

THESIS ON NATURAL AND EXACT SCIENCES B194

**Processes Influencing the Spatio-temporal
Dynamics of Nutrients and Phytoplankton in
Summer in the Gulf of Finland, Baltic Sea**

NATALJA BUHHALKO

TUT
PRESS

TALLINN UNIVERSITY OF TECHNOLOGY
Marine Systems Institute

This dissertation was accepted for the defence of the degree of Doctor of Philosophy in Oceanography on September 24, 2015.

Supervisor: Dr. Inga Lips, Marine Systems Institute at Tallinn University of Technology, Estonia

Opponents: Dr. Norbert Wasmund, Leibniz-Institute for Baltic Sea Research, Germany

Dr. Kai Piirsoo, Estonian University of Life Sciences, Institute of Agricultural and Environmental Sciences, Võrtsjärve Limnological Station, Estonia

Defence of the thesis: October 19, 2015

Declaration:

Hereby I declare that this doctoral thesis, my original investigation and achievement, submitted for the doctoral degree at Tallinn University of Technology has not been submitted for doctoral or equivalent academic degree.

Natalja Buhhalko

Copyright: Natalja Buhhalko, 2015
ISSN 1406-4723
ISBN 978-9949-23-844-6 (publication)
ISBN 978-9949-23-845-3 (PDF)

LOODUS- JA TÄPPISTEADUSED B194

**Toitainete ja fütoplanktoni ajalis-ruumilist
muutlikkust mõjutavad protsessid
suvel Soome lahes**

NATALJA BUHHALKO

Contents

LIST OF ORIGINAL PUBLICATIONS	7
INTRODUCTION	9
Background	9
Motivation and objectives	10
1. STUDY AREA	12
1.1 Seasonal changes of physical parameters	12
1.2 Seasonal changes of nutrient concentration and biological parameters	13
2. MATERIAL AND METHODS	15
2.1 Multi-disciplinary measurements using research vessel	15
2.2 Ships-of-opportunity	15
2.3 Autonomous moored water column profiler	16
2.4 Remote sensing	17
3. HORIZONTAL DISTRIBUTION OF CHLOROPHYLL <i>a</i> AND INORGANIC NUTRIENTS	18
3.1 Estuarine circulation	18
3.2 Stratification and vertical mixing	18
3.3 Upwelling and downwelling	19
4. VERTICAL DISTRIBUTION OF CHLOROPHYLL <i>a</i> AND INORGANIC NUTRIENTS	22
4.1 Stratification and vertical mixing	23
4.2 Upwelling and downwelling	26
5. CHLOROPHYLL <i>a</i> AND CHL <i>a</i> FLUORESCENCE FOR ENVIRONMENT ASSESSMENT	28
CONCLUSIONS	30
REFERENCES	32
PUBLICATIONS	39
Paper I	39
Paper II	51
Paper III	65
Paper IV	81
ACKNOWLEDGEMENTS	109
ABSTRACT	110
RESÜMEE	111
ELULOOKIRJELDUS	113
CURRICULUM VITAE	116

LIST OF ORIGINAL PUBLICATIONS

This thesis is based on four papers, in the following referred to by their Roman numerals:

I Kuvaldina, N., Lips, I., Lips, U., Liblik, T. (2010). The influence of a coastal upwelling event on chlorophyll *a* and nutrient dynamics in the surface layer of the Gulf of Finland, Baltic Sea. *Hydrobiologia*, 639(1), 221 - 230.

II Lips, U., Lips, I., Liblik, T., Kuvaldina, N. 2010. Processes responsible for the formation and maintenance of subsurface chlorophyll maxima in the Gulf of Finland. *Estuarine, coastal and shelf science*, 88, 339-349.

III Lips, U., Lips, I., Liblik, T., Kikas, V., Altoja, K., Buhhalko, N., Rünk, N. 2011. Vertical dynamics of summer phytoplankton in a stratified estuary (Gulf of Finland, Baltic Sea). *Ocean Dynamics*, 61, 903-915.

IV Uiboupin, R., Laanemets, J., Sipelgas, L., Raag, L., Lips, I., Buhhalko, N. 2012. Monitoring the effect of upwelling on the chlorophyll *a* distribution in the Gulf of Finland (Baltic Sea) using remote sensing and in situ data. *Oceanologia*, 54(3), 395-419.

Author's contribution

I – The author was responsible for chlorophyll *a* sampling, analysis of samples and data, and writing of the manuscript.

II – The author was responsible for chlorophyll *a* sampling, analysis of samples and data, and contributed to the writing of the manuscript.

III – The author participated in the field measurements, processed and analysed chlorophyll *a* data and contributed to the writing of the manuscript.

IV – The author was responsible for chlorophyll *a* sampling, analysis of samples and *in situ* data, and contributed to the writing of the manuscript.

INTRODUCTION

Background

Water eutrophication has become a worldwide environmental problem in recent decades, it is widespread all over the world and the severity is increasing (Yang *et al.*, 2008). Eutrophication is mostly described as an over enrichment of bioavailable nutrients. Within the EU, a common legislation defines eutrophication as “the enrichment of water by nutrients, especially compounds of nitrogen and phosphorus, causing accelerated growth of algae and higher forms of plant life to produce an undesirable disturbance to the balance of organisms present in the water and to the quality of water concerned” (Council Directive 91/271/EEC concerning urban waste water treatment, LEX-FAOC013224). Eutrophicated waterbody loses its functions: primary production is higher than during normal state, water transparency decreases, oxygen concentration is low or even anoxia develops near the bottom (Finni *et al.*, 2001). All that influences economy and development of society. It affects fisheries, recreation places, birds and animals connected to that eutrophicated waterbody. Therefore, a lot of attention is turned on finding the ways of preventing eutrophication (Yang *et al.*, 2008). In quantifying eutrophication, phytoplankton biomass, commonly measured as chlorophyll *a* (Chl *a*) concentration, is most often used to measure the trophic status of the water body.

Many factors and processes influence phytoplankton growth: human induced nutrient enrichment, hydrodynamics of waterbody, environmental factors as temperature, salinity, dissolved gases, balance of nutrients etc. Eutrophication causes some of the main problems in the Baltic Sea, such as cyanobacterial blooms in summer, decreased water transparency, and anoxic bottom layers (Baden *et al.*, 1990). Due to latter, the sediment effluxes of nutrients are one of the major sources of phosphorous and nitrogen for phytoplankton growth in the Baltic Sea (Lehtoranta *et al.*, 1997; Gran & Pitkänen, 1999). Hence, eutrophication in the Baltic Sea is a consequence of real external anthropogenic loading, and internal loading due to large resources of organic matter, which, for many decades have been stored into the sediments (Vahtera *et al.*, 2007).

Cyanobacterial blooms are common features in summer in the Baltic Sea but their increased intensity in last decades coinciding well with increased anthropogenic impact on the sea ecosystem (Finni *et al.*, 2001). The ecological importance of increased intensity of cyanobacterial blooms is through the functioning of ecosystem. Extreme gradients in the concentrations of cyanobacteria result in strong changes of the optical properties of water: colour and transparency (Kononen & Leppänen, 1997). Blooms of nitrogen fixing cyanobacteria in the Gulf of Finland are phosphorus limited (Vahtera *et al.*, 2007). One of the major sources of bioavailable phosphorus during summer in nutrient depleted upper layer is the internal loading from deeper layers through coastal upwelling events (Lips *et al.*, 2009). In summer, during upwelling, the water mass with higher nutrient concentration but low nitrogen to phosphorus (N: P) ratio is surfacing and can fuel the growth of cyanobacteria (if the

weather is calm and surface layer water temperature is above 16 C° after the collapse of upwelling event) and other phytoplankton species (Lips & Lips, 2010).

The horizontal and vertical distribution of phytoplankton is very heterogeneous and influenced, beside anthropogenic stress, by wide range of processes that include water mass circulation, light and nutrient availability, and biological interactions. In the World Ocean the circulation is dominated by meso-scale variability, which generally refers to ocean signals with space scales of 50-500 km and time scales of 10-100 days. The meso-scale processes in the Gulf of Finland is defined like a class of physical phenomena of spatial scales ranging from about five to ten kilometres and time scales ranging from a few days to several weeks (Alenius *et al.*, 2003). Meso-scale processes, such as coastal upwelling, eddies, jet currents (also dominant dynamical features of the Gulf of Finland; e.g. Fennel & Neumann, 1996), affect vertical dynamics of light, nutrients and phytoplankton populations, especially during periods when water column is strongly stratified (Delgadillo-Hinojosa *et al.* 1997; Pavelson *et al.*, 1999). In summer, sub-surface or deep chlorophyll *a* maxima are commonly observed in many stratified seas, including Baltic Sea (e.g. Kononen *et al.*, 1998, 2003; Deksheniaks *et al.*, 2001; Gentien *et al.*, 2005; Weston *et al.*, 2005; Lund-Hansen *et al.*, 2006). The hydrodynamic processes coupled with migratory behaviour of phytoplankton species is proposed to be the reason of such layers in the Baltic Sea (Pavelson *et al.*, 1999; Kononen *et al.*, 2003) and elsewhere (Deksheniaks *et al.*, 2001; McManus *et al.*, 2003).

To manage eutrophication in the interested water body, the best understanding of ecosystem functioning is achieved by combination of different monitoring approaches complemented with experimental and modelling research. Several eutrophication indicators are developed to help to assess the state of the sea. For the Baltic Sea, the indicators based on concentration of nutrients (nitrogen and phosphorus compounds) and Chl *a*, water transparency and oxygen conditions in the near bottom layer are developed (HELCOM, 2011).

Motivation and objectives

Understanding of natural processes, besides human induced, affecting changes in phytoplankton Chl *a* concentration leads to better understanding of mechanisms of water eutrophication. A combination of various approaches to measure phytoplankton Chl *a* and nutrient dynamics in the sea (monitoring, field studies using research vessel, ships-of-opportunity, autonomous buoys, remote sensing, modelling) enable more precisely register and assess environmental changes, see trends and make decisions for necessary actions.

The major purpose of this thesis is to verify the influence and importance of varying meso-scale hydrophysical processes on the dynamics of inorganic nutrients and Chl *a* in summer in the Gulf of Finland, Baltic Sea. The objective was to relate dynamics of Chl *a*, nutrients and different environmental variables obtained using high-frequent sampling approach in the Gulf of Finland. Multiparametric data collected with the autonomous systems were combined with data obtained during sampling aboard the research vessel within the periods of special interest.

This work consists of five chapters. Introduction gives an overview of topics discussed in dissertation and main objectives. The description and map of the study area illustrating the sampling transects are presented in chapter 1. In chapter 2 different methods and strategies used during present studies are described. The role of meso-scale hydrophysical processes controlling horizontal and vertical distribution of Chl *a* and inorganic nutrients in summer are outlined in chapters 3 and 4. The use of Chl *a* and Chl *a* fluorescence for environment assessments is discussed in chapter 5, followed by conclusions of the studies. The main results of the work are presented in more detail in four attached papers (denoted by Roman numerals **I** to **IV**).

1. STUDY AREA

Baltic Sea is a semi-enclosed brackish water continental sea. It has a restricted water exchange with the North Sea through narrow and shallow Danish Straits and due to that a relatively long water renewal time. Salt water inflow from the North Sea and large input of freshwater from more than 200 rivers create a south-north salinity gradient (Fennel & Seifert, 2008).

The Gulf of Finland is an elongated estuarine-like basin. The length of the gulf is about 400 km, the width varies from 48 to 135 km. The northern part of the gulf is shallower and the bottom slope is about 2 times lower than at the southern side (Laanemets *et al.*, 2009). Real bottom topography of the Gulf of Finland is complicated, especially near coasts, where islands and peninsulas divide coastal area into small bays.

The gulf has two main sources of water exchange. One is a freshwater runoff from rivers (mainly River Neva) and the second is saltier water inflow from the northern Baltic Proper. In general, the inflow of the saltier water occurs along the Estonian coast and the outflow of the less saline gulf water occurs along the Finnish coast (Alenius *et al.*, 1998) but the real flow pattern is strongly weather induced.

The field studies discussed in this dissertation were carried out in the central Gulf of Finland (Fig. 1).

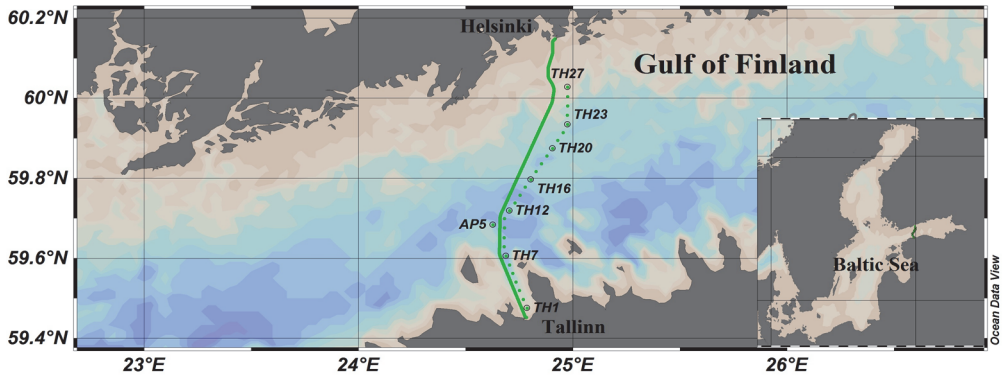


Figure 1. Map of the study area, the location of autonomous buoy station AP5, ferrybox transect (solid line) and stations visited abroad research vessel (dashed line with stations TH1-TH27). Ferrybox measurements reach more north compared with research vessel cruises.

1.1 Seasonal changes of physical parameters

Both, temperature and salinity have horizontal and vertical gradients in the Gulf of Finland. In the western gulf, a permanent halocline exists between depths 60-80 m preventing vertical mixing down to the bottom. In summer, thermocline exists at 10-20m depth. It vanishes in late autumn after convective mixing, and temperature of

waterbody is homogeneous at that time of the year. In winter, the gulf is usually covered with ice (Bergström *et al.*, 2001). In spring, after melting of ice cover, surface water temperature increases and leads to formation of seasonal thermocline. Horizontal temperature distribution in the surface layer is quite homogeneous in summer. The annual maximum surface layer temperature in the Gulf of Finland is typically as high as 17-22 °C. Horizontal salinity distribution is characterized by increase in salinity from 1-3 in the east to 6 in the west. Quasi-permanent salinity (density) front is formed at the entrance of the Gulf of Finland (Leppäranta & Myrberg, 2009). Front separates the northern Baltic Proper waters with higher salinity and less saline waters of the Gulf of Finland. The dynamics of the front is sensitive to wind and its direction. Up- and downwelling events are typical phenomena in the Baltic Sea, including Gulf of Finland, and have clear effects on horizontal temperature and salinity fields in summer when water mass is strongly stratified. During summer coastal upwelling events cold waters from intermediate layers surfacing (Lips *et al.*, 2009) and are well detectable with satellite remote sensing (Uiboupin & Laanemets, 2009).

1.2 Seasonal changes in nutrient concentration and biological parameters

A seasonal variation of inorganic nutrient concentrations is observed in the Baltic Sea upper layer: minimum values in summer and maximum in winter. Water pool is mixed down to the bottom or down to the halocline in autumn. In winter, concentrations of nutrients are high because deep vertical mixing and low light level prevent phytoplankton growth.

Phytoplankton primary production is highest in spring. The spring bloom dynamics, heterogeneity and intensity is influenced by winter level of inorganic nutrients in the surface layer and physical processes, such as prevailing circulation, development of stratification, upward and downward movement of the seasonal thermocline (Kahru & Nömmann, 1990; Lips *et al.*, 2014).

After the spring bloom, inorganic nutrients are almost depleted in the upper mixed layer and strong stratification prevents mixing between the nutrient depleted upper layer and the nutrient rich lower layers. That gives competitive advantages for cyanobacteria (Lips & Lips, 2008) able to fix molecular nitrogen and dinoflagellates able to migrate vertically in the water column (Jephson *et al.*, 2009). Filamentous cyanobacteria in the Baltic Sea have ability to fix molecular nitrogen and to use phosphates left in the upper water layer after spring bloom (Heiskanen, 1998). Vertically migrating phytoplankton species are known for the ability to assimilate necessary nutrients from the lower layer in order to use these in the euphotic layer for photosynthesis (Hall & Paerl, 2011).

In summer, during thermal stratification, when surface layer is depleted of inorganic nutrients, coastal upwelling plays an important role in replenishing the upper euphotic layer with nutrients and supporting the phytoplankton growth. In the intermediate water layer the N:P ratio is low, and hence, more phosphates in relation

to nitrates are brought to the surface layer (Lips *et al.*, 2009). Upwelling and downwelling are coupled in the Gulf of Finland affecting strongly both the horizontal and vertical pattern of inorganic nutrients and phytoplankton (Lips & Lips, 2010).

2. MATERIAL AND METHODS

The Baltic Sea is known as one of the most intensively observed marine areas (Fennel & Neumann, 1996). There are large datasets available from different areas of interest: physical, chemical, geological, and biological data, which gives us an opportunity to see long-term tendencies in ecology of the sea. At the same time, the short-term temporal and spatial heterogeneity is high and to understand the ecosystem functioning, dynamics of nutrients and phytoplankton in the pelagic ecosystem needs to be studied using high spatio-temporal approach (Benoit-Bird & McManus, 2012).

In the present study, investigations using different approaches were carried out: multi-disciplinary meso-scale surveys by research vessel (**I**, **II**), autonomous measurements and sampling on board commercial ferries (**III**), measurements using an autonomous moored water column profiler (**III**), and satellite remote sensing (**IV**). The combination of different approaches (**III**, **IV**) allowed following the high temporal and spatial heterogeneity and dynamics of nutrients and phytoplankton in the central part of the Gulf of Finland.

2.1 Multi-disciplinary measurements using research vessel

The main advantage of using research vessel is the possibility to conduct many measurements simultaneously. At the same time, the processes in the pelagic environment are often short, lasting only few days or weeks, making it difficult to organise measurements and sampling in appropriate sea area with the needed spatio-temporal coverage and resolution to link phenomena of pelagic biology to hydrophysical features, for instance.

The best strategy, which allows describing short-term changes, is to conduct high frequent field sampling (**I**, **II**) or combined approaches (**III**, **IV**). In 2006, seven surveys from 11 July until 29 August along the Tallinn-Helsinki ferry line were conducted. Weekly mappings (at 27 stations, distance between stations 2.5 km, Fig. 1) of hydrographical, -chemical and -biological (every second station) fields was performed along cross-gulf section (**I**, **II**). In July-August 2009 combined approach of ferrybox, autonomous profiling buoy measurements complemented with weekly horizontal and biweekly vertical sampling along the cross-gulf section and near the buoy station, respectively, was used (**III**). Detailed sampling dates and depths, together with methods used can be found in papers **I-III**.

2.2 Ships-of-opportunity

Commercial ferries can be used as carriers of autonomous measurement devices to enable to follow the high-resolution changes in the sea surface layer. The so called ships-of-opportunity or ferrybox technique allows to observe the dynamics of physical, chemical and biological properties in the upper layer in meso- and basin wide scale with high spatial and temporal frequency and relatively low cost (Rantajärvi & Leppänen, 1994). High-resolution transect yield gives much more

information than point measurements allowing to see the short-term dynamics and longer-term trends in phytoplankton growth and calculate several phytoplankton indexes for assessing the sea area (Pulliainen *et al.*, 2004; Fleming & Kaitala, 2006; Lips & Lips, 2008; Lips *et al.*, 2014). Obtained high-resolution surface layer data can be combined with other data to better explain the variability of different parameters (III). The ferrybox observations are found to be valuable in early warning systems of cyanobacterial bloom development as cyanobacterial bloom initiation phase is clearly detectable from ferrybox samples and the probability of formation of intense surface accumulations can be predicted in advance (Lips, 2005).

High-resolution surface layer temperature and salinity data obtained using autonomous ferrybox systems are also valuable for modelling. The ferrybox data have been used to simulate the observed evolution of Chl *a* on an alongshore transect in the coastal German Bight (North Sea) and to find out main mechanisms affecting that evolution of Chl *a* (Brandt & Wirtz, 2010). Ferrybox systems were used to study the partial pressure of carbon dioxide in the Baltic Sea (Schneider *et al.*, 2006) providing valuable validation data for modelling biogeochemical control of the coupled CO₂-O₂ system in the Baltic Sea (Omstedt *et al.*, 2014).

Part of the data used in the present thesis were obtained using the ferrybox system installed aboard the passenger ferry “Baltic Princess” plying between Tallinn and Helsinki. Ferrybox measurements and sampling in summer (July-August) 2009 were used (III). The width of the gulf in the study area is less than 80 km, and the parameters were registered in an approximately 72-km wide area along the ferry route (excluding an area of approximately 4 km close to each harbour). Water was pumped through the measuring system as the ferry travelled and the water intake was located at a depth of approximately 4 m. The temperature (T; PT-100 sensor), salinity (S; FSI Excell thermosalinograph), and Chl *a* fluorescence (SCUFA Turner Design) were recorded twice a day along the ferry route (Fig. 1) with a time resolution of 20 s, which corresponds approximately to a spatial resolution of 150 m between each collected data point. The water sampling from up to 17 locations along the ferry route was conducted using an automatic refrigerated (4 °C) sampler (Sigma 900 MAX) (Lips *et al.*, 2014). The collected samples were analysed to determine the concentration of Chl *a* and phytoplankton species composition and biomass. Detailed methods used for sample analysis can be found in paper (III).

2.3 Autonomous moored water column profiler

The time scales of pelagic biological processes are often short and it can be difficult to arrange surveys using research vessel only to register different processes and dynamics in the sea. The knowledge of the links between phytoplankton dynamics and meteorological and oceanographic forcing can be improved by using besides high-resolution autonomous horizontal *in situ* observations (e.g. ferrybox) also the high-resolution vertical *in situ* observations.

In the frame of present study, the autonomous profiler (Idronaut S.r.l.; surface buoy designed by Flydog Solutions Ltd.) was deployed close to the ferrybox line in

sea area with a bottom depth of 86 m (Fig. 1) in July-August 2009 (III). The vertical profiles of temperature, salinity and Chl *a* fluorescence (OceanSeven 316*plus* CTD probe) were registered in the water layer from 2-50 m with predefined time interval and vertical resolution (in our studies the time interval was 3 hours and vertical resolution was 10 cm). Additionally an ADCP (acoustic Doppler current profiler, Teledyne RDI, 300 kHz) was deployed close to the buoy from 27th July to 24th September in 2009 to measure the flow structure in the whole water column with a vertical resolution of 2 m.

2.4 Remote sensing

The traditional technique used to study phytoplankton dynamics is either microscopic examination or laboratory analyses of pigments in water samples. The major limitation of this methodology is often a temporal and spatial scope due to the amount of time involved in sample analysis. Spatio-temporal variability of different environmental parameters (including phytoplankton pigments) is widely studied using satellite imagery. The distribution patterns of different parameters are mapped in order to detect changes in either interannual, seasonal or meso-scale (Horstmann, 1983; Siegel *et al.*, 2005; Kahru *et al.*, 2007; Kononen *et al.*, 1997; Laanemets *et al.*, 2011). The detection of cyanobacteria surface accumulations in satellite imagery is probably one of the best tools available to map distributions of cyanobacterial surface accumulations during cloud-free periods. Satellite remote sensing, complemented with *in situ* measurements and wind information, enabled to analyse the spatial variability of phytoplankton Chl *a* promoted by upwelling event in 2006 (IV).

3. HORIZONTAL DISTRIBUTION OF CHLOROPHYLL *a* AND INORGANIC NUTRIENTS

The horizontal distribution of phytoplankton in the Gulf of Finland is heterogeneous and the spatial distribution of phytoplankton Chl *a* in the euphotic layer is usually affected by the physical variability of the water body (Kononen & Leppänen, 1997). The horizontal distribution of inorganic nutrients and phytoplankton is largely influenced by hydrophysical processes and structures like estuarine circulation, meso-scale eddies, fronts and coastal upwelling events in conjunction with life-strategy (e.g. migration) of plankton and nutrient limitation (Kononen *et al.*, 1996; Kanoshina *et al.*, 2003; Lips *et al.*, 2005). Due to the hydrophysical forcing phytoplankton is often transported from one place to another or growth enhancement may be followed in certain area.

3.1 Estuarine circulation

The intensity or even reversal of the estuarine circulation in the Gulf of Finland, characterized by an inflow in the deeper layers and an outflow in the surface layer, is depending on the prevailing winds (Elken *et al.*, 2003; Liblik & Lips, 2011). Usual circulation in the surface layer consists of inflow of saltier waters from Baltic Proper along the southern part of the gulf and outflow of less saline waters along the northern part of the gulf (Alenius *et al.*, 1998). Estuarine circulation is in general controlled by the inflow of rivers, rainfall, evaporation, and wind.

Estuarine circulation in the Gulf of Finland is intense and upward volume (and nutrient) transport may support the phytoplankton growth in the surface layer. The upward volume transport in the gulf is many-fold more intense in case of long-lasting easterly-north-easterly winds, in comparison to prevailing westerly-south-westerly winds (Liblik, 2012). In case of intensification of estuarine circulation, salinity in deep layers is higher, vertical stratification is stronger, and additional amounts of phosphorus is added into the Gulf of Finland (Lips *et al.*, 2008).

Wind-driven circulation in the Gulf of Finland is highly variable and often „breaks“ the classical estuarine circulation pattern. Several intense meso-scale features are initiated by variable wind pattern – eddies, upwelling or downwelling, coastal and frontal jet currents.

3.2 Stratification and vertical mixing

In summer, water column is thermally stratified in the Gulf of Finland and euphotic upper mixed layer is usually depleted of inorganic nutrients necessary for phytoplankton growth. Below the seasonal thermocline, inorganic nutrient ratio (DIN:DIP) is low creating favourable growth conditions to cyanobacteria after the upward transport of nutrient rich layers (Lips, 2005) as bloom forming filamentous cyanobacteria in the Baltic Sea are able to fix molecular nitrogen. In the Gulf of

Finland, any pre-bloom vertical mixing is potentially capable to support the growth of filamentous cyanobacteria after the re-establishment of vertical stratification. The other supporting aspect for cyanobacterial growth enhancement is the location of phosphocline, which is usually at a shallower depth (in the upper part of the seasonal thermocline; Laanemets *et al.*, 2004) than nitracline, hence vertical mixing will usually bring up water more rich in phosphates than nitrates and nitrites.

Not only physical and chemical factors affect the distribution of phytoplankton in the surface layer. Biological capabilities (e.g. vertical migration of phytoplankton) also play a great role. Many dinoflagellates are known to be capable of vertical migration (Smayda, 2010) in order to assimilate nutrients (mainly nitrogen) from lower layers and migrate back to photosynthesise in the well-lit upper layers (e.g. Fauchot *et al.*, 2005). Hence, keeping nutrient depleted upper layer productive and phytoplankton biomass high in certain sea areas (**III**; Lips & Lips, 2014) during summer stratification conditions.

3.3 Upwelling and downwelling

The overall horizontal distribution of temperature and phytoplankton Chl *a* in summer in the Gulf of Finland surface layer is usually quite homogeneous. The intense horizontal patterns develop during coastal upwelling events when steep gradients in horizontal temperature and salinity fields have been registered in the sea surface layer (e.g. Lips *et al.*, 2009) or were visible on satellite remote sensing images (e.g. Uiboupin & Laanemets, 2009). Coastal upwellings, induced by persistent or time variable winds, are important in bringing nutrient-rich waters from lower layers to the euphotic zone, and hence frequently associated with increased biological productivity (e.g. MacIsaac *et al.*, 1985; Cushing, 1989). Primary production in the major upwelling areas of the World Ocean is influenced by different factors, such as upwelling strength, duration and timing; the nutrient concentration of the upwelled waters, light, and the availability of phytoplankton seed stock (Mann, 2000). Upwellings in the Baltic Sea are not persistent, but short-time events. They depend on wind strength and duration.

The coastal upwelling-downwelling events are coupled in the Gulf of Finland because of the elongated shape of the gulf and relatively short distance (48–135 km) between northern and southern coasts. In the Gulf of Finland, the upwelling along the northern coast is induced by south-westerly winds and near the southern coast by north-easterly winds. Upwellings along the northern coast are more common, because south-westerly winds are dominating in the area (Soomere & Keevallik, 2003).

Very intense coastal upwelling observed along the southern coast of the Gulf of Finland in August 2006 had a clear influence to the spatial distribution of temperature, salinity, inorganic nutrients and phytoplankton (**I**, **II**, **IV**) in the upper layer. Water temperature in the surface layer along the studied cross-section was between 18 °C and 21°C at the end of July 2006. After the development of upwelling along the southern coast at the beginning of August, temperature of the surface layer in the southern part of the gulf decreased down to 5 °C. Cold and more saline water

(compared with pre upwelling situation) covered about $\frac{1}{3}$ of the cross-section in the study area (see Fig. 2 in paper I).

Before an upwelling event (in July 2006), the upper mixed layer was depleted of nutrients. During the upwelling, phosphate and nitrite+nitrate concentrations increased remarkably in the area covered with upwelled waters. Two weeks after the initiation of upwelling, by 15th August, nitrate+nitrite concentrations were already below the detection limit, while some phosphates were still left. A week later, after the relaxation of upwelling, concentration of both nutrients in the upper layer was below the lower detection range (see Fig 3 in paper I).

Phytoplankton Chl *a* in the surface layer of investigation area was strongly influenced by the observed upwelling event and circulation pattern (Fig. 2). The lowest Chl *a* values (below 2 mg m^{-3}) were measured in the upwelling water near the southern coast and highest (average 13 mg m^{-3}) near the northern coast, in zone of downwelling. The increase in Chl *a* concentration in the northern part of the study area was mostly due to the northward Ekman transport in the surface layer. However, possible influence of the along shore transport from adjacent coastal areas and growth enhancement stimulated by a smaller upwelling event in late July near the northern coast (II) cannot be ignored.

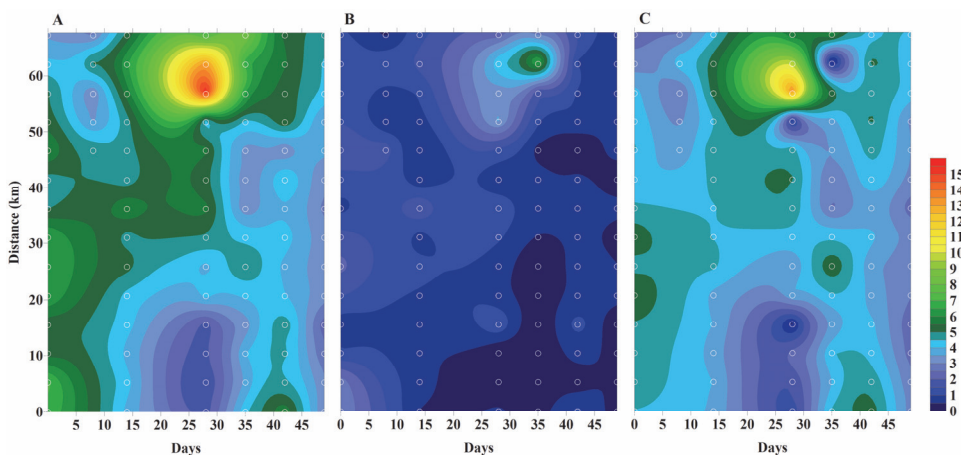


Figure 2. Horizontal distribution of total Chl *a* concentration (mg m^{-3} ; A), Chl *a* in $>20 \mu\text{m}$ size fraction (B) and Chl *a* in $<20 \mu\text{m}$ size fraction (C) in the upper mixed layer during the study period in July–August 2006. On the x-axis days from the beginning of the study are shown, and on the y-axis distance from the first (TH1) station is shown in kilometres. Circles on the map indicate sampling points.

After the relaxation of observed upwelling (by 22nd August), Chl *a* concentrations in the upper mixed layer were nearly similar as measured before the upwelling event. The fluctuations in Chl *a* concentration during the strong coastal upwelling indicate the advection of pre-upwelling communities away from the upwelling area and the time lag in increase of phytoplankton growth in the same area. As during upwelling

event water is brought from cold intermediate layers into the euphotic zone, the summer phytoplankton communities responds to changed light conditions and increased nutrient concentrations with small lag period (e.g. Vahtera *et al.*, 2005) which length is temperature and light dependant (Ishizaka *et al.*, 1983).

Chlorophyll *a* was mainly found in the <20- μm size fraction which also had faster response to changed nutrient conditions. From the results of this study, the increase in bigger phytoplankton size fraction after the upwelling relaxation due to the enrichment of nutrients during the upwelling event cannot be stated with very high confidence. We noticed, that the increase of Chl *a* in the >20- μm fraction in the area previously affected by upwelling equals with the decrease in concentration in this size fraction near the opposite coast (**I**). The temporal changes in smaller size fraction were similar to the changes of total Chl *a* content. It is also important to note, that the phytoplankton species composition of major upwelling areas worldwide are characterized by chain-forming and colonial diatoms, in the Baltic Sea, small-sized phytoplankton species (mainly nanoflagellates) benefit.

4. VERTICAL DISTRIBUTION OF CHLOROPHYLL *a* AND INORGANIC NUTRIENTS

Vertical gradients of nutrients and phytoplankton are often stronger than horizontal ones and are very much dependent on the water column stratification. Vertical distribution of phytoplankton is determined by availability of major resources (light and nutrients), grazing, divergence/convergence areas, buoyancy (Fennel & Boss, 2003). In summer, the strong thermal stratification develops in the Gulf of Finland. The upper mixed layer above the thermocline is usually exhausted of inorganic nutrients after the spring bloom while there are enough nutrients left below the thermocline but low light levels do not support the phytoplankton photosynthetic growth there.

In the stratified water column, when light is added from above and nutrients can be supplied from below, the sub-surface Chl *a* maxima may form (Klausmeier & Litchman, 2001). The sub-surface and deep Chl *a* maxima are quite often observed in the Baltic Sea (Kahru *et al.*, 1982; Kuosa, 1990; Kononen *et al.*, 1998; Pavelson *et al.*, 1999; II, III). Several mechanisms and processes, such as a two-layer current, temporal and spatial variation of pycnocline depth, estuarine structure of hydrographic fields, minimum of turbulent mixing, play an important role in the formation and dynamics of these Chl *a* layers (Dekshenieks *et al.*, 2001; McManus *et al.*, 2003).

The intensity and thickness of sub-surface Chl *a* maxima during present studies were detected as shown in Fig. 3. The difference between the sub-surface maximum of Chl *a* (Chl_{max}) and local minimum of Chl *a* above it (Chl_1), and the difference between the depth of local minimum (h_1) and the depth h_2 where Chl *a* values below the maximum decreased back to the same concentration (Chl_1) were estimated respectively.

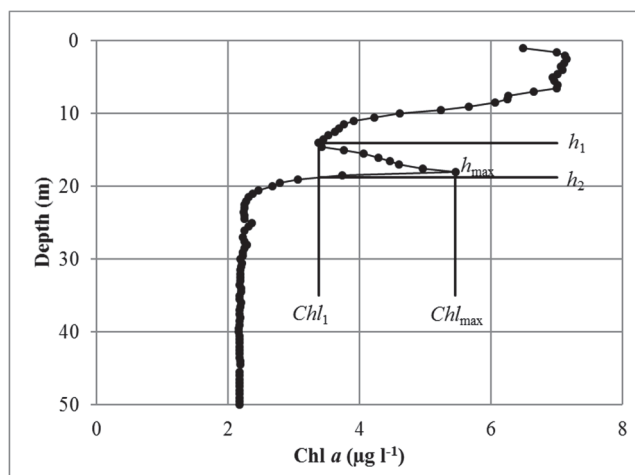


Figure 3. Sketch used to define the parameters of sub-surface Chl *a* maxima.

In July 2006 the sub-surface Chl *a* maxima with intensities $\geq 0.5 \mu\text{g l}^{-1}$ were registered at 37 stations out of 80 stations visited. The highest observed Chl *a* values in these layers were $10.5 \mu\text{g l}^{-1}$ on 11 July, $12.2 \mu\text{g l}^{-1}$ and $11.4 \mu\text{g l}^{-1}$ on 19-20 July, and $8.2 \mu\text{g l}^{-1}$ on 25 July. At the same time, the Chl *a* values at the surface layers were on average between $6\text{-}8 \mu\text{g l}^{-1}$. The depth of Chl *a* maxima varied between 14.5 and 35 m and the average depth of maxima was 23 ± 4.6 m.

4.1 Stratification and vertical mixing

Processes, which lead to vertical transport and mixing, are very important in the strongly stratified sea to the whole phytoplankton community, including the formation of sub-surface and deep phytoplankton biomass maxima (II, III).

Several studies have confirmed that phytoplankton sub-surface Chl *a* maximas are common in summer in stratified Gulf of Finland (II, III, Lips & Lips, 2014). These maxima usually locate at the base of thermocline and coincide well with the depth of nutriclines. The study in July 2006 revealed that these maxima were located an average at depth of 23 m. The concurrent light measurements allowed to show that these maxima were observed significantly below the photic depth (II). Several estimates based on the field measurements indicate that in certain conditions the upward nutrient fluxes may support formation and maintenance of sub-surface Chl *a* maxima (Sharples *et al.*, 2001; Lund-Hansen *et al.*, 2006; Hales *et al.*, 2009). During our study, the upward transport of nutrients seemed not to be the only mechanism to maintain the observed sub-surface maxima along the entire studied cross-section and hence, other processes responsible for development and maintenance of these maxima had to be analysed. The cross-transect geostrophic velocity distributions revealed that the sub-surface Chl *a* maxima layers detected in the Gulf of Finland in July 2006 were located mostly at the base of anti-cyclonic circulation cells where the isopycnals were depressed (Fig. 4).

The patchy distribution of Chl *a* in sub-surface and deep layers could be favoured by the combination of physical, chemical and biological processes. The ability of cells to migrate to deeper depths and maintain in these depths (the shallowest depth where high enough nutrient concentrations were available for growth, see Fig. 6 in paper II) together with horizontal convergence of waters along the depressed isopycnals at the base of anti-cyclonic circulation cells could have supported these maxima studied in 2006. A clear weakening of the stratification with the depth just below observed maxima could be considered as an indirect indication of vertical mixing and concurrent nutrient fluxes supporting the possible nutrient uptake there.

To confirm the hypothesis, that some species in summer phytoplankton community are able to perform such deep vertical migrations, the downward/upward migration of phytoplankton community dominated by dinoflagellate *Heterocapsa triquetra* Ehrenberg (Stein) in the Gulf of Finland in July 2009 was registered using the autonomous profiling buoy system complemented with vertical sampling aboard research vessel (III).

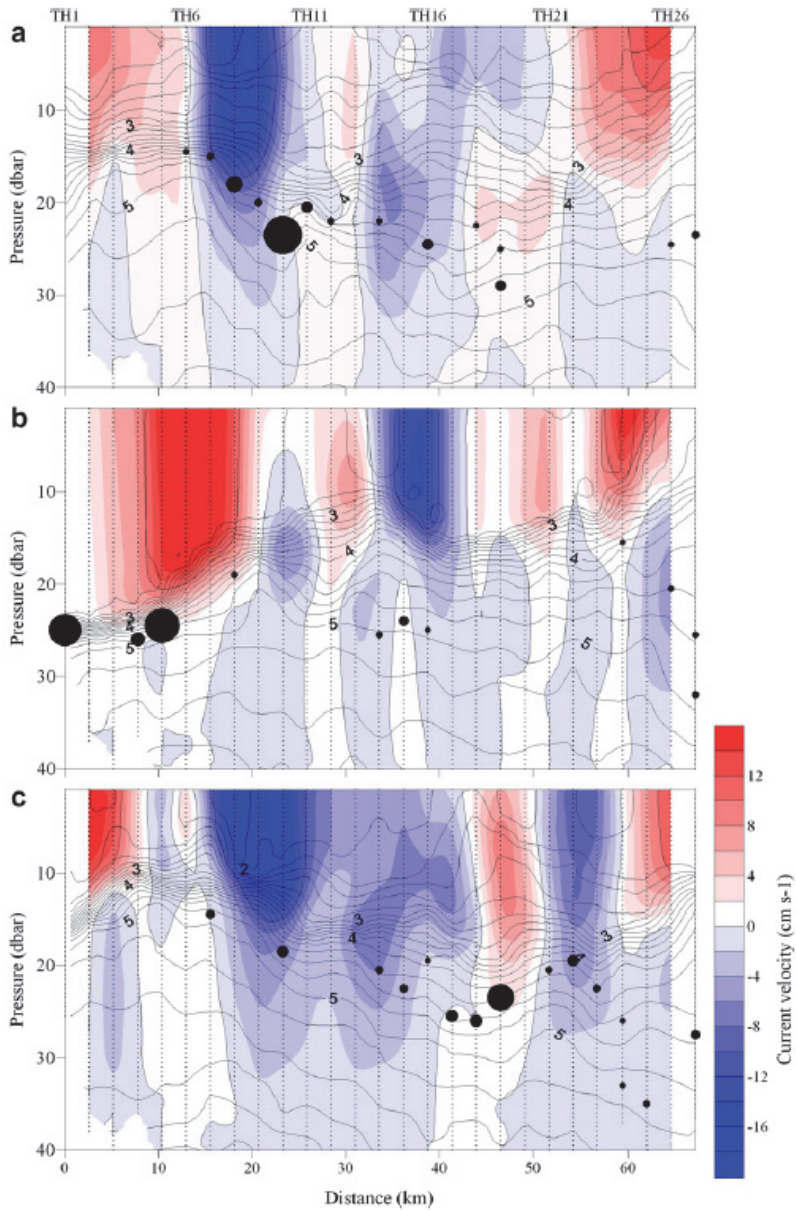


Figure 4. Vertical sections of cross-transect geostrophic current velocity on 11(a), 19-20 (b) and 25 (c) July 2006. The reference level of no motion was chosen at 40 dbar in the open gulf and at the seabed in the shallow areas. Corresponding density anomaly distribution (density – 1000 kg m⁻³) is shown by black contour lines. Dotted lines indicate profiles; values on x-axis are distance from the southernmost station (TH1); station numbers are shown above. Observed sub-surface Chl *a* maxima are indicated as black circles scaled proportionally to the intensity of maxima.

High-resolution vertical profiling revealed remarkable diurnal and bi-diurnal variations of the vertical distribution and temporal evolution of temperature, salinity and Chl *a* (see Fig. 2 in Paper III). It is showed by earlier studies that swimming enables nutrient deficient dinoflagellate cells to migrate to the deeper layers where they are able for dark-assimilation of nitrates (e.g. Fauchot *et al.*, 2005), including *H. triquetra* as observed by Paasche *et al.*, 1984). The diurnal (and possible bi-diurnal) vertical migration pattern was illustrated by a series of consecutive vertical profiles of Chl *a* registered by autonomous profiling buoy station with 3 h time interval within 30 h on 26-27 July 2009 (Fig. 5). The downward migration of phytoplankton was measured after 6 p.m. reaching the depth of 20 m 12 h later. During next 6 hours two maxima – one at 3 m depth (near the surface), the second at 27 m – developed.

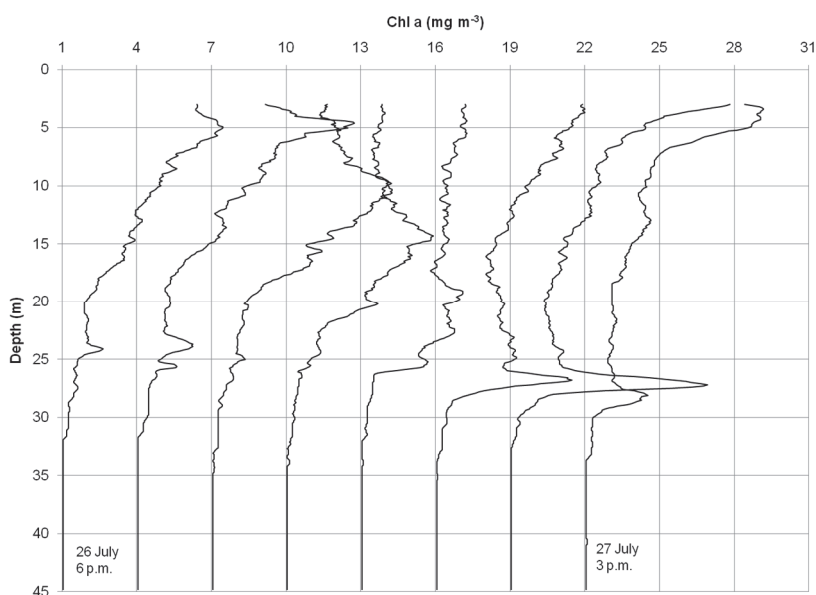


Figure 5. Changes in the vertical distribution of Chl *a* at the buoy station AP5 from noon on 26 July until 9 p.m. on 27 July 2009. Values on the x-axis are correct for the first profile. Each subsequent profile is shifted to the right by 3 mg m⁻³ in relation to the preceding one.

The thermocline was at the depth between 13 and 23 m. It was calculated that Chl *a* maximum moved downward during the night with an approximate speed of 1.6 m h⁻¹. The detectable amount of nutrients were measured below the strongest density gradient at depths >25 m (III). The depths of 28-34 m, where phytoplankton biomass maxima were observed in July 2009, are in principle reachable by diurnal migratory behaviour. However, the observed swimming speed of 1.6 m h⁻¹ is not enough for cells to migrate to a depth >25 m, assimilate nitrogen, and swim back to the surface within 24 h. As many profiles with two vertically separated maxima of Chl *a* were registered during our study, the migration cycle >24 h and the bimodal vertical

distribution as a consequence of asynchronous migration pattern was suggested (part of the community is migrating downwards and part is returning to the sea surface). Our results indicate that the downward migration is clearly synchronous while the upward migration could be asynchronous and depend on the time period needed to reach the nutrient rich layer and uptake enough nitrogen (see Fig. 6 in Paper **III**).

4.2 Upwelling and downwelling

Coastal upwellings can significantly contribute to the vertical mixing of the Gulf of Finland waters. Hence, being an important processes bringing nutrient rich waters from deeper layers to the surface during strong summer stratification period, and influencing the phytoplankton dynamics in the upper layer and in the whole water column (Vahtera *et al.*, 2005; Lips *et al.*, 2009; Lips *et al.*, 2010; **I**, **II**).

Coastal upwellings are frequent events in the Gulf of Finland and in the whole Baltic Sea (e.g. Myrberg & Andrejev, 2003). According to earlier studies, summer upwelling events usually transport nutrients from lower layers with excess of phosphorus in relation to the Redfield ratio (N: P of 16:1; Redfield *et al.*, 1963) into the surface layer in the Gulf of Finland (Haapala, 1994; Kononen *et al.*, 2003, Vahtera *et al.*, 2005, Lips *et al.*, 2009). Due to this, upwellings are one of the mayor internal sources of phosphorus for nitrogen fixing cyanobacterial blooms (Vahtera *et al.*, 2005; Lips & Lips, 2008). The major upwelling event observed in August 2006 along the southern (Estonian) coast brought phosphorus into the surface layer in amounts which is equal to the riverine load of total phosphorus to the entire Gulf of Finland during one month (HELCOM, 2004; Lips *et al.*, 2009).

A smaller upwelling event near the northern coast of study area was observed in mid July 2006 (**II**). Vertical profiles registered on 19-20 July demonstrate well the influence of coupled upwelling-downwelling event on the vertical distribution of temperature and Chl *a* along the cross-section (see paper **II**; Fig. 4 and 5). Vertical profiles of Chl *a* also revealed the occurrence of sub-surface maximum layers of phytoplankton at several sampling stations in the central part of the gulf cross-section in the beginning and end of July (Fig. 6) characterised with strong thermal stratification. After the development of small upwelling event near the northern coast of the gulf (registered on 19-20 July 2006), coupled with downwelling near the southern coast, the most intensive deep Chl *a* maxima were registered in the thermocline in the downwelling area. In this downwelling area, the thermocline had its deepest position but the horizontal convergence of waters could be expected. Therefore, it was concluded that intense Chl *a* maxima could be formed due to the accumulation of downward migrated phytoplankton near the base of the meso-scale features (**II**).

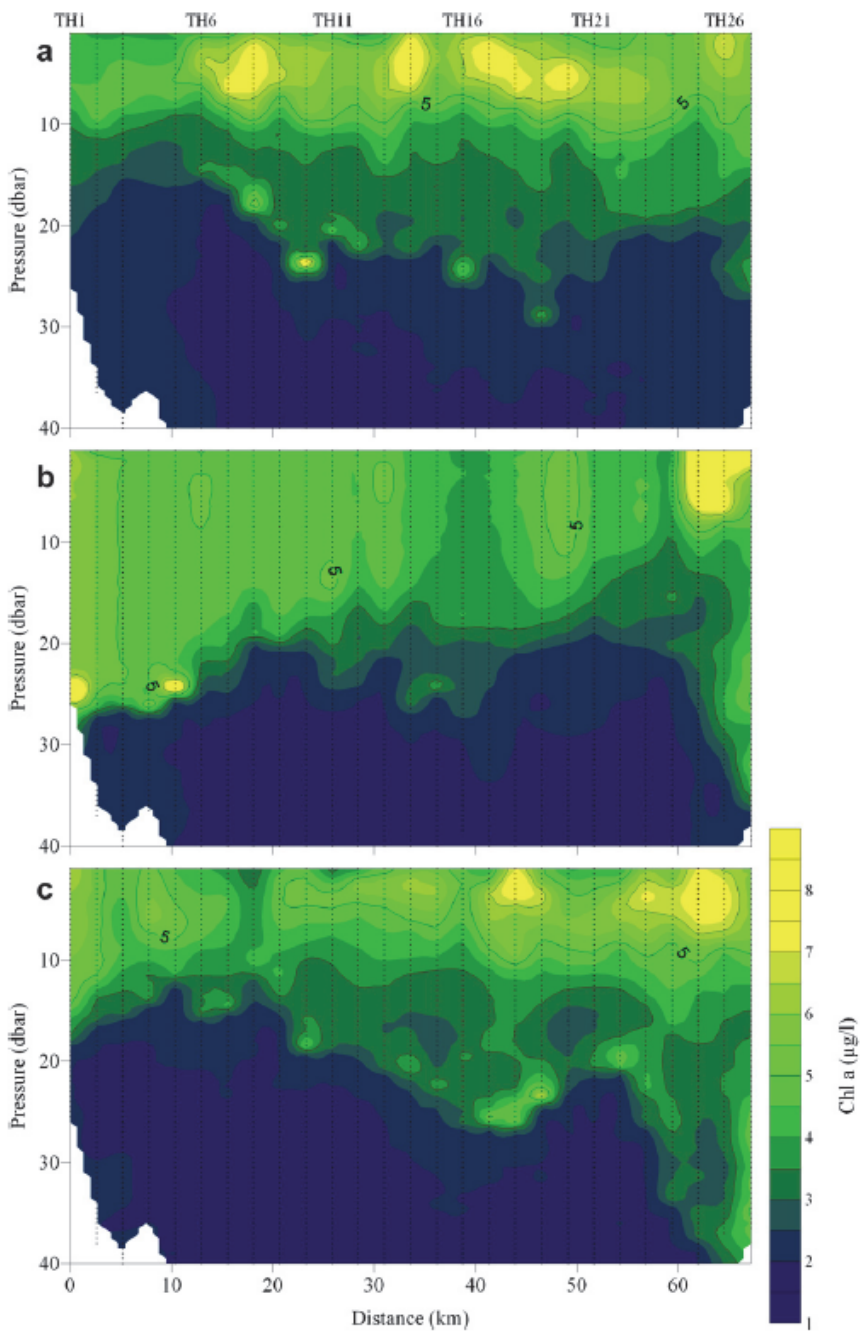


Figure 6. Vertical sections of Chl *a* on 11(a), 19-20 (b) and 25(c) July2006. Dotted lines indicate profiles; values on x-axis are distance from the southernmost station (TH1); station numbers are shown above.

5. CHLOROPHYLL *a* AND CHL *a* FLUORESCENCE FOR ENVIRONMENT ASSESSMENT

Countries surrounding the Baltic Sea being Contracting Parties to the Helsinki Convention have agreed to implement the Baltic Sea Action Plan (BSAP), first adopted in 2007 and updated in 2013 (www.helcom.fi/baltic-sea-action-plan). One of the main environmental problems tackled by the BSAP is eutrophication of the Baltic Sea. A number of measures to reduce external inputs of nitrogen and phosphorus to the sea were taken, however, the concentrations of nutrients have not declined proportionally yet. According to the model prediction, if nutrient reduction targets (agreed by HELCOM) are fulfilled, concentrations of nutrients will decline and the Baltic Sea ecosystem will recover. Due to the restricted water exchange and accumulation of nutrients in the system, it will take long time to reach the target levels of eutrophication status. Thus, nutrient reduction measures should be implemented as fast as possible.

Phytoplankton growth increases along with increased eutrophication, as a result of increased nutrient concentrations in the water body. Chlorophyll *a* concentration is often used as a proxy of phytoplankton biomass. Assessment of eutrophication status of the open sea areas of Baltic Sea is based on an integration of commonly agreed core indicators (HELCOM, 2014): inorganic nitrogen (DIN) concentration, inorganic phosphorus (DIP) concentration, Chl *a* concentration, water transparency (Secchi depth) and oxygen concentration (oxygen debt). Core indicators are developed to assess whether the agreed ecological objectives are achieved or not. According to the BSAP the ecological objectives under the eutrophication topic are: clear water, concentrations of nutrients (DIN, DIP) in the surface layer close to natural levels, natural level of algal blooms and natural oxygen levels.

Special attention in present thesis is paid on horizontal and vertical distribution of Chl *a* influenced by processes other than direct anthropogenic nutrient loading. Like pointed out above, the concentration of Chl *a* is used as an indicator in the assessment of the state of the marine environment. Analyses of Chl *a* are relatively cheap and fast, compared to the analyses of phytoplankton biomass and species composition. Hence, the number of samples to be taken and analysed is large, thereby the reliability of assessments is increased. However, one should have knowledge of possible hydrophysical processes affecting the Chl *a* dynamics. Low Chl *a* in the upwelling area is not a result of successful measures to tackle with eutrophication. Similarly, the high Chl *a* values in the downwelling area are not caused by the intensified external nutrient loading. Hence, in assessing the environmental status of the sea area, it is very important to understand and explain processes influencing the spatial pattern of phytoplankton. Measurements using satellite radiometers of water-leaving radiance in the visible range (ocean colour), are also widely used to determine the Chl *a* concentration in the sea surface layer and to register the spatial coverage of it. The satellite images obtained during cloud free periods significantly increase the understanding of Chl *a* dynamics. Hence, further development of algorithms specific

for different regions in the Baltic Sea, should be continued in order to use satellite remote sensing as one reliable tool in marine monitoring.

Measurements of Chl *a* are included in most eutrophication monitoring programmes, and Chl *a* represents the biological eutrophication indicator with the best geographical coverage at the European level (EEA, 2011). The present study demonstrates well that phytoplankton vertical distribution is not homogeneous and very high Chl *a* concentrations often exist at depths far lower compared where the water samples are collected during environmental monitoring. Using advanced monitoring technologies (e.g. measurements by ferrybox or autonomous buoy stations), high temporal and/or spatial measurements of Chl *a* fluorescence are performed. If fluorescence measurements are used to estimate Chl *a* content, we need to take into consideration that the relationship between fluorescence yield and Chl *a* concentration may differ depending on species composition and physiological condition of the phytoplankton, nutrient limitation, and photoquenching (Kelly-Gerreyn *et al.*, 2004). Photoquenching is dependent on the daily illumination history. When exposed to daylight, phytoplankton fluoresces less in comparison to evening and night. It is suggested by Kelly-Gerreyn *et al.* (2004) that error, which may arise due to the photoquenching effect of sunlight, can be minimised by making measurements during darkness. So, how time of the day affects the fluorescence data? Are the results affected significantly by solar radiation during the day time, and what would be the difference in the results in comparison with the Chl *a* estimates based on evening or night measurements when the solar activity is not high?

In order to assess how time of the measurements affects the estimates of Chl *a* concentration, a study was conducted in summer 2012. Ferrybox system on board of the passenger ferry Baltic Princess made measurements of fluorescence twice a day – in early afternoon, from 1.30 p.m. until 5 p.m. and evening, from 6.30 p.m. until 10.00 p.m. Thus, the fluorescence data along the same transect were recorded under conditions of different solar activity. Chl *a* concentrations were measured from the water samples collected during the both trips by the flow-through system of Ferrybox. Chl *a* fluorescence values obtained in the early afternoon were significantly lower at times of high solar radiation compared the ones obtained during lower solar radiation (Stoichescu *et al.*, unpublished data). As the use of autonomous devices in purpose of marine environment are increasing, the special conversion factors for different solar radiation conditions needs to be determined in order to use fluorescence data for marine monitoring purposes.

In conclusion, Chl *a* concentrations can be used to assess the effects of measures taken to reduce eutrophication and improve the ecological status of the water body. However, one have to be aware that due to variations in freshwater run-off, light climate, and internal cycling processes, trends in Chl *a* concentrations as such cannot be directly related to measures, but must be evaluated in a broader context.

CONCLUSIONS

This thesis investigated the influence and importance of varying meso-scale hydrophysical processes on the spatio-temporal dynamics of inorganic nutrients and phytoplankton chlorophyll *a* in the vertically stratified Gulf of Finland. In order to assess the anthropogenic influence to the marine ecosystem and take measures to control eutrophication, natural processes and climatic fluctuations need to be well understood. Today, Chl *a* is the most widely used phytoplankton metric providing high confident information for the ecological classification of the Baltic Sea waters.

This study is based on combination of different approaches, including traditional measurements aboard research vessel coupled with latest technological capabilities using autonomous horizontal and vertical high-resolution measuring devices. The interdisciplinary data collected in summer 2006 and 2009 in the central part of the Gulf of Finland are presented.

The horizontal and vertical dynamics of inorganic nutrients and Chl *a* influenced by different meso-scale hydrophysical processes were registered with high temporal and spatial resolution. The data were collected in vertical resolution from 10 cm up to 10 m with temporal resolution from 3 h up to 2 weeks, and horizontal resolution along the gulfs cross-section from approximately 150 m up to 5 km with temporal resolution from 1 day up to 1 week.

In summer, when the water column in the Gulf of Finland is thermally stratified and euphotic layer is mostly nutrient limited, phytoplankton growth and spatial distribution is highly influenced by prevailing hydrophysical features caused by variable wind impulses. Wind induced processes, like upwelling/downwelling, eddies, coastal currents and jets, in the background of estuarine circulation cause movements of water-masses (and substances in it) both horizontally and vertically. Besides physical, and connected chemical factors, the dynamics and distribution of phytoplankton communities is largely influenced by species-specific biological adaptations, like fixation of molecular nitrogen, storage of limiting nutrients in cells for later use, extensive vertical migration, dark assimilation of nutrient, fast response to short nutrient impulses etc.

The main results of the present thesis can be summarised as follows:

- As coastal upwelling and downwelling are coupled in the Gulf of Finland, the dramatic simultaneous changes in the inorganic nutrient field and distribution of phytoplankton communities in the surface layer near the northern and southern coast appear.
- During intensive upwelling events the horizontal Ekman transport is the major process shaping the distribution of phytoplankton biomass in size-fraction $>20 \mu\text{m}$. The warmer surface layer is transported towards the opposite coast off from the upwelling region, concentrating pre upwelling phytoplankton communities in the downwelling area. At the same time, the upwelled waters have low Chl *a* concentration.

- The summer phytoplankton communities respond to the nutrient inputs induced by coastal upwelling with certain time lag, and, unlikely from major World Ocean coastal upwelling areas, nanoflagellates show the fastest response to upwelled nutrients in the Gulf of Finland.
- In summer, strong thermal stratification inhibits the mixing between nutrient depleted surface layer and nutrient rich lower layers, hence separates the light and nutrients, necessary for phytoplankton growth. Under these conditions the ability to migrate vertically and assimilate nutrients in the dark, will make some phytoplankton species more competitive.
- Phytoplankton sub-surface or deep maxima are common features in summer in the stratified Gulf of Finland. The formation of sub-surface phytoplankton layers in the Gulf of Finland is not only due to the ability of some species to migrate vertically, but is the combination of physical, chemical and biological processes. Certain vertical mixing-stratification features are prerequisite for development and maintenance of such layers. Sub-surface maxima of Chl *a* are almost always found at the base of thermocline and coincide well with the depth of nutriclines. The thin layers of high Chl *a* concentration are often found at the base of anti-cyclonic circulating cells with horizontal convergence of water along the depressed isopycnals.
- The most prominent migrations through the strongest vertical density gradients towards nitracline, even below 30 m depth, were registered when dinoflagellate *Heterocapsa triquetra* (phytoplankton with cell size of 20-25 μm) dominated in the phytoplankton community.
- The diurnal and bi-diurnal migration patterns of *H. triquetra* with downward migration of 1.6 m h^{-1} were estimated on the basis of vertical dynamics of Chl *a*. This is the first documented migration speed record for this species in the field. The asynchronous migration patterns often create the bimodal distribution of Chl *a*.
- The ability to migrate in deep layers, assimilate nutrients in the dark followed by migration back to the surface layer will also act as “biological nutrient pump”, and will help to keep nutrient limited surface layer productive also during summer thermal stratification.
- High-resolution measurements and sampling revealed the high spatial and temporal variability in summer phytoplankton community. The spatio-temporal variability of Chl *a* estimated from MERIS data confirmed the strong influence of meso-scale processes to the spatial variability of phytoplankton Chl *a*.

REFERENCES

- Alenius, P., Myrberg, K., Nekrasov, A. 1998. Physical oceanography of the Gulf of Finland: a review. *Boreal Environmental Research*, 3, 97-125.
- Alenius, P., Nekrasov, A., Myrberg, K. 2003. Variability of the baroclinic Rossby radius in the Gulf of Finland. *Continental Shelf Research*, 23, 563-573.
- Baden, S.P. 1990. Cryptofauna of *Zostera marina* (L.): Abundance, biomass, population dynamics. *Netherlands Journal of Sea Research*, 27, 81-92.
- Benoit-Bird, K.J., McManus, M. 2012. Bottom-up regulation of a pelagic community through spatial aggregations. *Biological Letters*, 8 (5), 813-816.
- Bergström, S., Alexandersson, H., Carlsson, B., Josefsson, W., Karlsson, K.-G., Westring, G. 2001. Climate and hydrology of the Baltic basin. In: Wulff, F., Rahm, L., Larsson, P. (eds.), *A systems analysis of the Baltic Sea. Ecological studies*. Springer-Verlag, 148, 75-112.
- Brandt, G., Wirtz, K.W. 2010. Interannual variability of alongshore spring bloom dynamics in a coastal sea caused by the differential influence of hydrodynamics and light climate. *Biogeosciences*, 7, 371-386.
- Cushing, D.H. 1989. A difference in structure between ecosystems in strongly stratified waters and in those that are only weakly stratified. *Journal of Plankton Research*, 11, 1-13.
- Dekshenieks, M.M., Donaghay, P.L., Sullivan, J.M., Rines, J.E.B., Osborn, T.R., Twardowski, M.S. 2001. Temporal and spatial occurrence of thin phytoplankton layers in relation to physical processes. *Marine Ecology Progress Series*, 223, 261-271.
- Delgadillo-Hinojosa, F., Gaxiola-Castro, G., Segovia-Zavala, J.A., Muñoz-Barbosa, A., Orozco-Borbón, M.V. 1997. The effect of vertical mixing on primary production in a Bay of the Gulf of California. *Estuarine Coastal Shelf Science*, 45, 135-148.
- EEA, 2011, <http://www.eea.europa.eu/publications/annual-report-2011> (11.09.15)
- Elken, J., Raudsepp, U., Lips, U. 2003. On the estuarine transport reversal in deep layers of the Gulf of Finland. *Journal of Sea Research*, 49 (4), 267-274.
- Fauchot, J., Lévassieur, M., Roy, S. 2005. Daytime and nighttime vertical migrations of *Alexandrium tamarense* in the St. Lawrence estuary (Canada). *Marine Ecology Progress Series*, 296, 241-250.
- Fennel, K., Boss, E. 2003. Subsurface maxima of phytoplankton and chlorophyll: Steady-state solutions from a simple model. *Limnology and Oceanography*, 48 (4), 1521-1534.
- Fennel, W., Neumann, T. 1996. The meso-scale variability of nutrients and plankton as seen in a coupled model. *German Journal of Hydrography*, 48, 49-71.
- Fennel, W., Seifert, T. 2008. Oceanographic processes in the Baltic Sea. *Die Küste*, 74, 77-91.
- Finni, T., Kononen, K., Olsonen, R., Wallström, K. 2001. The history of cyanobacterial blooms in the Baltic Sea. *AMBIO*, 30, 172-178.

- Fleming, V., Kaitala, S. 2006. Phytoplankton spring bloom intensity index for the Baltic Sea estimated for the years 1992 to 2004. *Hydrobiologia*, 554, 57–65.
- Gentien, P., Donaghay, P.L., Yamazaki, H., Raine, R., Reguera, B., Osborn, T.R. 2005. Harmful algal blooms in stratified environments. *Oceanography*, 18, 172-183.
- Gran, V., Pitkanen, H. 1999. Denitrification in estuarine sediments in the eastern Gulf of Finland, Baltic Sea. *Hydrobiologia*, 393, 107-115.
- Haapala, J. 1994. Upwelling and its influence on nutrient concentration in the coastal area of the Hanko Peninsula, entrance to the Gulf of Finland. *Estuarine Coastal Shelf Science*, 38, 507-521.
- Hales, B., Hebert, D., Marra, J. 2009. Turbulent supply of nutrients to phytoplankton at the New England shelf break front. *Journal of Geophysical Research*, 114, C05010.doi:10.1029/2008JC005011.
- Hall, N.S., Paerl, H.W. 2011. Vertical migration patterns of phytoflagellates in relation to light and nutrient availability in shallow microtidal estuary. *Marine Ecology Progress Series*, 425, 1-19.
- Heiskanen, A.-S. 1998. Factors governing sedimentation and pelagic nutrient cycles in the northern Baltic Sea. *Monographs of the Boreal Environment Research*, 8, 50-67. Helsinki.
- www.helcom.fi/baltic-sea-action-plan (13.09.15)
- HELCOM, 2004. The Fourth Baltic Sea Pollution Load Compilation (PLC-4). *Baltic Sea Environment Proceedings*, 93, 1-188.
- HELCOM, 2011. Fifth Baltic Sea Pollution Load Compilation (PLC-5). *Baltic Sea Environment Proceedings*, 128, 1-217.
- HELCOM, 2014. Eutrophication status of the Baltic Sea 2007-2011 - A concise thematic assessment. *Baltic Sea Environment Proceedings*, 143, 1-41.
- Horstmann, U. 1983. Distribution patterns of temperature and water colour in the Baltic Sea as recorded in the satellite images: indications for phytoplankton growth. *Berichte Inst. Meereskunde, Univ. Kiel* 106.
- Ishizaka, J., Takahashi, M., Ichimura, S. 1983. Evaluation of coastal upwelling effects on phytoplankton growth by simulated culture experiments. *Marine Biology*, 76, 271-278.
- Jephson, T., Carlsson, P. 2009. Species- and stratification- dependent diel vertical migration behaviour of three dinoflagellate species in a laboratory study. *Journal of Plankton Research*, 31, 1353-1362.
- Kahru, M., Aitsam, A., Elken, J. 1982. Spatio-temporal dynamics of chlorophyll in the open Baltic Sea. *Journal of Plankton Research*, 4, 779-790.
- Kahru, M., Nömmann, S. 1990. The phytoplankton spring blooms in 1985, 1986: multitude of spatio-temporal scales. *Continental Shelf Research*, 10, 329-354.
- Kahru, M., Savchuk, O.P., Elmgren, R. 2007. Satellite measurements of cyanobacterial bloom frequency in the Baltic Sea: interannual and spatial variability. *Marine Ecology Progress Series*, 343, 15-23.

- Kanoshina, I., Lips, U., Leppänen, J.-M., 2003. The influence of weather conditions (temperature and wind) on cyanobacterial bloom development in the Gulf of Finland (Baltic Sea). *Harmful Algae*, 2, 29-41.
- Kelly-Gerrey, B. A., Qurban, M. A., Hydes, D. J., Miller, P. I., Fernand, L. 2004. Coupled FerryBox Ship of Opportunity and satellite data observations of plankton succession across the European Shelf Sea and Atlantic Ocean. ICES Council Meeting Papers.
- Klausmeier, A., Litchmann, E. 2001. Algal games: the vertical distribution of phytoplankton in poorly mixed water columns. *Limnology and Oceanography*, 46, 1998-2007.
- Kononen, K., Kuparinen, J., Mäkela, K., Laanemets, J., Pavelson, J., Nömmann, S. 1996. Initiation of cyanobacterial blooms in a frontal region at the entrance of the Gulf of Finland, Baltic Sea. *Limnology and Oceanography*, 43, 1089-1106.
- Kononen, K., Leppänen, J.-M. Patchiness, scales and controlling mechanisms of cyanobacterial blooms in the Baltic Sea: Application of a multiscale research strategy. 1997. In *Monitoring Algal Blooms*, edited by M. Kahru and C. W. Brown, Springer-Verlag, Berlin, 63-84.
- Kononen, K., Hällfors, S., Kokkonen, M., Kuosa, H., Laanemets, J., Pavelson, J., Autio, R. 1998. Development of a subsurface chlorophyll maximum at the entrance to the Gulf of Finland, Baltic Sea. *Limnology and Oceanography*, 43, 1089-1106.
- Kononen, K., Huttunen, M., Hällfors, S., Gentien, P., Lunven, M., Huttula, T., Laanemets, J., Lilover, M., Pavelson, J., Stips, A. 2003. Development of a deep chlorophyll maximum of *Heterocapsa triquetra* Ehrenb. at the entrance to the Gulf of Finland. *Limnology and Oceanography*, 48, 594-607.
- Kuosa, H. 1990. Subsurface chlorophyll maximum in the northern Baltic Sea. *Archiv für Hydrobiologie*, 118, 437-447.
- Laanemets, J., Kononen, K., Pavelson, J., Poutanen, E. L. 2004. Vertical location of seasonal nutriclines in the western Gulf of Finland. *Journal of Marine Systems*, 52, 1-13.
- Laanemets, J., Zhurbas, V., Elken, J., Vahtera, E. 2009. Dependence of upwelling mediated nutrient transport on wind forcing, bottom topography and stratification in the Gulf of Finland: model experiments. *Boreal Environment Research*, 14, 213-225.
- Laanemets, J., Väli, G., Zhurbas, V., Elken, J., Lips, I., Lips, U. 2011. Simulation of meso-scale structures and nutrient transport during summer upwelling events in the Gulf of Finland in 2006. *Boreal Environment Research*, 16(A), 15-26.
- Lehtoranta, J., Pitkänen, H., Sandman, O. 1997. Sediment accumulation of nutrients (N, P) in the eastern Gulf of Finland (Baltic Sea). *Water Air Soil Pollution*, 99, 477-486.
- Leppäranta, M., Myrberg, K. 2009. *Physical Oceanography of the Baltic Sea*. Springer-Praxis, Heidelberg, 378 pp.

- Liblik, T., Lips, U. 2011. Characteristics and variability of the vertical thermohaline structure in the Gulf of Finland in summer. *Boreal Environmental Research*, 16 (A), 73-83.
- Liblik, T. 2012. Variability of Thermohaline Structure in the Gulf of Finland in Summer. Thesis on natural and exact sciences B127. 159pp.
- Lips, I. 2005. Abiotic factors controlling the cyanobacterial bloom occurrence in the Gulf of Finland. *Dissertationes Biologicae Universitatis Tartuensis*, 108, 49pp.
- Lips, I., Lips, U., Kononen, K., Jaanus, A. 2005. The effect of hydrodynamics on the phytoplankton primary production and species composition at the entrance to the Gulf of Finland (Baltic Sea) in July 1996. *Estonian Academy of Science Biology Ecology*, 54, 3, 210-229.
- Lips, I., Lips, U. 2008. Abiotic factors influencing cyanobacterial bloom development in the Gulf of Finland (Baltic Sea). 2008. *Hydrobiologia*, 614, 133-140.
- Lips, I., Lips, U., Liblik, T. 2009. Consequences of coastal upwelling events on physical and chemical patterns in the central Gulf of Finland (Baltic Sea). *Continental Shelf Research*, 29, 1836-1847.
- Lips, I., Lips, U. 2010. Phytoplankton dynamics affected by the coastal upwelling events in the Gulf of Finland in July-August 2006. *Journal of Plankton Research*, 32, 1269-1282.
- Lips, I., Rünk, N., Kikas, V., Meerits, A., Lips, U. 2014. High-resolution dynamics of the spring bloom in the Gulf of Finland of the Baltic Sea. *Journal on Marine Systems*, 129, 135-149.
- Lips, U., Lips, I., Liblik, T., Elken, J. 2008. Estuarine transport versus vertical movement and mixing of water masses in the Gulf of Finland (Baltic Sea). US/EU-Baltic Symposium "Ocean Observations, Ecosystem-Based Management & Forecasting", Tallinn, 27-29 May, 2008. IEEE, 2008, (IEEE Conference Proceedings), 1-8.
- Lips, U., Lips, I. 2014. Bimodal distribution patterns of motile phytoplankton in relation to physical processes and stratification (Gulf of Finland, Baltic Sea). *Deep-Sea Research Part II: Topical Studies in Oceanography*, 101, 107-119.
- Lund-Hansen, L.C., Ayala, P.C.A., Reglero, A.F. 2006. Bio-optical properties and development of a sub-surface chlorophyll maxima (SCM) in south-west Kattegat, Baltic Sea. *Estuarine Coastal and Shelf Science*, 68, 372-378.
- Mann, K. H. 2000. Ecology of coastal waters: with implications for management. Second edition. Blackwell Science, Inc. 406 p.
- MacIsaac, J.J., Dugdale, R.C., Barber, R.T., Blasco, D., Packard, T.T. 1985. Primary production cycle in an upwelling center. *Deep-Sea Research*, 32, 503-529.
- McManus, M.A., Alldredge, A.L., Barnard, A., Boss, E., Case, J., Cowles, T.J., Donaghay, P.L., Eisner, L., Gifford, D.J., Greenlaw, C.F., Herren, C., Holliday, D.V., Johnson, D., MacIntyre, S., McGehee, D., Osborn, T.R., Perry, M.J., Pieper, R., Rines, J.E.B., Smith, D.C., Sullivan, J.M., Talbot, M.K., Twardowski, M.S., Weidemann, A., Zaneveld, J.R.V. 2003.

- Characteristics, distribution and persistence of thin layers over a 48 hours period. *Marine Ecology Progress Series*, 261, 1-19.
- Myrberg, K., Andrejev, O. 2003. Main upwelling regions in the Baltic Sea - a statistical analysis based on three-dimensional modelling. *Boreal Environmental Research*, 8(2), 97-112.
- Omstedt, A., Humborg, C., Pempkowiak, J., Pertillä, M., Rutgersson, A., Schneider, B., Smith, B. 2014. Biogeochemical control of the coupled CO₂-O₂ system of the Baltic Sea: a review of the results of Baltic-C. *AMBIO*, 43, 49-59.
- Paasche, E., Bryceson, I., Tangen, K. 1984. Interspecific variation in dark nitrogen uptake by dinoflagellates. *Journal of Phycology*, 20, 394-401.
- Pavelson, J., Kononen, K., Laanemets, J. 1999. Chlorophyll distribution patchiness caused by hydrodynamical processes: a case study in the Baltic Sea. *ICES Journal of Marine Science*, 56, 87-99.
- Pulliainen, J., Vepsäläinen, J., Kaitala, S., Hallikainen, M., Kallio, K., Fleming, V., Maunula, P. 2004. Regional water quality mapping through the assimilation of spaceborne remote sensing data to ship-based transect observations. *Journal of Geophysical Research*, 109, C12009, doi:10.1029/2003JC002167.
- Rantajärvi, E., Leppanen, J.-M. 1994. Unattended algal monitoring on merchant ships in the Baltic Sea. *TemaNord*, 546, 60 pp.
- Redfield, A.C., Ketchum, B.H., Richards, F.A. 1963. The influence of organisms on the composition of sea-water. In M.N. Hill ed.: *The Sea*. Vol.2, pp.554. John Wiley & Sons, New York.
- Siegel, D.A., Maritorena, S., Nelson, N.B., Behrenfeld, M.J. 2005. Independence and interdependencies of global ocean color properties; Reassessing the bio-optical assumption. *Journal of Geophysical Research*, 110, C07011, doi:10.1029/2004JC002527.
- Sharpley, J., Moore, C.M., Rippeth, T.P., Holligan, P.M., Hydes, D.J., Fisher, N.R., Simpson, J.H. 2001. Phytoplankton distribution and survival in the thermocline. *Limnology and Oceanography*, 46, 486-496.
- Schneider, B., Kaitala, S., Maunula, P. 2006. Identification and quantification of plankton bloom events in the Baltic Sea by continuous pCO₂ and chlorophyll *a* measurements. *Journal of Marine Systems*, 59, 238-248.
- Smayda, T. J. 2010. Adaptation and selection of harmful and other dinoflagellate species in upwelling system. Motility and migratory behaviour. *Progress in Oceanography*, 85, 71-91.
- Soomere, T., Keevallik, S. 2003. Directional and extreme wind properties in the Gulf of Finland. *Proceedings of the Estonian Academy of Science, Engineering*, 9, 73-90.
- Uiboupin, R., Laanemets, J. 2009. Upwelling characteristics derived from satellite sea surface temperature data in the Gulf of Finland, Baltic Sea. *Boreal Environmental Research*, 14, 297-304.
- Vahtera, E., Laanemets, J., Pavelson, J., Huttonen, M., Kononen, K. 2005. Effect of upwelling on the pelagic environment and bloom-forming cyanobacteria in

- the western Gulf of Finland, Baltic Sea. *Journal of Marine Systems*, 58, 67-82.
- Vahtera, E., Conley, D.J., Gustafsson, B.G., Kuosa, H., Pitkänen, H., Savchuk, O.P., Tamminen, T., Viitasalo, M. 2007. Internal ecosystem feedbacks enhance nitrogen-fixing cyanobacteria blooms and complicate management in the Baltic Sea. *AMBIO*, 36, 186-194.
- Weston, K., Fernand, L., Mills, D.K., Delahunty, R., Brown, J. 2005. Primary production in the deep chlorophyll maximum of the central North Sea. *Journal of Plankton Research*, 27, 909-922.
- Yang, X., Wu, X., Hao, H., He, Z. 2008. Mechanisms and assessment of water eutrophication. *Journal of Zhejiang University Science B. Mar*, 9(3), 197-209.

PUBLICATIONS

Paper I

Kuvaldina, N., Lips, I., Lips, U., Liblik, T. (2010). The influence of a coastal upwelling event on chlorophyll *a* and nutrient dynamics in the surface layer of the Gulf of Finland, Baltic Sea. *Hydrobiologia*, 639(1), 221 - 230.

The influence of a coastal upwelling event on chlorophyll *a* and nutrient dynamics in the surface layer of the Gulf of Finland, Baltic Sea

Natalja Kuvaldina · Inga Lips · Urmas Lips ·
Taavi Liblik

Published online: 13 December 2009
© Springer Science+Business Media B.V. 2009

Abstract Temporal variation and distribution of chlorophyll *a* and nutrients concentration was evaluated on the basis of field observations in August 2006 in the Gulf of Finland. Strong easterly winds in August 2006 generated an upwelling event along the Estonian coast of the Gulf of Finland. It caused a drop of the water-surface temperature and nutrient enrichment of the upper layer. At first, the chlorophyll *a* declined in the area affected by the upwelled water due to the strong advective transport of the chlorophyll *a* rich waters towards the northern coast and due to the intensive water mixing and low seed population in the upwelling waters. After stabilization of the upwelling, nutrients from the upper mixed layer were consumed fast: there were no nitrites + nitrates left one week later, and phosphate concentration was under the detection limit 2 weeks later. The smaller phytoplankton size fraction showed faster response to the upwelled nutrients compared with the bigger size fraction, showing the increase in

chlorophyll *a* content already during the stabilization of the upwelling. The increase in chlorophyll *a* concentration in >20- μ m size fraction at stations influenced by upwelling was observed only after the relaxation of the upwelling and formation of stratification.

Keywords Upwelling · Nutrients · Chlorophyll *a* · Gulf of Finland · Baltic Sea

Introduction

The availability of nitrogen and phosphorus is one of the factors regulating phytoplankton growth (Hecky & Kilham, 1988). The nutrient balance of the Gulf of Finland is governed by inputs from the catchment area, exchange between the Gulf and the Baltic Proper, as well as exchange between sea bed sediments and the water column (Pitkänen et al., 2001). There is a seasonal difference in the upper layer inorganic nutrient concentration in the Gulf of Finland: maximum values are observed in winter and minimum in summer. The summer period is characterized by the development of a strong thermocline which prevents mixing between the nutrient depleted upper layer and the nutrient-rich lower layers. Wind-induced vertical mixing and upwelling are important processes during this period in bringing nutrient-rich waters from deeper layers to the surface (Haapala, 1994; Lilover et al., 2003).

Guest editors: T. Zohary, J. Padisák & L. Naselli-Flores /
Phytoplankton in the Physical Environment: Papers from the
15th Workshop of the International Association for
Phytoplankton Taxonomy and Ecology (IAP), held at the
Ramot Holiday Resort on the Golan Heights, Israel, 23–30
November 2008

N. Kuvaldina (✉) · I. Lips · U. Lips · T. Liblik
Marine Systems Institute, Tallinn University of
Technology, Akadeemia Rd. 21B, 12618 Tallinn, Estonia
e-mail: natalja.kuvaldina@phys.sea.ee

In the world's oceans equator-ward winds along their eastern boundaries drive offshore surface Ekman transport and the upwelling of cold, nutrient-rich water into the euphotic zone, stimulating high phytoplankton production near the coast (Pauly & Christensen, 1995). Examples of such quasi-persistent phenomena include the California Current, the Humboldt Current, the Benguela Current and the Canary Current. Wind-induced coastal upwellings can also be temporary events forced by variable winds with time scales from a few days to a week. The consequences for the biota in such rapidly fluctuating regions are likely to be different to consequences of quasi-persistent upwelling systems, where more time is available for plankton blooms to develop transported persistently offshore. In a short-period oscillating system, the plankton community may not be moved far before being brought back again into the coastal area (Schumann, 1999). Also in short-period oscillating systems, the response of small- and bigger-sized phytoplankton community differs from the response in the major upwelling areas of the world (Wilkerson et al., 2006). Owing to the prevailing south-westerly winds, time variable upwelling events are relatively frequent along the northern coast of the Gulf of Finland (Myrberg & Andrejev, 2003). However, the high variability of atmospheric forcing in the Baltic region could often generate a series of variable, coupled upwelling–downwelling events in the elongated Gulf of Finland (Talpepp, 2008).

There have only been a small number of direct field observations of coastal upwellings in the Gulf of Finland (e.g. Kononen & Niemi, 1986; Haapala, 1994). The influence of such upwelling events on the phytoplankton growth and distribution were investigated 20 years ago under different nutrient limitation situation (phosphorus was suggested to be the limiting nutrient; Talpepp et al., 1994). In later investigations, the impacts on the phytoplankton growth, distribution and community composition were analysed mainly in relation to the temperature variations and horizontal advection associated with the upwelling events (e.g. Kanoshina et al., 2003). Chemical parameters have been included in the analysis only on a short term—during the upwelling and few days after (Vahtera et al., 2005). Longer term impacts of upwelling events on the nutrient content in the upper layer are based on modelling exercises (Zhurbas et al., 2008). The influence of the upwelled inorganic nutrients on

phytoplankton growth during and after the upwelling events have not been measured directly in the field, because there are only short periods, in which the wind conditions are favourable for development of upwelling events, and it is difficult to maintain the necessary readiness to take advantage of such wind conditions when they occur.

The objective of the present article is to describe the temporal variation and spatial distribution of nutrient concentrations and evaluate the consequent adjustment of phytoplankton expressed as chlorophyll *a* content on the basis of field observations before, during and after the major upwelling event in late summer 2006 in the Gulf of Finland (Baltic Sea).

Materials and methods

Weekly mappings of hydrographical, -chemical and -biological fields were done across the Gulf of Finland between Tallinn and Helsinki during the period in July–August 2006 (11 July, 19–20 July, 25 July, 8 August, 15–16 August, 22 August and 29 August). Vertical profiles of temperature, salinity and chlorophyll *a* fluorescence were recorded at 27 stations. Distance between stations was 2.6 km. Measurements were carried out using a NBIS Mark III CTD (conductivity, temperature and depth) probe and Seabird CTD probe (SBE 19) equipped with a Wetstar fluorimeter. Salinity data quality was checked on the basis of water sample analyses by a high precision salinometer AUTOSAL (Guildline).

Water samples for chemical analyses (PO_4^{3-} , $\text{NO}_2^- + \text{NO}_3^-$) were collected at 14 stations (every second station, distance between stations 5.2 km; except on 19–20 July when sampling was made only at the northernmost stations TH19-27). A rosette with 8 Niskin water samplers (volume 1.7 l) was used for sampling. Analyses were made from the pooled samples to represent the upper mixed layer (UML). The samples were prepared at all stations by pooling three water samples taken at different depths from the surface down to the seasonal thermocline, the depth of which was determined from the CTD casts. Nutrient analyses were carried out according to the guidelines of American Public Health Association (APHA, 1992), methods 4500-NO3 F and 4500-P F. Samples for phosphates (PO_4^{3-}) were mostly analysed immediately after sampling onboard research

vessel ‘Kake’, and samples for dissolved inorganic nitrogen compounds ($\text{NO}_2^- + \text{NO}_3^-$) determination were deep-frozen after collection and analysed later in the laboratory. Phosphates and nitrites + nitrates were analysed using automatic nutrient analyser $\mu\text{Mac 1000}$ (Systea S.r.l.). The lower detection range for phosphate-phosphorus and nitrate + nitrite-nitrogen was 2 ppb (corresponds to 0.06 and 0.14 $\mu\text{mol l}^{-1}$, respectively).

The pooled water samples from the UML, prepared as described above, were analysed for chlorophyll *a* (Chl *a*) content in two size fractions—the separation of the $>20\text{-}\mu\text{m}$ size fraction was made to assess the growth of filamentous cyanobacteria, bigger dinoflagellates (e.g. *Heterocapsa triquetra*, *Dinophysis* spp.) and photosynthetic ciliates (*Mesodinium rubrum*). The size fractionated chlorophyll *a* was achieved by pouring the pooled sample through a $20\text{-}\mu\text{m}$ mesh. The Chl *a* concentration in the pooled sample (total Chl *a* concentration) and in the $<20\text{-}\mu\text{m}$ size fraction were determined on Millipore APFF glass-fibre filters following the extraction at the room temperature in dark with 96% ethanol for 24 h. Chlorophyll *a* content

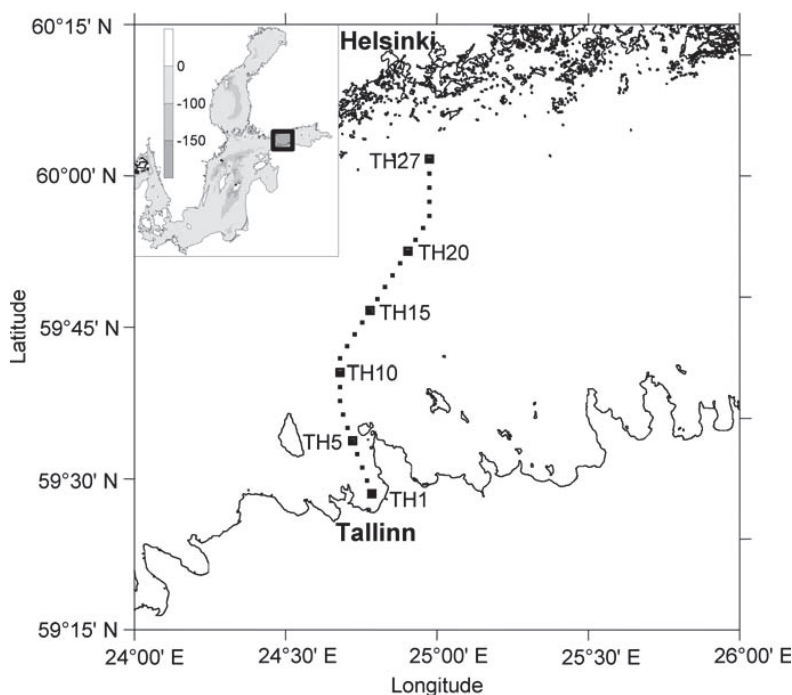
from the extract was measured spectrophotometrically (Thermo Helios γ ; photometric accuracy: $\pm 0.005 \text{ A}$ at 1 A) in laboratory (HELCOM, 1988). In order to obtain the Chl *a* concentration in $>20\text{-}\mu\text{m}$ size fraction the concentrations of $<20\text{-}\mu\text{m}$ size fraction were subtracted from the total concentration.

Additional water samples for Chl *a* analyses were collected at each station from different depths to validate the fluorescence measurements conducted using SBE 19 equipped with Wetstar fluorimeter. In total 85 Chl *a* values were obtained and used to get a calibration line for converting measured fluorescence (FI) values to Chl *a*. One calibration line Chl *a* = $0.50 \times \text{FI} + 1.71$ ($r^2 = 0.49$; $P < 0.01$) for the whole data set was used. All fluorescence measurements described in this article were made during daylight hours (Fig. 1).

Results

At the end of July, the vertical temperature and salinity distribution was characteristic for the summer

Fig. 1 The map of the study area in the Gulf of Finland and the locations of sampling stations (TH1–TH27)



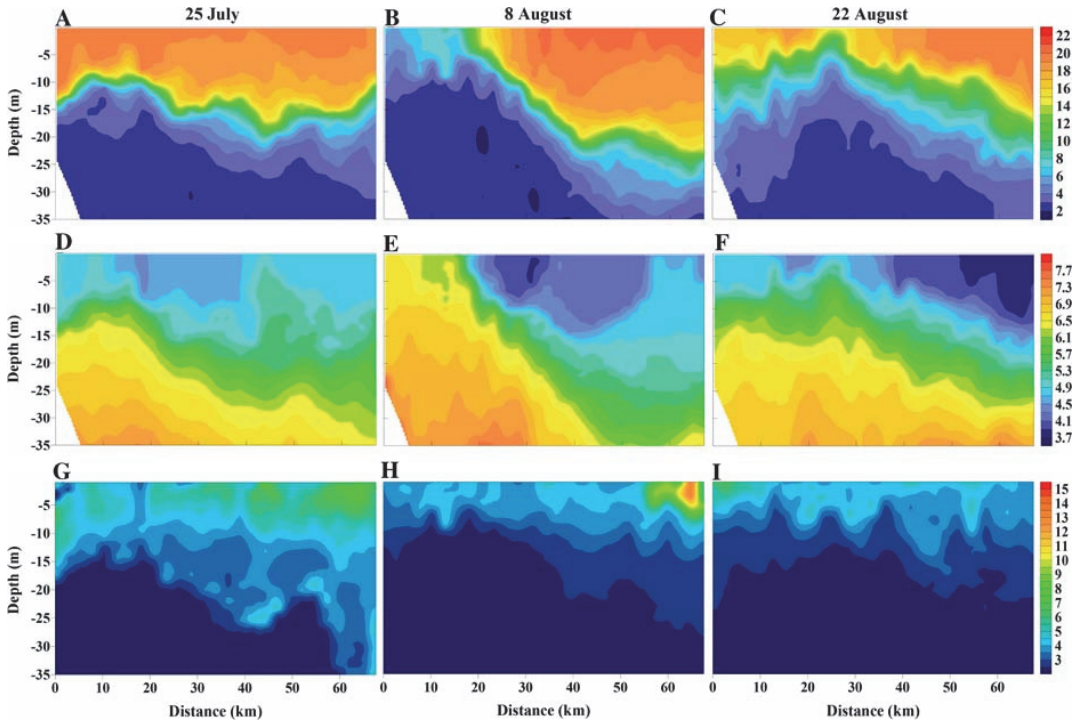


Fig. 2 Vertical section of temperature ($^{\circ}\text{C}$; **A–C**), salinity (‰ **D–F**) and chlorophyll *a* (mg m^{-3} ; **G–I**) on 25th July, 8th and 22nd August 2006. On the *x*-axis distance is shown in kilometers starting from the first (TH1) station

period in this region of the Baltic Sea. The thermocline was mostly situated at depths of 10–20 m (Fig. 2A). A nearly linear downward increase of salinity (Fig. 2D) in the thermocline strengthened the stratification. The thermocline was narrower in the southern part and wider in the northern part of the cross-section. Water temperature in the upper 10 m layer was between 15 and 21 $^{\circ}\text{C}$. At the beginning of August, after the development of an upwelling along the southern coast of the Gulf of Finland (close to the Estonian coast), low temperature values were recorded in the surface waters of the southern part of the cross-section (down to 5 $^{\circ}\text{C}$; Fig. 2B). The cold water covered about 1/3 of the cross-section during the upwelling event. Higher surface water temperatures, with maximum of 21 $^{\circ}\text{C}$, and downward shifted thermocline were observed in the central and northern part of the Gulf (Fig. 2B). Two weeks later the upwelling vanished. At this time, a narrower warm surface layer (temperatures between 15 and 19 $^{\circ}\text{C}$ and depth between 3 and 12.5 m) together with wider

thermocline compared with pre-upwelling time had been formed (Fig. 2C).

Salinity distribution in the UML along the measured transect was quite even at the end of July (Fig. 2D). An increase in salinity from 4.6–4.8 ‰ to 6.2–6.4 ‰ near the southern coast was measured during the upwelling event on 8th August 2006 (Fig. 2E) and low salinity surface water mass was observed in the second half of August in the northern part of the cross-section (Fig. 2F) after the relaxation of the upwelling.

Chlorophyll *a* values obtained by converting fluorescence data using the found calibration equation showed concentrations near the surface of up to 6.5 mg m^{-3} in the northern part of the Gulf on 25th July (Fig. 2G). There were some patches of subsurface Chl *a* maxima observed in the lower part of the thermocline before the upwelling event. During the upwelling, the Chl *a* concentrations in the upwelled colder water were below 2 mg m^{-3} and at the same time, high Chl *a* concentrations (average 13 mg m^{-3})

were measured near the northern coast (Fig. 2H). By 22nd August, after the relaxation of observed upwelling, the Chl *a* concentrations in the upper layer were more or less evenly distributed along the cross-section, and were in the same range, with concentrations measured before the upwelling event (Fig. 2I).

At the beginning of the study, the UML was depleted of both nitrites + nitrates and dissolved inorganic phosphorus (DIP; Fig. 3), and nutriclines were located just below or in the lower part of the thermocline (Lips et al., 2009; Fig. 5a, b). During the upwelling event (measurements on 8th August), high nutrient concentrations were measured in the upwelling region—0.7 and 0.4 $\mu\text{mol l}^{-1}$ for nitrites + nitrates and DIP, respectively. By 15th August all nitrites + nitrates were depleted from the surface layer (Fig. 3A), while there was still DIP left (Fig. 3B). On 22nd August, both nitrites + nitrates and DIP concentrations in the UML were below the lower detection range. The higher DIP values in the southern part of the Gulf on 29th August are due to the development of a next upwelling event.

Total Chl *a* concentrations measured in the pooled samples from the UML in July before the upwelling

event were between 3.4 and 7.1 mg m^{-3} (Fig. 4A). On 11th and 19th July higher values of Chl *a* were measured in the southern and central part of the cross-section, while lower values were detected in the northern part. The distribution of Chl *a* concentration measured at the end of July was opposite to the previous period—higher concentrations were measured at the northern part of the cross-section. Chlorophyll *a* was found mainly in the $<20\text{-}\mu\text{m}$ size fraction before the upwelling (between 2.3 and 4.9 mg m^{-3} on 11th July and between 3.3 and 4.7 mg m^{-3} on 25th July; Fig. 4C) forming a slightly higher (84% of total) portion on 25th July in the seven southernmost stations compared with concentrations on 11th July at the same region (71% of total). The highest concentrations of the $>20\text{-}\mu\text{m}$ fraction before the upwelling were measured on 11th July at stations TH1 and TH3 (2.9 and 2.8 mg m^{-3} , respectively; distance 0–5.2 km on Fig. 4B) forming 40% of the total Chl *a* concentration.

During the upwelling, the total Chl *a* concentrations in the UML along the cross-section changed considerably (1.6–15.5 mg m^{-3} ; Fig. 4A). It remained below 2 mg m^{-3} in the area affected by the upwelling (stations TH1–TH7, distance 0–15.6 km) and

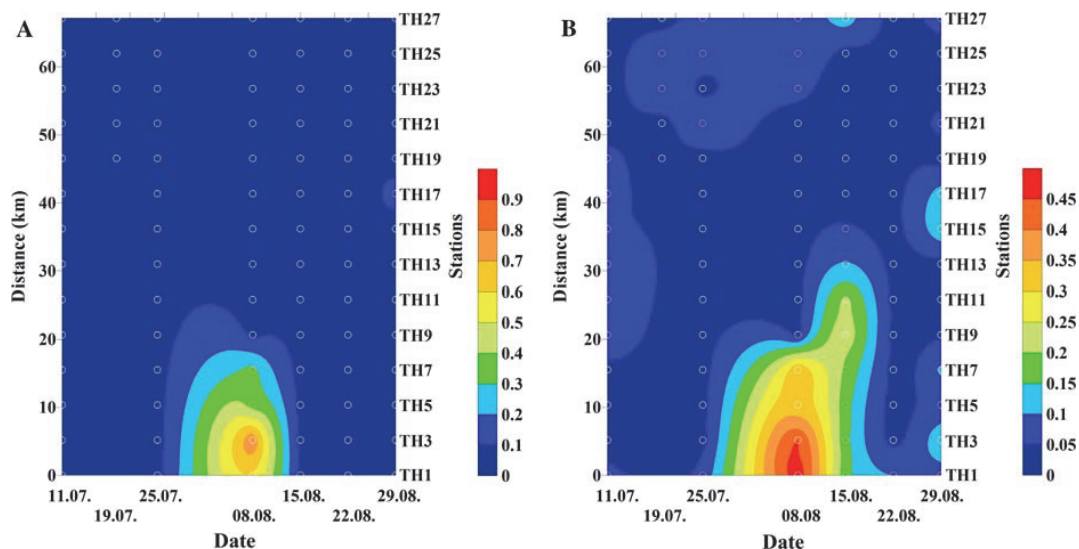


Fig. 3 Horizontal distribution of dissolved inorganic nitrogen compounds (**A**; $\text{NO}_2^- + \text{NO}_3^-$; $\mu\text{mol l}^{-1}$) and dissolved inorganic phosphorus (**B**; $\mu\text{mol l}^{-1}$) in the upper mixed layer during the study period in July–August 2006. On the *x*-axis

dates of the study are shown, and on the *y*-axis distance from the first (TH1) station is shown in kilometers. Circles on the map indicate sampling points

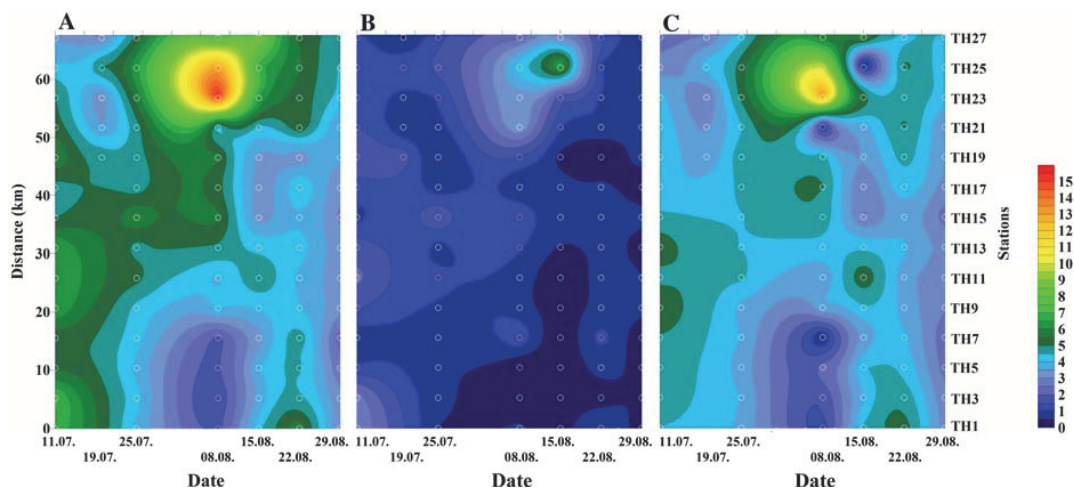


Fig. 4 Horizontal distribution of total chlorophyll *a* concentration (mg m^{-3} ; **A**), chlorophyll *a* in $>20 \mu\text{m}$ size fraction (**B**) and chlorophyll *a* in $<20 \mu\text{m}$ size fraction (**C**) in the upper mixed layer during the study period in July–August 2006. On

the *x*-axis dates of the study are shown, and on the *y*-axis distance from the first (TH1) station is shown in kilometers. Circles on the map indicate sampling points

showing the highest values at the northern end of the cross-section (Fig. 4A). The Chl *a* concentrations in the $>20\text{-}\mu\text{m}$ size fraction in the upwelling water were very low ($0.02\text{--}0.6 \text{ mg m}^{-3}$) and still low, but on average 2.5 times higher in the central part of the cross-section ($0.7\text{--}1.5 \text{ mg m}^{-3}$; Fig. 4B). Even the total concentration of Chl *a* was low in the area affected by upwelling, the proportion of $>20\text{-}\mu\text{m}$ size fraction was surprisingly high at station TH7 (80%) when compared with the average contribution of this size fraction to the total value (31%; contribution range between 1 and 80%) in the upwelling region.

After the stabilization of the upwelling on 15–16th August, the total Chl *a* values near the southern coast (stations TH1–TH7, distance 0–15.6 km from the southern coast) reached to the same level compared with the pre-upwelling concentrations ($3.3\text{--}4.4 \text{ mg m}^{-3}$; Fig. 4A). On average only 3% of total Chl *a* concentration was formed by $>20\text{-}\mu\text{m}$ size fraction ($0\text{--}0.3 \text{ mg m}^{-3}$). In the central part of the cross-section (stations TH9–TH19, distance 20.8–46.8 km), the total Chl *a* concentrations were in the similar range ($3.3\text{--}4.9 \text{ mg m}^{-3}$), but the contribution of the $>20\text{-}\mu\text{m}$ size fraction to the total (Fig. 4A, B) was higher (on average 12% of the total concentration compared with the 3% at stations TH1–TH7) and a noticeable rising gradient towards north

was detected (values between 0 and 1.1 mg m^{-3}). At the northern end of the cross-section, the total Chl *a* values were between 4.5 and 8.5 mg m^{-3} of which on average 28% was formed by the $>20\text{-}\mu\text{m}$ size fraction.

On 22nd August, the highest values ($4.6\text{--}5.9 \text{ mg m}^{-3}$) of total Chl *a* during the whole study period in July–August were measured at stations TH1–TH7. The northern part of the cross-section (stations TH21–TH27) was characterized with more or less even and slightly higher total Chl *a* concentrations ($5.3\text{--}5.6 \text{ mg m}^{-3}$) compared with more patchy central part (stations TH9–TH19; $3.9\text{--}4.6 \text{ mg m}^{-3}$). The contribution of $>20\text{-}\mu\text{m}$ size fraction to the total concentration was low ($0.2\text{--}1.5 \text{ mg m}^{-3}$) forming on average 16, 18 and 20% of the total Chl *a* concentration at southern, central and northern part, respectively, on that day.

The 29th August is characterized by lowest total Chl *a* concentrations ($2.2\text{--}4.8 \text{ mg m}^{-3}$) during the measurements period. A continuous increase in concentrations towards north due to the development of a next upwelling event along the southern coast of Gulf of Finland was observed, but the contribution of bigger size class was the lowest for the entire study period (on average 12% of the total with concentrations below 1 mg m^{-3}).

There was a clear difference in the growth response to the upwelled nutrients and stabilization of water column observed in smaller and bigger size fractions. The Chl *a* concentration in smaller size fraction increased already during the stabilization of observed upwelling on 15th August (Fig. 5b), while the increase in bigger size fraction was observed after the relaxation of upwelling on 22nd August (Fig. 5a). At the same time, the temporal variations of Chl *a* concentrations in the smaller and bigger size fractions were similar to each other in the northernmost part of the cross-section (Fig. 5c, d). The highest Chl *a* concentration was observed on 8th August, when a coupled downwelling was developed near the northern coast.

Discussion

Coastal upwellings, induced by persistent or time variable winds, bring nutrient-rich water up into the euphotic zone, and thus are frequently associated with increased biological productivity (e.g. MacIsaac et al., 1985; Cushing, 1989). The effect of time-variable upwelling on summer phytoplankton in the Baltic Sea depends on the duration of the upwelling/relaxation cycle, the phytoplankton species composition before the upwelling both in the upper layer and in the thermocline, and the nutrient ratios and temperature of the upwelled water. During the coastal upwelling described in the present article, the consecutive surface temperature and salinity values

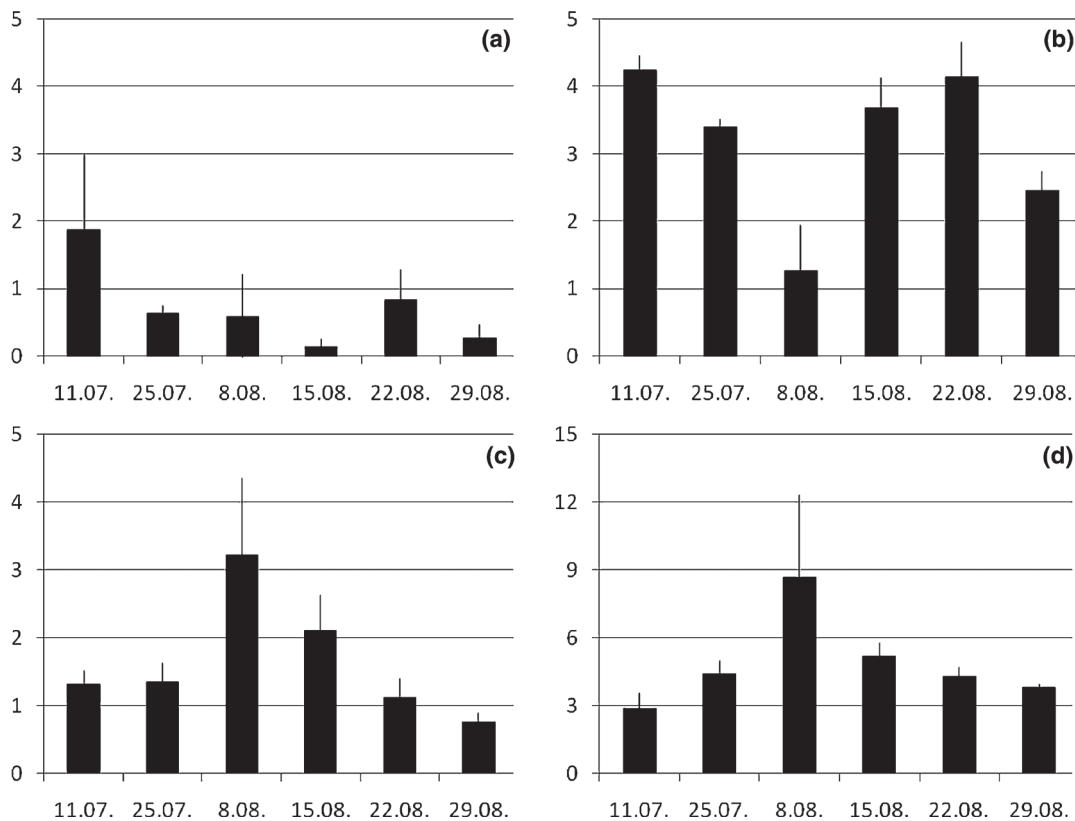


Fig. 5 Average concentrations and standard deviations of chlorophyll *a* (mg m⁻³) in >20-µm size fraction at stations TH1–TH7 (a) and TH21–TH27 (c), and average concentrations

and standard deviations of chlorophyll *a* in <20-µm size fraction at stations TH1–TH7 (b) and TH21–TH27 (d; note the different scale) during the study period in summer 2006

as well as concentrations of dissolved inorganic nutrients and phytoplankton chlorophyll *a* revealed large changes in only a few weeks. Answers to the key question on the consequences of an upwelling event seem to depend on the temporal and spatial scales of the processes involved.

According to Myrberg (1998), the overall horizontal distribution of the surface water temperature in the Gulf of Finland during summer is usually quite homogeneous. In July 2006, before the upwelling event, a warm surface layer (around 20°C) was observed along the whole cross-section (Fig. 2A). During the upwelling, strong horizontal gradients developed (Fig. 2B), while quite homogeneous temperature distribution along the cross-section was measured again 2 weeks later (Fig. 2C). It has been shown in earlier studies (Haapala, 1994; Alenius et al., 1998) that the surface-layer water temperature may drop more than 10°C within hours and nutrient concentrations may increase markedly during coastal upwellings in the Gulf of Finland. During this study, the surface-layer temperature dropped from 20°C to 5–11°C (Fig. 2A, B). At the same time, the concentrations of inorganic nutrients increased remarkably: before the upwelling the concentrations of phosphates (DIP) and nitrites + nitrates in the surface layer were below the lower detection range, while during the upwelling the values as high as 0.3–0.8 $\mu\text{mol l}^{-1}$ for nitrites + nitrates (Fig. 3A) and 0.3–0.5 $\mu\text{mol l}^{-1}$ for DIP (Fig. 3B) were measured.

The response of phytoplankton growth to the observed meso-scale processes is described on the basis on Chl *a* data. Phytoplankton Chl *a* in the investigation area was strongly influenced by the observed upwelling event and circulation pattern by two means: new nutrient input enhancing growth and by passive advection/accumulation of the existing phytoplankton biomass. In open ocean upwelling systems, phytoplankton move offshore and concentrate at some distance from the coast (Dugdale et al., 1990), while in the relatively narrow Gulf of Finland coastal upwelling events are coupled with downwelling near the opposite coast.

In the beginning of August, the observed upwelling caused a clear decrease in Chl *a* concentration in the UML near the southern coast and an increase in Chl *a* near the northern coast of the Gulf of Finland (Figs. 4, 5). We suggest that the increase near the northern coast was mostly due to the northward

Ekman transport in the surface layer and accumulation of the phytoplankton biomass in the convergence zone built up there. However, possible influence of the along shore transport from adjacent coastal areas and growth enhancement stimulated by a previous relatively weak upwelling event near the northern coast in the mid-July cannot be excluded.

The fluctuations in nutrient and Chl *a* concentration in the upwelling area indicate that in the beginning of the upwelling, the pre-upwelling phytoplankton community was advected out from the area, and was not able to take advantage of upwelled nutrients. At the same time, the upwelled phytoplankton community had low biomass and needed some time to adapt to the well-lighted conditions in the near surface layer, but still in cold waters. As the water is brought into the euphotic zone, algae respond to high light and nutrients by switching on nutrient uptake mechanisms and starting to photosynthesize (e.g. Largier et al., 2006). During simulated upwelling condition experiments in the laboratory Ishizaka et al. (1983) have observed that there is a lag period preceding the increase of phytoplankton Chl *a*, and that the length of the time lag is temperature and light dependant. It has been shown in several coastal shelf field and modelling studies that the upwelled nutrients are taken up fast after the relaxation of the system (within 3–9 days; e.g. Dugdale et al., 1990; Wilkerson et al., 2006). During this study, the low Chl *a* period in the beginning of August was followed by phytoplankton growth after stabilization of upwelling by 15th August when an increase of Chl *a*, and a decrease of nutrient concentrations in the upwelling water were observed. The nutrients were consumed from the upper layer quite fast—there were no nitrites + nitrates left one week later, and the DIP concentrations were under the lower detection range 2 weeks later in the UML (Fig. 3). Nitrogen was depleted faster because the nitrites + nitrates to DIP ratio in the upwelling water (molar ratio being about 2) was much lower than the Redfield optimum. This is compatible with previous conclusions of Kivi et al. (1993) that phytoplankton growth in the western and central Gulf of Finland is nitrogen limited.

Chlorophyll *a* was found mainly in the <20- μm size fraction, and the temporal changes in this size fraction were similar to the changes of total Chl *a* content (Fig. 4). Chlorophyll *a* concentrations were relatively low and variable in upwelling waters on

8th August in both size fractions (Fig. 5a, b). The higher Chl *a* concentration in >20- μm size fraction and lower in <20- μm size fraction at station TH7 (Fig. 4B, C) compared with other stations in the upwelling area (TH1–TH5) was most probably due to the effect of an upwelling front (see salinity front in Fig. 2E). A similar pattern in Chl *a* concentrations in different size fractions can be noticed in the second frontal area near the northern coast at station TH21 (Figs. 2E and 4B, C). During the upwelling, the initial phytoplankton community in the surface waters was replaced by the community above, in and below the thermocline and lower concentrations measured in >20- μm size fraction compared with higher concentrations measured in <20- μm size fraction on 15th August is a clear sign that bigger size fraction needed longer ‘response time’ to the increased nutrient concentrations and more stable growth environment (stronger stratification) compared with the smaller size fraction.

As nitrites + nitrates were depleted from the UML already by 15th August (when also lowest Chl *a* concentrations in >20- μm size fraction were measured) and DIP by 22nd August, the increase in >20- μm size fraction could have been obtained either using the accumulated intracellular nutrient reserves or depending on regenerated nutrients. It has been shown in previous studies that a significant proportion of nutrients used in primary production after an upwelling pulse may be supplied by the regeneration of the phytoplankton biomass in the same area where upwelling occurs (review by Bode et al., 1997). The studies in the Gulf of Finland have shown that the typical summer bloom communities dominated by cyanobacteria will be changed by the ones dominated by euglenophytes and the autotrophic ciliate *Mesodinium rubrum* (Kanoshina et al., 2003; Vahtera et al., 2005) during the upwelling event. Studies of Wilkerson & Grunseich (1990) in the Peru upwelling system have shown the capability of *M. rubrum* to take up nitrate and to develop large blooms. *Eutreptiella* spp. has been noted to be an opportunistic bloom species adapted to decaying turbulence and high nutrient conditions, and it can form almost unialgal blooms in the Baltic Sea (Olli et al., 1996).

The separation of the >20- μm fraction was mainly done because the filamentous cyanobacteria

(dominating in the summer phytoplankton community) have been demonstrated to retain on the 20- μm plankton net (Kononen et al., 1999), and hence the dynamics in this size fraction could give an indication about the response of filamentous cyanobacteria to the upwelled nutrients. From the results of this study based on Chl *a* measurements, we cannot be confident that the increase in Chl *a* concentration in the >20- μm fraction was due to the enrichment of nutrients during the upwelling event as one can also notice that the increase of Chl *a* in the >20- μm fraction in the upwelling area on 22nd August (Fig. 5a) equals with the decrease in concentration in this size fraction near the opposite coast (Fig. 5c; stations TH21–TH27). Hence, the increase in the upwelling water might have resulted from the relaxation of upwelling and homogenization of the water masses along the cross-section. A further increase of Chl *a* concentration did not take place most probably due to the next upwelling event observed near the southern coast on 29nd August. This is in accordance with previous suggestions that a cyanobacterial bloom would develop in 2–3 weeks after the upwelling (e.g. Vahtera et al., 2005). The time span between two upwelling events in August 2006 was less than 10 days.

Upwelling is one of the most important sources of nutrients in the Gulf of Finland. The importance of vertical transport of nutrients from the deeper water layers and its role in the nutrient budget of the eutrophicated Baltic Sea and its sub-basins needs further studies. The studies in summer 2006 with high temporal and spatial resolution gave new information for understanding the functioning of the ecosystem compared with maximum 2-week studies usually conducted in this sea area. Still further high-resolution in situ measurements of biological, chemical and physical parameters are needed to provide a comprehensive synoptic picture of the highly variable near-shore processes in the Gulf of Finland.

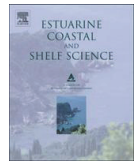
Acknowledgments This study was financially supported by the Estonian Science Foundation (grant no. 6752) and Foundation Innove (grant no. 1.0101-0279). This study was presented as a contributed article at the Bat Sheva de Rothschild seminar on Phytoplankton in the Physical Environment, the 15th workshop of the International Association of phytoplankton taxonomy and ecology (IAP). ESF Programm DoRa and a student scholarship from the Bat Sheva de Rothschild Fund supported financially the participation of Natalja Kuvaldina at this seminar.

References

- Alenius, P., K. Myrberg & A. Nekrasov, 1998. Physical oceanography of the Gulf of Finland: a review. *Boreal Environment Research* 3: 97–125.
- APHA, 1992. APHA, AWWA, and WPCF standard methods for the examination of water and wastewater, 18th ed. American Public Health Association, Washington DC.
- Bode, A., J. A. Botas & E. Fernández, 1997. Nitrate storage by phytoplankton in a coastal upwelling environment. *Marine Biology* 129: 399–406.
- Cushing, D. H., 1989. A difference in structure between ecosystems in strongly stratified waters and in those that are only weakly stratified. *Journal of Plankton Research* 11: 1–13.
- Dugdale, R. C., F. P. Wilkerson & A. Morel, 1990. Realization of new production in coastal upwelling areas: a means to compare relative performance. *Limnology and Oceanography* 35: 822–829.
- Haapala, J., 1994. Upwelling and its influence on nutrient concentration in the coastal area of the Hanko peninsula, entrance to the Gulf of Finland. *Estuarine, Coastal and Shelf Science* 38: 507–521.
- Hecky, R. E. & P. Kilham, 1988. Nutrient limitation of phytoplankton in freshwater and marine environments: a review of recent evidence on the effects of enrichment. *Limnology and Oceanography* 33: 796–822.
- HELCOM, 1988. Guidelines for the Baltic Monitoring Programme for the third stage. *Baltic Sea Environment Proceedings* 27D.
- Ishizaka, J., M. Takahashi & S. Ichimura, 1983. Evaluation of coastal upwelling effects on phytoplankton growth by simulated culture experiments. *Marine Biology* 76: 271–278.
- Kanoshina, I., U. Lips & J.-M. Leppänen, 2003. The influence of weather conditions (temperature and wind) on cyanobacterial bloom development in the Gulf of Finland (Baltic Sea). *Harmful Algae* 2: 29–42.
- Kivi, K., S. Kaitala, H. Kuosa, J. Kuparinen, E. Leskinen, R. Lignell, B. Marcussen & T. Tamminen, 1993. Nutrient limitation and grazing control of the Baltic plankton community during annual succession. *Limnology and Oceanography* 38: 893–905.
- Kononen, K. & Å. Niemi, 1986. Variation in phytoplankton and hydrography in the outer archipelago at the entrance to the Gulf of Finland in 1968–1975. *Finnish Marine Research* 253: 35–51.
- Kononen, K., M. Huttunen, I. Kanoshina, J. Laanemets, P. Moisaner & J. Pavelson, 1999. Spatial and temporal variability of a dinoflagellate-cyanobacterium community under a complex hydrodynamical influence: a case study at the entrance to the Gulf of Finland. *Marine Ecology Progress Series* 186: 43–57.
- Largier, J. L., C. A. Lawrence, M. Roughan, D. M. Kaplan, E. P. Dever, C. E. Dorman, R. M. Kudela, S. M. Bollens, F. P. Wilkerson, R. C. Dugdale, L. W. Botsford, N. Garfield, B. Kuebel Cervantes & D. Koračin, 2006. WEST: a northern California study of the role of wind-driven transport in the productivity of coastal plankton communities. *Deep Sea Research II* 53: 2833–2849.
- Lilover, M.-J., J. Laanemets, T. Kullas, A. Stips & K. Kononen, 2003. Late summer vertical nutrient fluxes estimated from direct turbulence measurements: a Gulf of Finland case study. *Proceedings of the Estonian Academy of Sciences: Biology, Ecology* 52: 193–204.
- Lips, U., U. Lips & T. Liblik, 2009. Consequences of coastal upwelling events on physical and chemical patterns in the central Gulf of Finland (Baltic Sea). *Continental Shelf Research*. doi:10.1016/j.csr.2009.06.010.
- MacIsaac, J. J., R. C. Dugdale, R. T. Barber, D. Blasco & T. T. Packard, 1985. Primary production cycle in an upwelling center. *Deep-Sea Research* 32: 503–529.
- Myrberg, K., 1998. Analysing and modelling the physical processes of the Gulf of Finland in the Baltic Sea. *Monographs of the Boreal Environment Research* 10: 9–49.
- Myrberg, K. & O. Andrejev, 2003. Main upwelling regions in the Baltic Sea- a statistical analysis based on three-dimensional modelling. *Boreal Environment Research* 8: 97–112.
- Olli, K., A.-S. Heiskanen & J. Seppälä, 1996. Development and fate of *Eutroptiella gymnastica* bloom in nutrient-enriched enclosures in the coastal Baltic Sea. *Journal of Plankton Research* 18: 1587–1604.
- Pauly, D. & V. Christensen, 1995. Primary production required to sustain global fisheries. *Nature* 374: 255–257.
- Pitkänen, H., J. Lehtoranta & A. Räike, 2001. Internal nutrient fluxes counteract decreases in external load: the case of the estuarial eastern Gulf of Finland, Baltic Sea. *Ambio* 30: 195–201.
- Schumann, E. H., 1999. Wind-driven mixed layer and coastal upwelling processes off the south coast of South Africa. *Journal of Marine Research* 57: 671–691.
- Talpsepp, L., 2008. On the influence of the sequence of coastal upwellings and downwellings on surface water salinity in the Gulf of Finland. *Estonian Journal of Engineering* 14: 29–41.
- Talpsepp, L., T. Nõges, T. Raid & T. Kõuts, 1994. Hydro-physical and hydrobiological processes in the Gulf of Finland in summer 1987: characterization and relationship. *Continental Shelf Research* 14: 749–763.
- Vahtera, E., J. Laanemets, J. Pavelson, M. Huttunen & K. Kononen, 2005. Effect of upwelling on the pelagic environment and bloom-forming cyanobacteria in the western Gulf of Finland, Baltic Sea. *Journal of Marine Systems* 58: 67–82.
- Wilkerson, F. P. & G. Grunseich, 1990. Formation of blooms by symbiotic ciliate *Mesodinium rubrum*: the significance of nitrogen uptake. *Journal of Plankton Research* 12: 973–989.
- Wilkerson, F. P., A. M. Lassiter, R. C. Dugdale, A. Marchi & V. E. Hogue, 2006. The phytoplankton bloom response to wind events and upwelled nutrients during the CoOP WEST study. *Deep-Sea Research II* 53: 3023–3048.
- Zhurbas, V., J. Laanemets & E. Vahtera, 2008. Modeling of the mesoscale structure of coupled upwelling/downwelling events and the related input of nutrients to the upper mixed layer in the Gulf of Finland, Baltic Sea. *Journal of Geophysical Research* 113: C05004.

Paper II

Lips, U., Lips, I., Liblik, T., Kuvaldina, N. 2010. Processes responsible for the formation and maintenance of subsurface chlorophyll maxima in the Gulf of Finland. *Estuarine, coastal and shelf science*, 88, 339-349.



Processes responsible for the formation and maintenance of sub-surface chlorophyll maxima in the Gulf of Finland

Urmas Lips*, Inga Lips, Taavi Liblik, Natalja Kuvaldina

Marine Systems Institute, Tallinn University of Technology Akadeemia 21B, 12618 Tallinn Estonia

ARTICLE INFO

Article history:

Received 28 December 2009

Accepted 21 April 2010

Available online 10 May 2010

Keywords:

sub-surface chlorophyll maxima
seasonal thermocline
nutrients
meso-scale processes
Gulf of Finland
Baltic Sea

ABSTRACT

Vertical cross-sections of temperature, salinity and Chl *a* fluorescence distributions in the Gulf of Finland were mapped on 11, 19–20 and 25 July 2006. The sub-surface Chl *a* maximum layers with thickness varying between 1.5 and 9 m and intensity up to $7.6 \mu\text{g l}^{-1}$ were observed in the lower part of the seasonal thermocline within the depth range of 14.5–35 m. Nutrient (PO_4^{3-} , $\text{NO}_2^- + \text{NO}_3^-$) analyses of water samples collected from the thermocline revealed the coincidence of the location of Chl *a* maxima and nutriclines. We suggest that the observed Chl *a* maxima were formed by dinoflagellate *Heterocapsa triquetra* capable for vertical migration and nutrient uptake in dark. The upward flux of nutrients caused by estuarine circulation and vertical turbulent mixing created favourable conditions for the formation and maintenance of sub-surface Chl *a* maxima. We explain the observed horizontal patchiness of sub-surface Chl *a* maxima by meso-scale processes – by the accumulation of phytoplankton along the depressed isopycnals at the base of anti-cyclonic circulation cells and by the horizontal convergence of waters in the downwelling area.

© 2010 Elsevier Ltd. All rights reserved.

1. Introduction

The distribution of phytoplankton in water bodies (including the Baltic Sea) is highly heterogeneous, both horizontally and vertically. Horizontal distribution of phytoplankton in the euphotic layer is often related to the meso-scale hydrophysical processes and structures – meso-scale eddies, fronts and coastal upwelling events (in the Gulf of Finland e.g. Talpsepp et al., 1994; Kononen et al., 1996; Kanoshina et al., 2003; Lips et al., 2005). Vertical distribution of phytoplankton is determined by availability of major resources – light and nutrients – as well as grazing and divergence/convergence of sinking and buoyancy (see e.g. Fennel and Boss, 2003). In a stratified water column the contrasting gradients of resources – light that is supplied from above and nutrients that are often supplied from below – will lead to the development of a sub-surface biomass/chlorophyll (Chl *a*) maximum (Klausmeier and Litchman, 2001).

The sub-surface Chl *a* maxima have been observed in the Baltic Sea quite often (e.g. Kahru et al., 1982; Kuosa, 1990; Kononen et al., 1998; Pavelson et al., 1999) and a variety of mechanisms of their formation has been suggested. It is known that the sub-surface Chl

a maxima are located just above the nutricline(s) which could be developed by an intrusion of nutrient rich water into the sea area under consideration (Lund-Hansen et al., 2006). In some cases the sub-surface Chl *a* maxima are observed well below the euphotic layer (e.g. Kononen et al., 2003). As mechanisms of the formation of such deep maxima, the hydrodynamic processes (Pavelson et al., 1999) and changing migratory behavior of *Heterocapsa triquetra* after an upwelling event (Kononen et al., 2003) have been proposed.

Sub-surface Chl *a* maxima are commonly observed in the summer stratified North Sea (Weston et al., 2005) and in the Celtic Sea (Hickman et al., 2009). It has been argued that accumulated new production in these layers in summer may be greater than that occurring in the spring bloom in the same regions (Richardson et al., 2000). No estimates of the role of sub-surface maxima in the total primary production during summer months are available yet for the Baltic Sea.

Development of measuring equipment in the last years has triggered an enhanced interest to sub-surface maximum layers of phytoplankton and zooplankton biomass, their fine-scale structure and ecology. Typical fine-scale layers range in thickness from a few centimetres to a few meters and they are described in the literature as “thin layers” (e.g. McManus et al., 2003). Physical processes can play an important role in the formation and dynamics of thin layers of phytoplankton and zooplankton (Dekshenieks et al., 2001; McManus et al., 2003). The measurements in the East Sound

* Corresponding author.

E-mail addresses: urmas.lips@phys.sea.ee (U. Lips), inga@sea.ee (I. Lips), taavi.liblik@phys.sea.ee (T. Liblik), natalja.kuvaldina@phys.sea.ee (N. Kuvaldina).

revealed that over 71% of thin layers were located in the base of, or within, the pycnocline (Deksheniaks et al., 2001). The regions of occurrence of thin layers are relatively sheltered bays or straits with two-layer vertical structure. A two-layer current, temporal and spatial variation of pycnocline depth, caused by meso-scale hydrophysical processes and estuarine structure of hydrographic fields, and minimum of turbulent mixing are conditions favourable for formation of thin layers (McManus et al., 2003; Lund-Hansen et al., 2006). Recent observations have shown that thin layers of Chl *a* maxima can exist in both weak and strong turbulent conditions, however, under strong turbulence a weakening of the thin layer was evident (Wang and Goodman, 2010).

The Gulf of Finland as an elongated basin has a weak, characteristic to an estuary, circulation pattern superimposed by quite energetic, wind-driven meso-scale motions. In summer, the upper layer of the gulf is nutrient depleted while in the layers below the seasonal thermocline high nutrient reserves are available. Meso-scale processes cause vertical movements and mixing of water masses – upwelling events bring water from below the thermocline into the upper layer (e.g. Lips et al., 2009) and downwelling events generate downward transport of upper layer waters containing phytoplankton (Pavelson et al., 1999; Laanemets et al., 2005). Vertical stratification characterised by two strong pycnoclines serves as a pre-requisite for formation of layered current structure in the gulf. Thus, we can assume that a coincidence of certain factors could lead to favourable conditions for the formation of sub-surface Chl *a* maxima and thin layers in the Gulf of Finland.

The aim of the present paper is to define the pre-conditions and physical processes responsible for the formation and maintenance of sub-surface Chl *a* maxima observed in the Gulf of Finland in July 2006. We show that similarly to the horizontal distribution of phytoplankton in the euphotic layer, the distribution pattern of sub-surface Chl *a* maxima and occurrence of maxima complying with the “thin layer” definition are affected by the meso-scale processes.

2. Material and methods

Three surveys of hydrographic, -chemical and -biological fields were carried out in the central part of the Gulf of Finland in July 2006 – on 11, 19–20 and 25 July. Vertical profiles of temperature, salinity and Chl *a* fluorescence were recorded at 27 stations (Fig. 1, distance between stations 2.6 km) and water samples for inorganic nutrient (PO_4^{3-} , $\text{NO}_2^- + \text{NO}_3^-$) analyses were collected at 14 stations (distance between stations 5.2 km) from the upper mixed layer and from the thermocline with a vertical resolution of 2.5–5 m. In order to convert fluorescence values to Chl *a* content, the water samples at 6 to 10 stations per survey were collected from different depths. Full sampling program was completed on 11 and 25 July while on 19–20 July we were able to take water samples only at the northernmost stations (TH19–TH27). Samples for phytoplankton analyses were collected mainly from the upper mixed layer, except a few samples collected in the thermocline on 11 and 25 July.

Vertical profiles of temperature, salinity and Chl *a* fluorescence in the upper 50-m layer were recorded using an SBE 19 CTD probe (Sea-Bird) equipped with a WETStar fluorometer (WET Labs). Sampling rate and lowering speed of the probe were 2 Hz and 0.5–1 m s⁻¹, respectively. In data processing, standard software package SEASOFT (Sea-Bird) was used where constant time shifts of 0.5 s for conductivity sensor, 1.0 s for temperature sensor and 2.5 s for Chl *a* fluorescence sensor were applied in order to compensate the time constant differences and different location of sensors while water was pumped through the sensors. The time shifts used in data processing were defined as the values ensuring the best conformity between downcast and upcast profiles (by visual

comparison of them). Salinity data were quality checked against the water sample analyses by a high precise salinometer AUTOSAL (Guildline). In order to assure that the measured fluorescence peaks reflect the stable structures, the downcast and upcast profiles were both taken into account and an average profile at every station was analysed.

Nutrient analyses were carried out according to the guidelines of American Public Health Association (APHA, 1992; methods 4500-NO₃-F and 4500-P-F). Samples for phosphates (PO_4^{3-}) were mostly analysed immediately after the sampling onboard research vessel and samples for dissolved nitrogen compounds ($\text{NO}_2^- + \text{NO}_3^-$; henceforth called as NO_x) determination were deep-frozen after collection and analysed later in the on-shore laboratory. Phosphates and nitrates + nitrites were analysed using automatic nutrient analyzer μMac 1000 (Systea S.r.l.). The lower detection range for phosphate-phosphorus and nitrate + nitrite-nitrogen was 2 ppb (parts per billion; 0.06 mmol m⁻³ and 0.14 mmol m⁻³, respectively).

Chl *a* concentration in the water samples was determined on Millipore APFF glass-fibre filters following the extraction at the room temperature in dark with 96% ethanol for 24 h. Chl *a* content from the extract was measured spectrophotometrically (Thermo Helios γ) in laboratory (Helsinki Commission, 1988). Results of analyses of 16 water samples collected on 11 and 25 July were used to get a calibrations line for converting measured fluorescence values to the Chl *a* content. The corresponding fluorescence values were obtained as 2-m average values around the water sampling depth. We applied only one calibration line for the whole data set: $\text{Chl} = 0.58 \times F + 1.37$ ($r^2 = 0.75$, where F is fluorescence in arbitrary units and Chl *a* content (Chl) is obtained in $\mu\text{g l}^{-1}$).

Phytoplankton samples were preserved with acid Lugol solution and analysed using the Utermöhl (1958) technique and PhytoWin software by Kahma Ky. Cyanobacterial filaments were counted as 100- μm segments and other phytoplankton species as single cells or colonies.

The intensity and thickness of sub-surface Chl *a* maxima were detected as shown in a sketch in Fig. 2. The maximum Chl *a* value (Chl_{max}) below 10 m depth and the minimum above it (Chl_1) were defined at every profile. The intensity of Chl *a* maximum was estimated as the difference between the values of Chl_{max} and Chl_1 . The thickness of maximum layer was defined as the difference between the depth of local minimum Chl_1 (h_1) and the depth h_2 where the Chl *a* values below the maximum decreased back to the same concentration (Chl_1). The depth, temperature, salinity and density values associated to the maximum were recorded as these values at the depth of Chl_{max} (h_{max}). Only Chl *a* maxima with an intensity of $\geq 0.5 \mu\text{g l}^{-1}$ were taken into account.

The upper mixed layer (UML) depth at each station was determined using smoothed (2.5 m moving average) vertical density profiles. First, the density difference (Δd_{tot}) between the cold intermediate layer and the surface layer was estimated as the density at the depth of minimum temperature minus the minimum density value in the surface layer. The UML depth was defined as the shallowest depth at which the vertical density gradient exceeded a criterion calculated as $C_{\text{up}} \times \Delta d_{\text{tot}}$, where $C_{\text{up}} = 1/30 \text{ m}^{-1}$. In order to determine the base of thermocline, the temperature difference between the UML and the cold intermediate layer was found. The shallowest depth, at which the temperature differs from the maximum value in the UML more than 90% of this difference, was defined as the base of thermocline.

The upper boundary of phosphocline and nitracline was defined as the deepest depth at which the nutrient (PO_4^{3-} or NO_x , respectively) concentration below the lower detection range was measured. When comparing the depths of Chl *a* maximum, thermocline and nutriclines it has to be kept in mind that the water

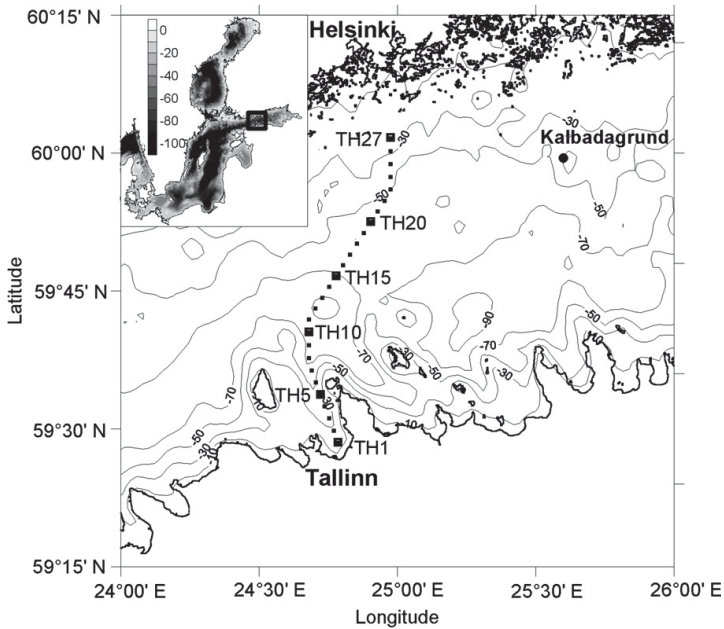


Fig. 1. Map of the study area and location of stations.

samples were collected with a vertical resolution of 2.5 m while the analysed temperature, salinity and fluorescence profiles had a vertical resolution of 0.5 m.

A primitive equation, sigma coordinate, free surface, hydrostatic model with a second moment turbulent closure sub-model embedded – Princeton Ocean Model (POM; Blumberg and Mellor, 1983) – was used with the aim to simulate the hydrophysical processes and related nutrient transport in the Gulf of Finland from 10 July until 31 August 2006 (Laanemets et al., in press). Since the nutrient uptake by phytoplankton was not taken into account in the model calculations, the difference between the modelled and

measured changes of nutrient concentrations in the upper water layer (comprising UML and thermocline) was taken as an estimate of the amount of consumed nutrients.

Fine structure of vertical stratification related to the observed Chl *a* maxima was analysed using vertical profiles of Brunt–Väisälä frequency estimated as $N^2 = -g/\rho \cdot \partial\rho/\partial z$, where g is acceleration due to gravity, ρ is density and $\partial\rho/\partial z$ is vertical density gradient. The flow structure in the study area at the time of surveys was characterised by vertical profiles of relative cross-transect geostrophic velocity, which were estimated on the basis of CTD data as: $u = 1/fL \int_{p_{ref}}^p (\delta_{p,i} - \delta_{p,i+2}) dp$, where f is the Coriolis parameter, L – the distance between the stations i and $i + 2$ (about 5.2 km) and $\delta_{p,i}$ and $\delta_{p,i+2}$ – vertical profiles of specific volume anomaly at stations i and $i + 2$. The reference level of no motion (p_{ref}) was chosen at 40 dbar in the open gulf and at the seabed in the shallower areas.

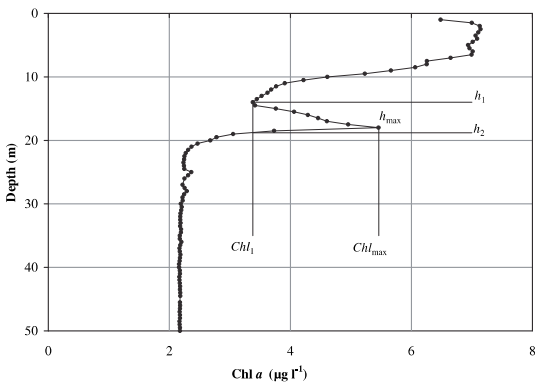


Fig. 2. Sketch used to define the parameters of sub-surface Chl *a* maxima (vertical profile is obtained at station TH8 on 11 July). Chl_{max} , h_{max} – maximum Chl *a* value below 10 m depth and depth of this maximum; Chl_1 , h_1 – minimum Chl *a* value above h_{max} and depth of this minimum; h_2 – depth where the Chl *a* values below the maximum decrease back to Chl_1 .

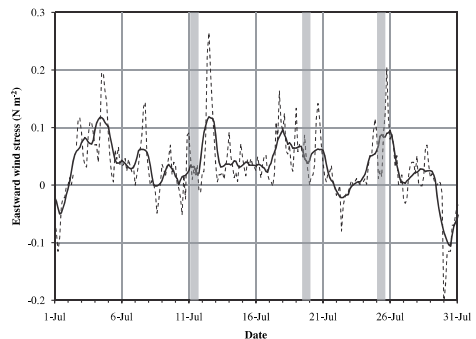


Fig. 3. Eastward wind stress (dashed line) in July 2006 estimated using wind data from Kalbadagrund meteorological station. Daily average wind stress is shown as solid line and vertical grey areas indicate the periods of sampling.

3. Results

According to the wind stress estimates southward cross-gulf Ekman drift (due to the eastward wind stress; Fig. 3) prevailed in the surface layer of the Gulf of Finland in July 2006. The surveys on 11 July and on 25 July were conducted after the periods of relatively weak winds from varying direction. The survey on 19–20 July was conducted when moderate westerly winds have been prevailed for a week. It resulted in an upwelling near the northern coast and a downwelling near the southern coast of the gulf. A more detailed description of upwelling and downwelling events in the Gulf of Finland in summer 2006 is given by Lips et al. (2009).

Vertical profiles of Chl *a* registered in July 2006 in the Gulf of Finland revealed the occurrence of sub-surface maximum layers of phytoplankton at many sampling stations (Fig. 4). Even if in most cases the maximum Chl *a* values were observed in UML, local maxima in the thermocline layer were quite common on the vertical profiles during all surveys. The Chl *a* content in UML on 11 July was higher in the open gulf – up to $6\text{--}8\ \mu\text{g l}^{-1}$ – than that in the coastal areas. On 19–20 July, the UML Chl *a* content was $<6\ \mu\text{g l}^{-1}$ except in the upwelling front at the northernmost part of the study transect where the maximum values exceeded $10\ \mu\text{g l}^{-1}$. On 25 July, higher Chl *a* values were observed in the northern part – reaching $7\text{--}8\ \mu\text{g l}^{-1}$ and lower values in the southern part – mostly $<6\ \mu\text{g l}^{-1}$.

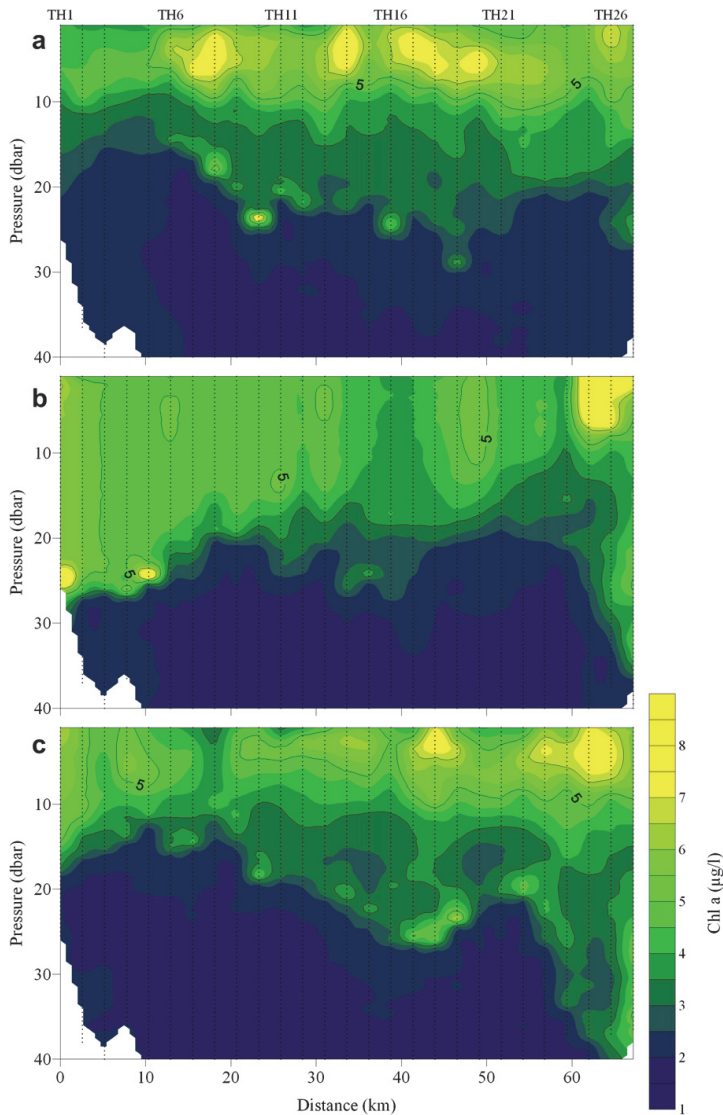


Fig. 4. Vertical sections of Chl *a* on 11 (a), 19–20 (b) and 25 (c) July 2006. Dotted lines indicate profiles; values on x-axis are distance from the southernmost station (TH1); station numbers are shown above.

In total the sub-surface Chl *a* maxima with intensities $\geq 0.5 \mu\text{g l}^{-1}$ were observed at 37 stations out of analysed 80 stations, $\geq 1.0 \mu\text{g l}^{-1}$ at 19, $\geq 2.0 \mu\text{g l}^{-1}$ at 7 and $\geq 5.0 \mu\text{g l}^{-1}$ at 4 stations. The characteristics of observed sub-surface Chl *a* maximum layers are summarised in Table 1. The highest observed Chl *a* values in these maximum layers were $10.5 \mu\text{g l}^{-1}$ on 11 July (at station TH10), $12.2 \mu\text{g l}^{-1}$ and $11.4 \mu\text{g l}^{-1}$ on 19–20 July (at stations TH1 and TH5, respectively) and $8.2 \mu\text{g l}^{-1}$ on 25 July (at station TH19). If excluding the sub-surface Chl *a* maximum observed close to the seabed at the shallowest station (TH1) on 19–20 July, all other three most intense maximum layers comply with the “thin layer” definition in regard of the optical signal (Deksheniaks et al., 2001). While their intensities estimated as shown in Fig. 2 were $7.6 \mu\text{g l}^{-1}$, $6.9 \mu\text{g l}^{-1}$ and $5.1 \mu\text{g l}^{-1}$, the Chl *a* fluorescence values measured in maxima where at least three times greater than the background Chl *a* fluorescence level. The depth of maxima varied between 14.5 and 35 m while the average depth of maxima was 23.0 ± 4.6 m (arithmetic mean and standard deviation are given, median was 23.5 m). Average values of temperature, salinity and density anomaly (density minus 1000 in kg m^{-3}) in the observed maxima were 4.73 ± 1.75 °C (median 4.46 °C), 5.85 ± 0.30 (median 5.86) and 4.61 ± 0.28 kg m^{-3} (median 4.65 kg m^{-3}), respectively.

The occurrence of Chl *a* maximum layers was found to be very well related to the registered vertical temperature structure (Fig. 5).

An ordinary vertical distribution of temperature was observed on 11 July 2006 with sea surface temperature >20 °C at almost all stations and the seasonal thermocline situated at the depths of 10–20 m. Eight days later an upwelling event was observed near the northern coast and downwelling in the southernmost part of the study transect. On 25 July, the sea surface temperature was between 19 and 20 °C and the thermocline was steeper than in the beginning of study period. The UML depth was on average 7 m on 11 July, 12 m on 19–20 July and 8 m on 25 July. The base of thermocline was situated at 24 m on 11 July, 23 m on 19–20 July and 21 m on 25 July. While on 19–20 July the thermocline characteristics were affected by a coupled upwelling-downwelling event, on 11 and 25 July the observed thermocline characteristics could be considered as typical ones in July in the Gulf of Finland. According to these two surveys the UML was shallower in the northern gulf than that in the southern part. In contrary, the base of thermocline was shallower in the southern gulf. As a consequence a very pronounced (steep) thermocline with vertical temperature and density gradients up to 2.43 °C m^{-1} and 0.48 kg m^{-4} was observed in the southern gulf while thermocline was thicker in the northern gulf.

As seen from the vertical cross-sections of temperature (Fig. 5) the Chl *a* maxima followed almost precisely the base of thermocline. On 11 July, the maxima were situated just above the base of

Table 1

Characteristics of sub-surface Chl *a* maximum layers with intensities $\geq 0.5 \mu\text{g l}^{-1}$ observed in the Gulf of Finland in July 2006. The maxima with fluorescence signal more than three times greater than the background signal are indicated in bold.

Date	Station	Chl <i>a</i> flores. (a.u.)	Chl <i>a</i> ($\mu\text{g l}^{-1}$)	Depth (m)	Intensity flores. (a.u.)	Intensity Chl <i>a</i> ($\mu\text{g l}^{-1}$)	Thickness (m)	Temp. (°C)	Salin.	Density anomaly (kg m^{-3})
11/07	TH6	4.3	3.8	14.5	0.9	0.5	2.5	6.67	5.58	4.34
11/07	TH7	4.8	4.1	15.0	1.5	0.8	2.5	5.77	5.66	4.44
11/07	TH8	8.1	6.0	18.0	4.8	2.8	4.5	4.39	5.52	4.38
11/07	TH9	4.8	4.1	20.0	1.7	1.0	4.0	5.35	5.74	4.53
11/07	TH10	15.9	10.5	23.5	13.2	7.6	2.5	4.38	5.99	4.75
11/07	TH11	6.0	4.8	20.5	3.1	1.8	5.5	5.36	5.69	4.48
11/07	TH12	4.8	4.1	22.0	1.5	0.9	4.5	5.68	5.39	4.24
11/07	TH14	3.7	3.5	22.0	1.0	0.6	3.5	5.43	5.53	4.35
11/07	TH16	5.7	4.6	24.5	2.8	1.6	4.5	4.79	5.60	4.43
11/07	TH18	3.5	3.4	22.5	0.9	0.5	6.0	6.19	5.36	4.19
11/07	TH19 ^a	3.7	3.5	25.0	1.1	0.6	2.5	5.02	5.84	4.61
11/07	TH19 ^a	5.0	4.3	29.0	2.8	1.6	3.0	3.73	6.13	4.88
11/07	TH26	3.0	3.1	24.5	1.0	0.6	4.0	3.87	5.88	4.68
11/07	TH27	4.4	3.9	23.5	1.6	0.9	6.5	3.81	5.95	4.73
19/07	TH1	18.9	12.2	25.0	11.0	6.4	5.0 ^b	11.81	5.73	3.97
19/07	TH4	8.9	6.5	26.0	3.9	2.2	2.0	5.67	6.08	4.78
19/07	TH5	17.4	11.4	24.5	11.9	6.9	3.0	6.52	6.01	4.68
19/07	TH8	5.3	4.4	19.0	1.2	0.7	1.5	8.19	5.80	4.40
19/07	TH14	3.4	3.3	25.5	1.2	0.7	6.0	2.54	6.31	5.03
19/07	TH15	4.5	4.0	24.0	2.4	1.4	3.0	2.79	6.21	4.95
19/07	TH16	2.9	3.0	25.0	1.0	0.6	5.5	2.99	6.20	4.94
19/07	TH24	4.1	3.7	15.5	0.9	0.5	4.0	6.39	5.15	4.01
19/07	TH26	4.3	3.8	20.5	1.0	0.6	4.0	4.5	5.81	4.60
19/07	TH27 ^a	6.5	5.1	25.5	1.2	0.7	7.0	3.58	5.99	4.77
19/07	TH27 ^a	5.9	4.7	32.0	1.4	0.8	5.0	3.04	6.19	4.93
25/07	TH7	5.4	4.4	14.5	2.2	1.3	2.5	4.42	6.32	5.02
25/07	TH10	6.2	4.9	18.5	3.2	1.8	6.5	4.09	5.91	4.69
25/07	TH14	4.6	4.0	20.5	1.6	0.9	3.5	4.83	5.71	4.52
25/07	TH15	4.3	3.8	22.5	2.0	1.1	4.5	4.61	5.76	4.57
25/07	TH16	4.0	3.7	19.5	1.1	0.6	7.0	6.67	5.56	4.31
25/07	TH17	6.7	5.2	25.5	3.4	2.0	5.0	3.29	6.03	4.81
25/07	TH18	6.8	5.3	26.0	3.5	2.0	5.0	3.53	5.95	4.73
25/07	TH19	11.9	8.2	23.5	8.9	5.1	5.5	3.52	5.88	4.68
25/07	TH21	4.1	3.7	20.5	1.3	0.8	5.0	4.34	5.68	4.51
25/07	TH22	5.8	4.7	19.5	3.0	1.7	5.5	4.80	5.49	4.35
25/07	TH23	4.9	4.2	22.5	1.8	1.0	8.0	4.63	5.66	4.48
25/07	TH24 ^a	4.2	3.8	26.0	1.0	0.6	7.0	3.97	5.93	4.71
25/07	TH24 ^a	3.6	3.4	33.0	1.0	0.6	4.5	2.27	6.46	5.15
25/07	TH25	3.6	3.4	35.0	1.4	0.8	5.0	2.41	6.47	5.16
25/07	TH27	6.1	4.9	27.5	2.2	1.3	9.0	3.53	6.02	4.79

^a Two sub-surface Chl *a* maxima were found on the profile.

^b Lower border of Chl *a* maximum layer was defined as the deepest measurement point on the profile.

thermocline and were related to the isotherm 5 °C (average temperature at maxima was 5.0 ± 0.9 °C), except a secondary maximum at station TH19. On 19 July, the most intensive maxima were observed in the thermocline in the downwelling area and less pronounced maxima in the central part of the study transect below the thermocline. The initial pattern of maxima distribution was re-established on 25 July; however, the maxima were less pronounced and they were registered almost precisely at the base of thermocline and at slightly lower temperatures than those on 11 July (average temperature at maxima on 25 July was 4.1 ± 1.1 °C).

The vertical structure of salinity field was characterised by low values in the surface layer – from 4.5 to 5.3 on 11 July, from 4.7 to 5.2 on 19–20 July and from 4.5 to 5.1 on 25 July – and by a continuous increase of salinity in the seasonal thermocline and below it. The Chl *a* maxima were mostly observed in the salinity range from 5.8 to 6.2.

The vertical sections of nutrients on 11 and 25 July revealed low nutrient concentrations in the upper layer – UML and upper part of the thermocline – and higher values with relatively patchy distribution in the deeper layer below the thermocline (Fig. 6). According to both surveys the nitrates + nitrites were completely consumed

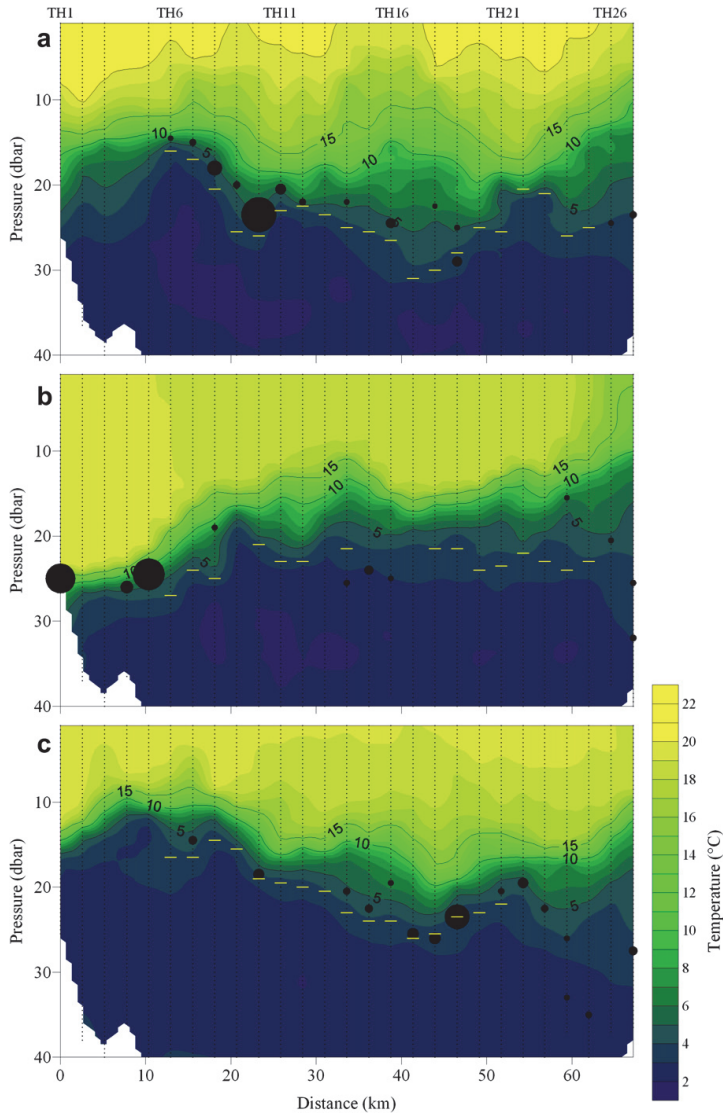


Fig. 5. Vertical sections of temperature on 11 (a), 19–20 (b) and 25 (c) July 2006. Dotted lines indicate profiles; values on x-axis are distance from the southernmost station (TH1); station numbers are shown above. Observed sub-surface Chl *a* maxima are indicated as black circles scaled proportionally to the intensity of maxima; the base of thermocline is shown by yellow/light dashes (the base of thermocline was not determined if the profile did not reach the minimum temperature).

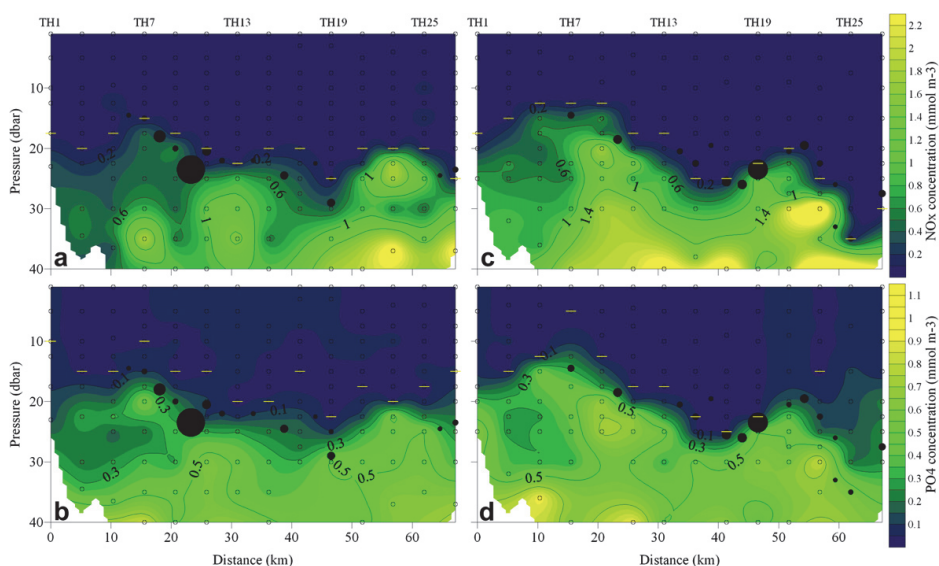


Fig. 6. Vertical sections of nutrient concentrations: (a) – NO_x on 11 July, (b) – PO_4 on 11 July, (c) – NO_x on 25 July and (d) – PO_4 on 25 July. Dots indicate the sampling points; values on x-axis are distance from the southernmost station (TH1); station numbers are shown above. Observed sub-surface Chl *a* maxima are indicated as black circles scaled proportionally to the intensity of maxima; the depth of nutriclines (nitracline and phosphocline, respectively) is shown by yellow/light dashes.

from the UML while detectable concentrations of phosphates were measured at some stations in the central part on 11 July and at some stations in the coastal areas on 25 July. A comparison of corresponding nutrient distributions in the maximum layer on 11 and 25 July shows that slightly higher concentrations, especially in the southern part and for nitrates + nitrites, were observed during the latter survey. The registered sub-surface Chl *a* maxima coincided well with the nutriclines, especially with the nitracline. Since the vertical resolution of water sampling was 2.5 m or more and the samples were taken not at all stations it is not possible to indicate the exact nutrient concentrations in the maximum layers. However, at most of the stations with sub-surface maxima the concentrations of NO_x were below the lower detection range in the samples taken above the Chl *a* maximum layer and detectable concentrations were measured in the samples taken just below the maxima.

According to the model results the average NO_x concentration in the upper 0–25 m layer increased in a two-week period from 11 to 25 July by 0.16 mmol m^{-3} (Laanemets et al., in press), which corresponds to an average nitrate flux at the 25 m depth level of $0.3 \text{ mmol N m}^{-2} \text{ d}^{-1}$. On the basis of measurements, the increase of NO_x concentration in the upper 0–25 m layer between surveys on 11 and 25 July was only 0.04 mmol m^{-3} . If assuming that this discrepancy between measurements and model might be related to the nutrients transported upward and taken up by phytoplankton in the thermocline one can suppose that about $3/4$ of nitrates was consumed. Given that the local wind forcing before 11 July was similar to that within the period from 11 to 25 July (see Fig. 3) we may assume that an upward nutrient flux of similar intensity ($0.3 \text{ mmol N m}^{-2} \text{ d}^{-1}$) occurred also before our first survey on 11 July.

Filamentous cyanobacteria species/groups and dinoflagellate *H. triquetra* (Ehrenberg) Stein were dominating in the UML phytoplankton community in the Gulf of Finland in July 2006 (more detailed description of phytoplankton dynamics in the UML can be found in (Lips and Lips, 2010)). Wet weight biomass up to

1039 mg m^{-3} (54% of total phytoplankton biomass) on 11 July, up to 1013 mg m^{-3} (56%) on 19–20 July and up to 542 mg m^{-3} (39%) on 25 July of the latter species known to be forming sub-surface maxima was observed. Only one quantitative phytoplankton sample from a sub-surface Chl *a* maximum was analysed. The sample was collected at station TH19 on 25 July from 22.5 m depth where the Chl *a* fluorescence value was a half of that at the fluorescence peak registered at 23.5 m depth (see Fig. 7a; relative depth 1 m). The phytoplankton community at this sampling point was dominated by *H. triquetra* (288 mg m^{-3} , 33%), *Aphanizomenon* sp. (L.) Ralfs (203 mg m^{-3} , 23%) and *Dinophysis acuminata* Claparède and Lachmann (147 mg m^{-3} , 17%). The two former species had a similar share while the latter species was absent in the UML community at the same station.

Vertical profiles of Brunt–Väisälä frequency estimated over 2 m intervals and presented as functions of the relative depth (calculated as the distance from the depth of maximum Chl *a* value – h_{max}) revealed a quite high variability (Fig. 7b). Nevertheless, an average profile indicates a clear weakening of stratification with the depth in the vicinity of h_{max} . The two most intense Chl *a* maxima were associated with the weakest stratification in the water layer from 1 to 3 m below h_{max} . While a sharp drop of Chl *a* values below h_{max} was observed at almost all stations (Fig. 7a) the profiles were more variable above h_{max} . At some stations, where the stratification was stronger just above h_{max} , the Chl *a* maximum layers were thicker (station TH19 on 25 July as an example) and at stations with a weaker stratification above h_{max} , thinner Chl *a* maximum layers were observed (among them the most intense sub-surface Chl *a* maximum sampled at station TH10 on 25 July).

According to the cross-transect geostrophic velocity distributions in the upper 40-m layer (Fig. 8), an outflow prevailed in the central part of the gulf and an inflow in the southernmost and northernmost areas on 11 July. Next survey on 19–20 July revealed a cross-transect jet current associated with the upwelling front in the northern part of the study transect and another jet current

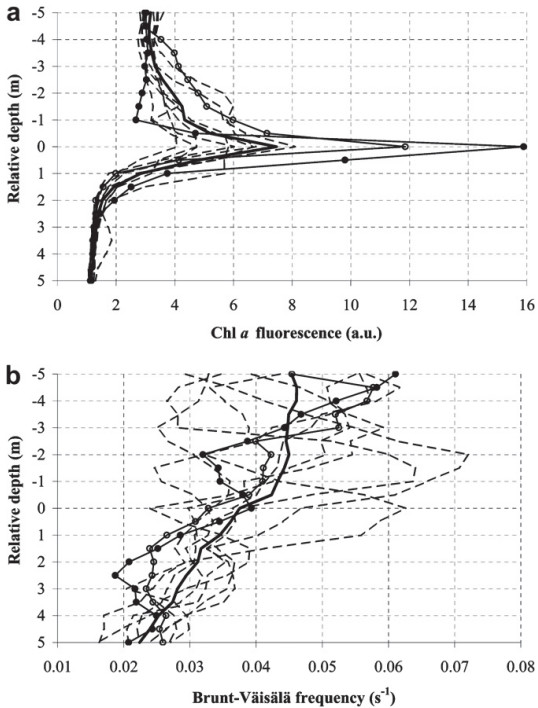


Fig. 7. Vertical profiles of Chl *a* fluorescence (a) and Brunt–Väisälä frequency (b) at selected stations (TH8–TH12 on 11 July and TH17–TH19, TH21–TH22 on 25 July) as functions of the relative depth (calculated as the vertical distance from the depth of maximum Chl *a* value – h_{\max}). Brunt–Väisälä frequency was estimated over 2 m intervals. Average profiles are shown as thick solid lines, profiles at station TH10 on 11 July as thin solid lines with filled circles and at station TH19 on 25 July as thin solid lines with empty circles.

coupled with the downwelling in the southern gulf. Only a narrow outflow region in the central gulf was evident on 19–20 July. The geostrophic current structure was characterised mainly by an outflow in the upper layer except narrow inflow regions in the northernmost, southernmost and central parts of the study transect on 25 July.

Presented geostrophic velocity distributions with alternating flow directions along the study transect could be interpreted as a sequence of meso-scale eddies or as a sequence of cyclonic and/or anti-cyclonic circulation cells. On 11 July, two of such anti-cyclonic circulation cells were evident – first in the southern part between 15 and 30 km and second in the central part within the thermocline between 33 and 48 km. On 25 July a similar to the latter circulation cell with higher velocities in the thermocline was observed between 33 and 48 km. As seen in Fig. 8, most of the detected sub-surface maximum layers, especially those with the highest intensities, were located at the base of the described meso-scale features (anti-cyclonic circulation cells). On 19–20 July, the Chl *a* maxima were observed mainly in the downwelling area which could be also characterised as an anti-cyclonic circulation cell with horizontal convergence of water masses.

4. Discussion

Our measurements in July 2006 along the study transect Tallinn–Helsinki in the Gulf of Finland confirm that the sub-surface Chl

a maximum layers can exist in a stratified water column in summer when the upper layer is depleted of nutrients while high reserves of nutrients are available below the seasonal thermocline. The detected maxima were almost all located at the base of thermocline and coincided well with the depth of nutriclines. The former indicates that the vertical stratification and related hydrodynamic conditions, such as mixing and/or current shear, could play an important role in formation of the observed Chl *a* maxima. The latter points either to the nutrient availability as a major factor controlling the formation of sub-surface Chl *a* maxima or to the nutrient uptake by the phytoplankton in the Chl *a* maxima at the base of thermocline that maintained the nutriclines exactly at these depths.

The Chl *a* maxima were located at the depths between 14.5 and 35 m with an average of 23 m. Since the Secchi disk depth in the study area during all surveys did not exceed 5 m, very low irradiances could be assumed at the depths of the observed maxima. We estimated PAR attenuation coefficient K_d on the basis of optical measurements in the upper 3 m layer in the study area on 11 July (T. Kutser and L. Metsamaa, personal communication). According to these estimates of K_d (from 0.33 to 0.55 m^{-1}) the photic depth varied between 8.4 and 13.9 m, which are clearly less than the average depth of observed sub-surface maxima. Similar relatively deep Chl *a* maxima observed in the Gulf of Finland in July 1998 at low irradiances (<0.1% of the sea surface irradiance) were formed by *H. triquetra* (Kononen et al., 2003). Phytoplankton community data suggest that the Chl *a* maximum layers observed in July 2006 were also dominated by *H. triquetra*, as it was the dominating species in the sample collected close to a sub-surface Chl *a* fluorescence peak and one of the dominant species in the UML in our study area. Since the Chl *a* maximum layers were observed during all three surveys conducted within two weeks in July 2006, the favourable conditions should have existed for a relatively long period to support their formation and maintenance. Among these favourable conditions the hydrodynamic processes producing upward flux of nutrients and/or the nutrient conditions or hydrodynamic processes triggering downward migration of phytoplankton could be referred.

Several estimates based on the field measurements are available indicating that in certain conditions the upward nutrient fluxes may support formation and maintenance of sub-surface Chl *a* maxima. In the studies by Sharples et al. (2001) and Hales et al. (2009) the vertical turbulent nitrate fluxes were estimated at 0.8–5.2 $\text{mmol N m}^{-2} \text{d}^{-1}$ which could support a net phytoplankton productivity of 64–360 $\text{mg C m}^{-2} \text{d}^{-1}$. In the southwest Kattegat, Baltic Sea where a sub-surface Chl *a* maximum was observed in October 2003 the nitrate flux as high as 17 $\text{mmol N m}^{-2} \text{d}^{-1}$ was estimated (Lund-Hansen et al., 2006). One of the favourable conditions supporting the development of sub-surface maxima is the functioning of estuarine circulation with opposite flow directions in the layers above and below the thermocline resulting in an upward volume (and nutrient) flux in the gulf interior (Elken et al., 2003; Lips et al., 2008). A modelling study (Laanemets et al., in press) gave an estimate of average nitrate flux of 0.3 $\text{mmol N m}^{-2} \text{d}^{-1}$ at the 25 m depth level in the central Gulf of Finland in July 2006, which according to our assumption was in a large extent consumed by phytoplankton in the sub-surface layer. This estimate of nitrate flux is one order of magnitude lower than those referred above. It has to be noted that the contribution of vertical ammonium flux (ammonium was not measured in our study) could double the flux of available dissolved inorganic nitrogen due to the high concentrations of ammonium in the Gulf of Finland deep layers (e.g. Pitkänen et al., 2008). However, it appears that the upward nutrient flux was still not large enough to maintain the sub-surface Chl *a* maxima along the entire study

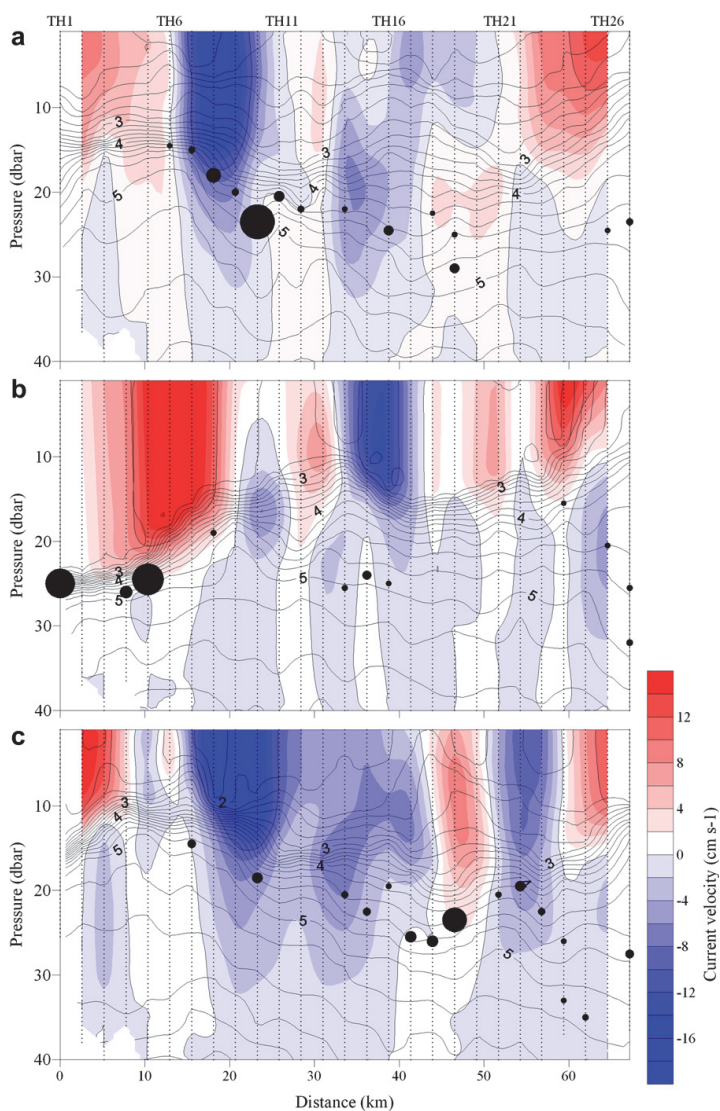


Fig. 8. Vertical sections of cross-transect geostrophic current velocity on 11 (a), 19–20 (b) and 25 (c) July 2006. The reference level of no motion was chosen at 40 dbar in the open gulf and at the seabed in the shallower areas. Corresponding density anomaly distribution (density – 1000 kg m⁻³) is shown by black contour lines. Dotted lines indicate profiles; values on x-axis are distance from the southernmost station (TH1); station numbers are shown above. Observed sub-surface Chl *a* maxima are indicated as black circles scaled proportionally to the intensity of maxima.

transect at all three surveys in July 2006. As a result the sub-surface maxima were observed at about 50% of stations and only a few of them revealed at least three times greater optical signal than the background level. Thus, it needs to be analysed what processes were responsible for the observed patchiness of horizontal distribution of sub-surface maxima.

Many earlier studies have revealed evidences that the meso-scale processes shape the horizontal distribution of phytoplankton both in the surface layer and in the sub-surface layer whereas pure advection of biomass as well as local growth enhancement might

cause the observed patchiness. It is well documented that eddy/wind interactions can generate high sub-surface diatom biomass in mode-water eddies (McGillicuddy et al., 2007). The tracer measurements were used to estimate the vertical advection and turbulent diffusion of deep-water nutrients into a sub-surface Chl *a* layer and the flux of dissolved inorganic nitrogen was found to be large enough to maintain the observed high diatom biomass (Ledwell et al., 2008). On the other hand, Johnston et al. (2009) related the appearance of thin layers in a coastal upwelling zone to the advection and current shear and argued that initially thick

sub-surface Chl *a* maxima were transformed into thin layers by current shear on the flanks of the eddies, filaments, and fronts. The peak values in the observed thin layers exceeded concentrations in the upwelled source waters and stayed unexplained by the available data.

The cross-transect geostrophic velocity distributions revealed that the sub-surface Chl *a* maximum layers detected in the Gulf of Finland in July 2006 were located mostly at the base of anti-cyclonic circulation cells. Although the highest Chl *a* maxima observed on 11 and 25 July were related to the meso-scale circulation cells similar to mode-water eddies, our results differ from those referred above (McGillicuddy et al., 2007; Ledwell et al., 2008), first, the scales are non-comparable and, secondly, the maxima were found at the base of circulation cells where the isopycnals were depressed (not at the domed isopycnals above, see Fig. 8). On 19–20 July, the most intense sub-surface Chl *a* maxima were found in the downwelling area where the thermocline had the deepest position but the horizontal convergence of waters could be expected. Therefore, we conclude that the most intense maxima could be formed due to the accumulation of downward migrated phytoplankton cells near the base of the meso-scale features.

The formation of such patches of high biomass of phytoplankton could be favoured both by the ability of cells to reach and maintain these depths (the shallowest depth where high enough nutrient concentrations were available for the growth) and by the horizontal convergence of waters along the depressed isopycnals at the base of anti-cyclonic circulation cells. It has been reported that the swimming speed of *H. triquetra* in a turbulent environment could be as high as 0.5–0.75 m h⁻¹ (Anderson and Stolzenbach, 1985). We have recorded downward migration of phytoplankton community dominated by *H. triquetra* in the Gulf of Finland in July 2009 of about 20 m during a 24 h period (unpublished data). Thus, the phytoplankton can reach the observed depths of Chl *a* maxima within a day. A clear weakening of stratification with the depth just below the observed maxima could be considered as an indirect indication of vertical mixing and nutrient fluxes supporting the possible nutrient uptake there. Unlike to many other dinoflagellates *H. triquetra* might assimilate nitrate in the dark as efficiently as in the light (Paasche et al., 1984) and that explains the coinciding depth of Chl *a* maxima and nitracline.

5. Conclusions

Our measurements in July 2006 showed that the sub-surface Chl *a* maximum layers are common in the Gulf of Finland stratified water column in summer. The Chl *a* maxima were mostly located at the base of thermocline and coincided well with the depths of nutriclines. We suggest that downward migration of phytoplankton capable for nutrient uptake in dark and upward flux of nutrients caused by estuarine circulation and vertical turbulent mixing created favourable conditions for the formation and maintenance of sub-surface Chl *a* maxima. The observed horizontal patchiness of sub-surface Chl *a* maximum layers could be related to the meso-scale processes. The accumulation of phytoplankton was observed along the depressed isopycnals at the base of anti-cyclonic circulation cells and in the downwelling area characterised by the horizontal convergence of waters.

Acknowledgments

This work was financially supported by the Estonian Science Foundation (grants no. 6752 and 6955) and Foundation Innove (grant no. 1.0101-0279). Authors appreciate the help of colleagues and crew members who participated in the field measurements.

We express our gratitude to Dorrit Talts who first analysed the fluorescence profiles presented here during her Master studies. We thank Liisa Metsamaa and Tiit Kutser for providing us with data of optical measurements and the Finnish Meteorological Institute for wind data at Kalbådgrund station.

References

- Anderson, D.M., Stolzenbach, K.D., 1985. Selective retention of two dinoflagellates in a well-mixed estuarine embayment: the importance of diel vertical migration and surface avoidance. *Marine Ecology Progress Series* 25, 39–50.
- APHA, 1992. APHA, AWWA, and WPCF Standard Methods for the Examination of Water and Wastewater, 18th ed. American Public Health Association, Washington, DC.
- Blumberg, A.F., Mellor, G.L., 1983. Diagnostic and prognostic numerical calculation studies of the South Atlantic Bight. *Journal of Geophysical Research* 88 (C8), 4579–4592.
- Deksheniaks, M.M., Donaghay, P.L., Sullivan, J.M., Rines, J.E.B., Osborn, T.R., Twardowski, M.S., 2001. Temporal and spatial occurrence of thin phytoplankton layers in relation to physical processes. *Marine Ecology Progress Series* 223, 261–271.
- Elken, J., Raudsepp, U., Lips, U., 2003. On the estuarine transport reversal in deep layers of the Gulf of Finland. *Journal of Sea Research* 49, 267–274.
- Fennel, K., Boss, E., 2003. Subsurface maxima of phytoplankton and chlorophyll: steady-state solutions from a simple model. *Limnology and Oceanography* 48, 1521–1534.
- Hales, B., Hebert, D., Marra, J., 2009. Turbulent supply of nutrients to phytoplankton at the New England shelf break front. *Journal of Geophysical Research* 114, C05010. doi:10.1029/2008JC005011.
- Helsinki Commission, 1988. Guidelines for the Baltic Monitoring Programme for the third stage. Part D. Biological determinands. *Baltic Sea Environment Proceedings* 27D, 1–161.
- Hickman, A.E., Holligan, P.M., Moore, C.M., Sharples, J., Krivtsov, V., Palmer, M.R., 2009. Distribution and chromatic adaptation of phytoplankton within a shelf sea thermocline. *Limnology and Oceanography* 54, 525–536.
- Johnston, T.M.S., Cheriton, O.M., Pennington, J.P., Francisco, P.C., 2009. Thin phytoplankton layer formation at eddies, filaments, and fronts in a coastal upwelling zone. *Deep-Sea Research II* 56, 246–259.
- Kahru, M., Aitsam, A., Elken, J., 1982. Spatio-temporal dynamics of chlorophyll in the open Baltic Sea. *Journal of Plankton Research* 4, 779–790.
- Kanoshina, I., Lips, U., Leppänen, J.-M., 2003. The influence of weather conditions (temperature and wind) on cyanobacterial bloom development in the Gulf of Finland (Baltic Sea). *Harmful Algae* 2, 29–42.
- Klausmeier, A., Litchman, E., 2001. Algal games: the vertical distribution of phytoplankton in poorly mixed water columns. *Limnology and Oceanography* 46, 1998–2007.
- Kononen, K., Kuparinen, J., Mäkelä, K., Laanemets, J., Pavelson, J., Nömmann, S., 1996. Initiation of cyanobacterial blooms in a frontal region at the entrance of the Gulf of Finland, Baltic Sea. *Limnology and Oceanography* 41, 98–112.
- Kononen, K., Hällfors, S., Kokkonen, M., Kuosa, H., Laanemets, J., Pavelson, J., Autio, R., 1998. Development of a subsurface chlorophyll maximum at the entrance to the Gulf of Finland, Baltic Sea. *Limnology and Oceanography* 43, 1089–1106.
- Kononen, K., Huttunen, M., Hällfors, S., Gentien, P., Lunven, M., Huttala, T., Laanemets, J., Lilover, M., Pavelson, J., Stips, A., 2003. Development of a deep chlorophyll maximum of *Heterocapsa triquetra* Ehrenb. At the entrance to the Gulf of Finland. *Limnology and Oceanography* 48, 594–607.
- Kuosa, H., 1990. Subsurface chlorophyll maximum in the northern Baltic Sea. *Archiv für Hydrobiologie* 118, 437–447.
- Laanemets, J., Väli, G., Zhurbas, V., Elken, J., Lips, I., Lips, U., Simulation of mesoscale structures and nutrient transport during summer upwelling events in the Gulf of Finland in 2006. *Boreal Environment Research*, in press.
- Laanemets, J., Pavelson, J., Lips, U., Kononen, K., 2005. Downwelling related mesoscale motions at the entrance to the Gulf of Finland: observations and diagnosis. *Oceanological and Hydrobiological Studies* 34 (2), 15–36.
- Ledwell, J.R., McGillicuddy, D.J., Anderson, L.A., 2008. Nutrient flux into an intense deep chlorophyll layer in a mode-water eddy. *Deep-Sea Research II* 55, 1139–1160.
- Lips, I., Lips, U., Kononen, K., Jaanus, A., 2005. The effect of hydrodynamics on the phytoplankton primary production and species composition at the entrance to the Gulf of Finland (Baltic Sea) in July 1996. *Proceedings of Estonian Academy of Sciences. Biology*, *Ecology* 54 (3), 210–229.
- Lips, I., Lips, U., Liblik, T., 2009. Consequences of coastal upwelling events on physical and chemical patterns in the central Gulf of Finland (Baltic Sea). *Continental Shelf Research* 29, 1836–1847.
- Lips, I., Lips, U., 2010. Phytoplankton dynamics affected by the coastal upwelling events in the Gulf of Finland in July–August 2006. *Journal of Plankton Research*. doi:10.1093/plankt/fbq049.
- Lips, U., Lips, I., Liblik, T., Elken, J., 2008. Estuarine Transport versus Vertical Movement and Mixing of Water Masses in the Gulf of Finland (Baltic Sea). *US/EU-Baltic International Symposium*, 27–29 May 2008. Institute of Electrical and Electronics Engineers/Oceanic Engineering Society (IEEE/OES), Tallinn. doi:10.1109/BALTIC.4625535.

- Lund-Hansen, L.C., Ayala, P.C.A., Reglero, A.F., 2006. Bio-optical properties and development of a sub-surface chlorophyll maxima (SCM) in south-west Kattegat, Baltic Sea. *Estuarine, Coastal and Shelf Science* 68, 372–378.
- McGillicuddy, D.J., Anderson, L.A., Bates, N.R., Bibby, T., Buesseler, K.O., Carlson, C., Davis, C.S., Ewart, C., Falkowski, P.G., Goldthwait, S.A., Hansell, D.A., Jenkins, W.J., Johnson, R., Kosnyrev, V.K., Ledwell, J.R., Li, Q.P., Siegel, D.A., Steinberg, D.K., 2007. Eddy-wind interactions stimulate extraordinary mid-ocean plankton blooms. *Science* 316, 1021–1026.
- McManus, M.A., Alldredge, A.L., Barnard, A., Boss, E., Case, J., Cowles, T.J., Donaghay, P. L., Eisner, L., Gifford, D.J., Greenlaw, C.F., Herren, C., Holliday, D.V., Johnson, D., MacIntyre, S., McGehee, D., Osborn, T.R., Perry, M.J., Pieper, R., Rines, J.E.B., Smith, D.C., Sullivan, J.M., Talbot, M.K., Twardowski, M.S., Weidemann, A., Zaneveld, J.R.V., 2003. Characteristics, distribution and persistence of thin layers over a 48 hours period. *Marine Ecology Progress Series* 261, 1–19.
- Paasche, E., Bryceson, I., Tangen, K., 1984. Interspecific variation in dark nitrogen uptake by dinoflagellates. *Journal of Phycology* 20 (3), 394–401.
- Pavelson, J., Kononen, K., Laanemets, J., 1999. Chlorophyll distribution patchiness caused by hydrodynamical processes: a case study in the Baltic Sea. *ICES Journal of Marine Science* 56 (S), 87–99.
- Pitkänen, H., Lehtoranta, J., Peltonen, H., 2008. The Gulf of Finland. In: Schiewer, U. (Ed.), *Ecology of Baltic Coastal Waters*. Ecological Studies 197. Springer, Berlin, pp. 285–308.
- Richardson, K., Visser, A.W., Pedersen, F.B., 2000. Subsurface phytoplankton blooms fuel pelagic production in the North Sea. *Journal of Plankton Research* 22, 1663–1671.
- Sharples, J., Moore, C.M., Rippeth, T.P., Holligan, P.M., Hydes, D.J., Fisher, N.R., Simpson, J.H., 2001. Phytoplankton distribution and survival in the thermocline. *Limnology and Oceanography* 46, 486–496.
- Talpepp, L., Nöges, T., Raid, T., Köuts, T., 1994. Hydrophysical and hydrobiological processes in the Gulf of Finland in summer 1987: characterization and relationship. *Continental Shelf Research* 14, 749–763.
- Utermöhl, H., 1958. Zur Vervollkommnung der quantitativen Phytoplanktonmethode. *Mitteilungen des Internationale Vereinigung für Theoretische und Angewandte Limnologie* 9, 1–38.
- Wang, Z., Goodman, L., 2010. The evolution of a thin phytoplankton layer in strong turbulence. *Continental Shelf Research* 30, 104–118.
- Weston, K., Fernand, L., Mills, D.K., Delahunty, R., Brown, J., 2005. Primary production in the deep chlorophyll maximum of the central North Sea. *Journal of Plankton Research* 27, 909–922.

Paper III

Lips, U., Lips, I., Liblik, T., Kikas, V., Altoja, K., Buhhalko, N., Rünk, N. 2011. Vertical dynamics of summer phytoplankton in a stratified estuary (Gulf of Finland, Baltic Sea). *Ocean Dynamics*, 61, 903-915.

Vertical dynamics of summer phytoplankton in a stratified estuary (Gulf of Finland, Baltic Sea)

Urmas Lips · Inga Lips · Taavi Liblik · Villu Kikas ·
Kristi Altoja · Natalja Buhhalko · Nelli Rünk

Received: 30 September 2010 / Accepted: 31 March 2011 / Published online: 20 April 2011
© Springer-Verlag 2011

Abstract We present the results of multiparametric observations designed to follow the phytoplankton dynamics and interrelated physical, chemical and biological processes in the Gulf of Finland (Baltic Sea). Data were acquired by an autonomous moored water column profiler, an acoustic Doppler current profiler, a flow-through system installed aboard a ferry and by profiling and discrete water sampling aboard research vessels in July and August 2009. The main aim of the study was to investigate the processes responsible for the formation and maintenance of sub-surface maxima of phytoplankton biomass. We suggest that the environmental conditions caused by the prevailing atmospheric and oceanographic forcing (wind; vertical stratification; basin-wide, mesoscale and sub-mesoscale processes) are preferred by certain species/taxonomic groups and explain the migration patterns of phytoplankton. Nocturnal downward migration of phytoplankton with a swimming speed up to 1.6 m h^{-1} occurred when the community was dominated by the dinoflagellate *Heterocapsa triquetra*. The observed splitting of the population into two vertically separated biomass maxima suggests that the *H. triquetra* cells, which reached the sub-surface layers with high nutrient concentrations, experienced bi-diurnal or asynchronous (when swimming upwards) vertical migration. The most intense sub-surface biomass maxima, on some occa-

sions with the biomass much higher than that in the surface layer, were detected in connection to the sub-mesoscale intrusions below the depth of the strongest vertical density gradient.

Keywords Phytoplankton dynamics · Stratification · *Heterocapsa triquetra* · Vertical migration · Autonomous profiler · Gulf of Finland

1 Introduction

The Gulf of Finland is a stratified and wide estuary with considerable fresh water inflow at the eastern end and relatively open water exchange with the Baltic proper through the gulf's western boundary. In April–May, a seasonal thermocline begins to form, and during the productive season, the Gulf is strongly stratified. The upper mixed layer depth is typically 10–20 m, and temperature drops in summer from about 15–20°C at the top of the thermocline to about 2–4°C in the cold intermediate layer. Estuarine circulation is characterized by an inflow into the Gulf in the deeper layers and an outflow in the surface layer; however, depending on the prevailing winds, the circulation pattern might be reversed (Elken et al. 2003). Residual circulation in the surface layer consists of an outflow of gulf water in the northern part and an inflow of open Baltic Sea water to the southern part of the Gulf (Alenius et al. 1998).

The seasonal dynamics of nutrient concentrations in the surface layer of the Gulf of Finland is characterized by a maximum in winter and a minimum in summer. After the spring bloom, in the middle of May, the euphotic layer becomes depleted of dissolved inorganic nitrogen (DIN). Dissolved inorganic phosphorus (DIP) concentration usu-

Responsible Editor: Aida Alvera-Azcárate

This article is part of the Topical Collection on *Multiparametric observation and analysis of the Sea*

U. Lips (✉) · I. Lips · T. Liblik · V. Kikas · K. Altoja ·
N. Buhhalko · N. Rünk
Marine Systems Institute, Tallinn University of Technology,
Akadeemia Rd. 15A,
12168 Tallinn, Estonia
e-mail: urmas.lips@phys.sea.ee

ally reaches a minimum in late June–early July before the late summer bloom that is dominated by cyanobacteria or, in some years, by the dinoflagellate *Heterocapsa triquetra* (Ehrenberg) Stein (Kononen et al. 1996; HELCOM 2002).

The wind-driven circulation in the Gulf of Finland is highly variable and characterized by intense mesoscale features—eddies, upwelling/downwelling and coastal and frontal jet currents. Upwelling events cause substantial vertical nutrient transport (Zhurbas et al. 2008; Lips et al. 2009) and influence the phytoplankton dynamics in the upper layer in the Gulf of Finland (Vahtera et al. 2005; Lips and Lips 2010). The upward transport of nutrients from below the seasonal thermocline could create favourable conditions for the growth of nitrogen-fixing cyanobacteria due to the low DIN/DIP ratio in the upwelled waters. Furthermore, any vertical mixing could support the growth of cyanobacteria, since the phosphocline is usually located in the upper part of the seasonal thermocline (Laanemets et al. 2004). Less attention has been paid to downwelling events, although they are associated with the horizontal convergence of waters and substances that could lead to vertical transport and mixing and, for instance, to support the formation of sub-surface phytoplankton biomass maxima (Lips et al. 2010).

Earlier studies in the Gulf of Finland carried out during the late summer phytoplankton bloom have mostly dealt with cyanobacteria (Kononen et al. 1996; Kanoshina et al. 2003; Lips and Lips, 2008). A few studies only have investigated the dynamics of communities dominated by cyanobacteria/dinoflagellates (e.g. Kononen et al. 2003) or the dynamics of the whole phytoplankton community (e.g. Lips and Lips 2010). The co-dominance of functionally different phytoplankton species (*Aphanizomenon* sp. (L.) Ralfs and *H. triquetra*) in the summer community in the upper layer has been explained by Kononen et al. (2003) by the dynamic hydrographic field and species-specific adaptation to water movements.

The sub-surface maxima of phytoplankton biomass, among them the relatively deep biomass maxima of *H. triquetra*, have been observed in the Gulf of Finland in summer (e.g. Pavelson et al. 1999; Kononen et al. 2003). In July 2006, sub-surface chlorophyll *a* (Chl *a*) maximum layers with thicknesses varying between 1.5 and 9 m and an intensity up to 7.6 mg m^{-3} were observed in the lower part of the seasonal thermocline within the depth range of 14.5 to 35 m (Lips et al. 2010). Nutrient analyses of water samples collected from the thermocline revealed the coincidence of the location of Chl *a* maxima and nutriclines. However, until 2009, continuous/high-resolution vertical profiling data were not available for the Gulf of Finland, and we did not have observational evidence of the formation of sub-surface biomass maxima by vertical migration of phytoplankton.

Studies of sub-surface maxima of phytoplankton biomass or “thin layers” have been carried out in many coastal regions of the world, for example, in Monterey Bay (e.g. Sullivan et al. 2010) and in Ria de Pontevedra (Velo-Suarez et al. 2010). The conditions in these coastal ocean regions and in our study area differ due to the relatively turbid waters in the Gulf of Finland and occurrence of sub-surface phytoplankton maxima (dominated by *H. triquetra*) in the water layer below the euphotic depth. However, many questions are common to the studies of sub-surface biomass maxima at all sites, such as, is it possible to explain the formation and maintenance of maxima mainly by physical processes, and what is the role of vertical migration due to different physiological states of the phytoplankton cells?

The main motivation of the present study was to show that knowledge of the links between phytoplankton dynamics and meteorological and oceanographic forcing can be improved by using high-resolution autonomous in situ observations. We aimed to define more precisely the physical, chemical and biological processes responsible for the formation of sub-surface maxima of phytoplankton biomass in the Gulf of Finland.

2 Materials and methods

A multiparametric observation program was designed to follow the phytoplankton dynamics and interrelated physical, chemical and biological processes in the Gulf of Finland (Baltic Sea) in the summer, 2009. The measurements were performed using an autonomous moored water column profiler, a bottom mounted acoustic Doppler current profiler (ADCP), an autonomous system installed aboard a ferry (Ferrybox system) and measurement and sampling devices aboard the research vessel SALME and hydrographic vessel EVA-318. The data collected with the autonomous systems were transferred via mobile phone network immediately after every profiling from the buoy station and once a day from the ferry. The operational data gathering enabled us to perform additional measurements and sampling aboard the research vessel within the periods of special interest.

The autonomous profiler (Idronaut S.r.l.; surface buoy designed by Flydog Solutions Ltd.) was deployed in the Gulf of Finland from 30 June to 28 August in a sea area with a bottom depth of 86 m (see location in Fig. 1). Vertical profiles of temperature, salinity and Chl *a* fluorescence in the water layer from 2 to 45 (50) m were acquired with a time resolution of 3 h and a vertical resolution of 10 cm. Measurements were conducted using an Ocean Seven 316*plus* CTD probe (Idronaut S.r.l.) equipped with a Seapoint Chl *a* fluorometer. An ADCP (Teledyne RDI, 300 kHz) was deployed close to the buoy

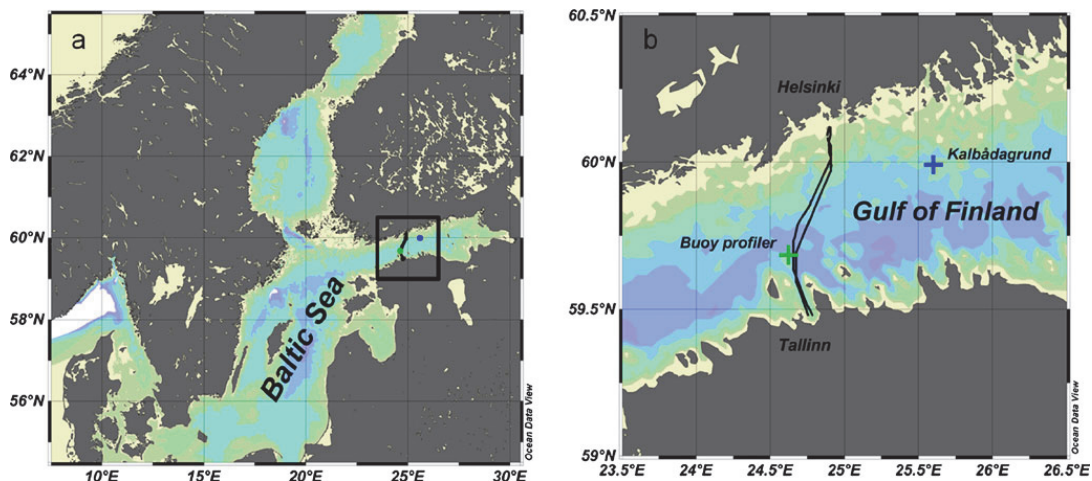


Fig. 1 Map of the Baltic Sea (a) and observation sites in the Gulf of Finland (b) where locations of moored profiler and ADCP (green cross), ferry track from Tallinn to Helsinki and back (solid curves) and

Kalbådagrund meteorological station (blue cross) are shown. Maps are created using ODV software (Shlitzer 2010)

profiler from 23 July until 24 September to measure flow structure in the whole water column with a vertical resolution of 2 m.

The Ferrybox system installed aboard the passenger ferry “Baltic Princess” (AS Tallink Group) travelling between Tallinn and Helsinki was used for measurements and sampling in the surface layer. Water intake was located approximately at 4 m depth. Temperature, salinity and Chl *a* fluorescence were recorded along the ferry route (Fig. 1) twice a day with a time resolution of 20 s corresponding approximately to a spatial resolution of 150 m. Water sampling at 17 locations distributed evenly along the ferry route was conducted on 5, 12 and 19 July and 2, 9 and 23 August. The collected water samples were analysed for Chl *a* content and phytoplankton species composition and biomass.

CTD measurements using an Ocean Seven 320plus CTD probe (Idronaut S.r.l.) equipped with a Seapoint Chl *a* fluorometer and water sampling aboard the research vessel were performed on 28 July, 31 July and 11–12 August. The locations of stations and the sampling depths were defined on the basis of autonomously acquired data and vertical profiles of Chl *a* fluorescence at each sampling station. Vertical resolution of water sampling was from 2 to 5 m. Water samples were analysed for inorganic nutrient (PO_4^{3-} and $\text{NO}_2^- + \text{NO}_3^-$) concentrations, Chl *a* content and phytoplankton species composition and biomass.

Nutrient analyses were carried out according to the guidelines of the American Public Health Association (APHA 1992; methods 4500-NO₃ F and 4500-P F). The samples were deep-frozen after collection and analysed at

the on-shore laboratory using an automatic nutrient analyser ($\mu\text{Mac 1000}$, Systea S.r.l.). The lower detection range for phosphate–phosphorus and nitrate + nitrite–nitrogen was 1 ppb (parts per billion; 0.03 and 0.07 μM , respectively; with a measurement uncertainty of 20% near detection limit).

Chl *a* concentration in the water samples was determined on Whatman GF/F glass fibre filters following extraction at room temperature in the dark with 96% ethanol for 24 h. Chl *a* content from the extract was measured spectrophotometrically (Thermo Helios γ) in the laboratory (HELCOM 1988). Phytoplankton samples were preserved with acid Lugol’s solution and analysed using the Utermöhl (1958) technique and PhytoWin software by Kahma Ky. Cyanobacterial filaments were counted as 100- μm segments and other phytoplankton species as single cells or colonies. All biomass data are given in wet weight concentrations.

Fluorescence data were calibrated against Chl *a* measured in the water samples collected aboard the research vessel on 28 July, 31 July and 11–12 August. Sixty data pairs were used to find the best linear fit (using least mean square criteria) between fluorescence and Chl *a*: $\text{Chl } a = 2.11 \times F + 0.63$ ($r^2 = 0.69$, where F is fluorescence in arbitrary units and Chl *a* content is obtained in milligram per cubic metre). The applicability of the same equation to convert the fluorescence values measured by another Seapoint fluorometer attached to the moored profiler was confirmed by very good agreement between the simultaneous vertical Chl *a* fluorescence profiles obtained by the moored profiler and the profiler aboard the research vessel.

Two stratification parameters were calculated for each vertical density profile measured at the buoy station—upper mixed layer (UML) depth (h_{UML}) and depth of the strongest density gradient (depth of the maximum Brunt-Väisälä frequency— h_{maxN}). Profiles with a vertical resolution of 0.5 m were used, and only those profiles were taken into account where the profiling depth was ≥ 30 m. The UML depth was derived as the depth at which the density exceeded the surface density (taken at 4 m depth) by 0.25 kg m^{-3} .

Wind data with a time resolution of 3 h obtained from the Kalbådgrund meteorological station (Finnish Meteorological Institute; see location in Fig. 1) were used to characterize local atmospheric forcing.

3 Results

3.1 Vertical temperature, salinity and Chl *a* distribution

High-resolution vertical profiling at the buoy station revealed remarkable temporal variations of the vertical distributions of temperature and salinity in the Gulf of Finland in July–August 2009 (Fig. 2a, b). Although the general temporal pattern was superimposed by short-time variations, the deployment period could be divided into several sub-periods with distinct vertical structure (and/or changes) of temperature and salinity fields. At the beginning of July, the UML temperature and depth were $13\text{--}15^\circ\text{C}$ and $5\text{--}9$ m, respectively. Surfacing of colder and more saline subsurface layer water was observed in the first half of July. Later, a less saline water mass with temperature and salinity ranging from 14°C to 15.5°C and from 4.2 to 4.5 m, respectively, appeared in the UML. A fast deepening of the UML from 7–9 to 16–18 m occurred on 25 July and a more saline water mass occupied the UML on 26 July—the UML salinity increased up to 5.0. After 31 July, considerable warming of the sea surface and formation of a secondary thermocline at 7–10 m depth were observed. It was followed by a drastic deepening of the UML from 13–15 m (on 15–16 August) to 26–30 m (on 20–21 August) accompanied by an increase of the UML salinity up to 5.7. While in most cases the depth of the strongest density gradient followed the temporal evolution of the UML depth, separation of about 10 m between these depths occurred from 29 July to 12 August.

The general dynamics of Chl *a* were characterized by an interchange of periods with different Chl *a* distribution patterns (Fig. 2c). Three periods with deep distribution patterns of Chl *a* were related to the deepening of the UML after 12 July, 25 July and 16 August. The highest Chl *a* concentrations in the UML were observed on 3–10 August when the highest UML temperature (up to 19.2°C) and

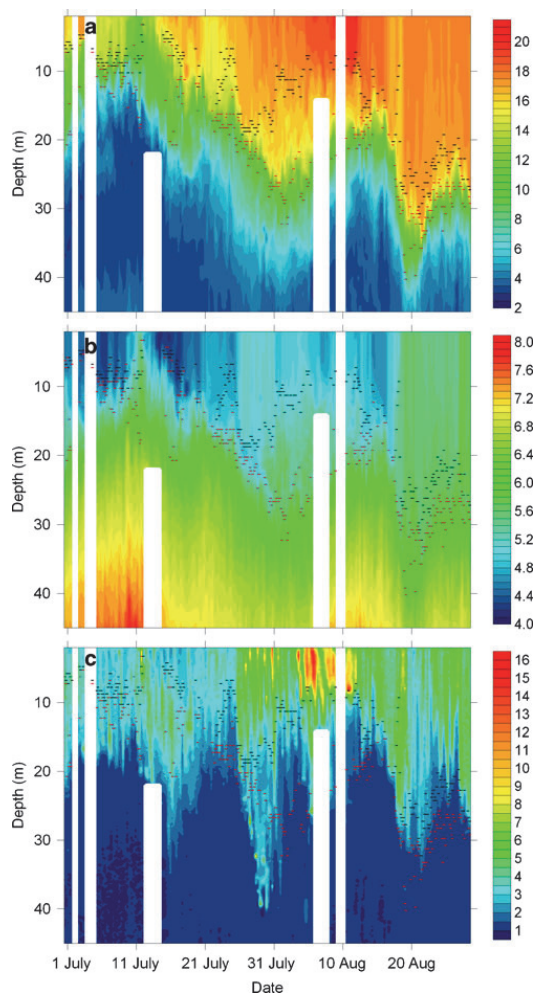


Fig. 2 Variations of the vertical distribution of temperature (a, degree Celsius), salinity (b) and Chl *a* (c, milligram per cubic metre) as measured by autonomous profiler in the Gulf of Finland from 30 June to 28 August 2009. Blanked areas correspond to the periods when vertical profiles were not available for 24 h or more. Black dashes indicate the UML depth and red dashes the depth of the strongest density gradient

secondary thermocline occurred. The three mentioned periods of relatively high Chl *a* concentration in the subsurface layer differ from each other regarding the depths of Chl *a* penetration and the concurrent UML depth and depth of the strongest density gradient (Fig. 2c). In the period after 12 July, the highest Chl *a* values were observed mainly in the thermocline between the UML depth and the depth of the strongest density gradient, i.e. the Chl *a* concentrations in the UML were lower than those in the

thermocline. On 26–31 July, relatively high Chl *a* concentrations were observed in the UML, while patches of very high Chl *a* were detected also in the sub-surface layer below the depth of the strongest density gradient. The overall Chl *a* concentration maximum, measured by the buoy profiler, was registered also within this period in the sub-surface layer (19.8 mg m^{-3} at 32 m on 28 July). During the third period of deep Chl *a* distribution (after 16 August), high Chl *a* concentrations were observed only in the UML (however, the UML was deep), and no patches of elevated Chl *a* content were detected below the depth of the strongest density gradient. Relatively high Chl *a* values were measured below the depth of the highest density gradient on 5–9 July when the UML was very shallow and h_{maxN} was located close to the UML depth. It has to be pointed out that the described general Chl *a* dynamics was superimposed with short-term variations, often having a diurnal signal in the whole water column where noticeable Chl *a* concentrations were measured.

3.2 Atmospheric and oceanographic forcing

Wind measurements at the Kalbådgrund meteorological station (see location in Fig. 1) revealed high variability of the wind but some periods with characteristic wind forcing (Fig. 3) leading to certain current patterns (data available since 23 July) or coastal upwelling/downwelling events. South-easterly winds, which are favourable for upwelling near the southern coast, prevailed in the Gulf of Finland area from 6 to 12 July. The temperature and salinity data collected in the surface layer along the Tallinn–Helsinki ferry route confirmed that an upwelling event occurred near the southern coast on 7–13 July (Fig. 4) and that upwelling waters reached the buoy station on 10 July resulting in a temporal temperature decrease and salinity increase measured by the profiler on 10–12 July. Mainly westerly–south-

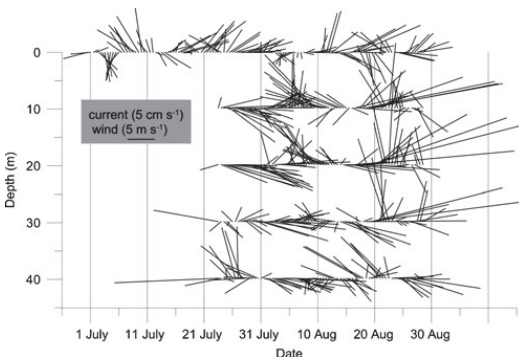


Fig. 3 Daily mean wind velocity measured at the Kalbådgrund meteorological station from 30 June to 28 August 2009 (upper row of vectors) and daily mean currents at the depths of 10, 20, 30 and 40 m

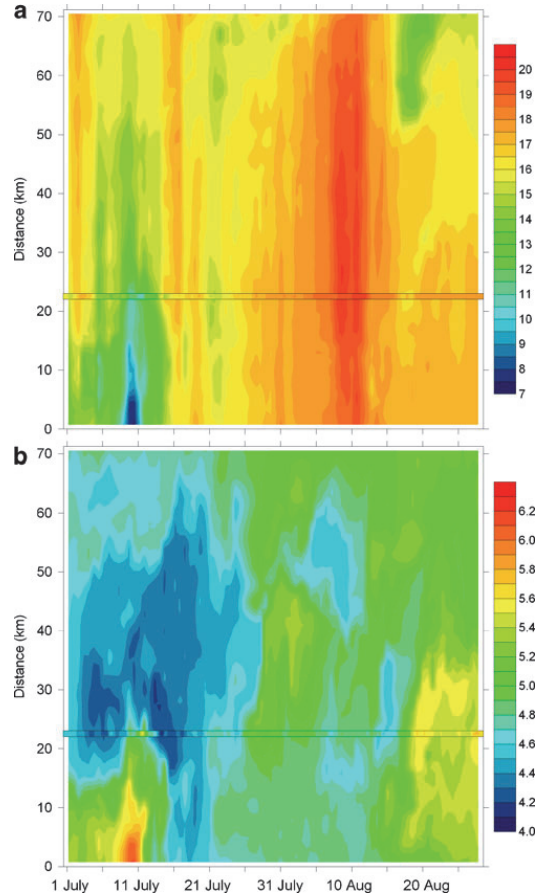


Fig. 4 Variations of temperature (a, degree Celsius) and salinity (b) in the surface layer along the ferry route Tallinn–Helsinki from 30 June until 28 August 2009. Distance in kilometres from a fixed starting point of Ferrybox measurements near Tallinn is shown on the y-axis. Simultaneous data acquired at the buoy profiler (at the depth of 4 m) are shown at the distance of 22–23 km

westerly winds prevailed in the area from 15 July until the end of July. This period was characterized by deepening of the thermocline (h_{maxN} , see Fig. 2a). South-eastward flow in the 20-m upper layer and north-westward flow below the thermocline were observed from 24 July (Fig. 3). The appearance of more saline water in the UML on 26 July (Figs. 2b and 4b) could be related to this flow structure.

A period of weak winds was observed during the first 10 days of August. The flow structure was characterized by a northward (north-westward) flow in the surface layer and an eastward flow below the thermocline (30 and 40 m in Fig. 3). Strong wind pulses from variable directions were observed from 10 August until the end of the measurement

period. First, simultaneous diurnal current oscillations occurred in the whole water mass (not seen in Fig. 3 where daily mean velocities are presented). Later, a clear two-layer flow structure was established with similar changes of current speed and direction in the upper 30 m layer and mostly opposite flow below. Strong westerly and north-westerly winds on 15–20 August caused downwelling near the southern coast of the Gulf, which was detected at our measurement site as the sharp deepening of the UML from 17 to 19 August. According to the Tallinn–Helsinki Ferrybox data, an intensive upwelling event developed simultaneously near the northern coast (Fig. 4).

3.3 Phytoplankton dynamics in the surface layer

Phytoplankton biomass and species composition in the surface layer changed during the study period and, according to the sampling using the Ferrybox system, differed between the regions along the ferry route. On the basis of combined Ferrybox and research vessel data collected near the buoy profiler (Fig. 5), phytoplankton biomass values were relatively low (420–880 mg m⁻³, expressed as total wet weight concentrations) at the beginning of July. Euglenophytes *Eutreptiella* spp. de Cunha (16–30% of total wet weight biomass), the filamentous cyanobacterium *Aphanizomenon* sp. (13–26%) and the dinoflagellate *Dinophysis acuminata* Claparède and Lachmann (19–27%) were the dominant species in the phytoplankton community. In the area influenced by a coastal upwelling near the southern coast, *Eutreptiella* spp. were most prominent (28–58%) on 12 July, and the community was dominated by *Aphanizomenon* sp. (32–50%) and *D. acuminata* (12–27%) on 19 July. At the same time, the three Ferrybox samplings in July revealed that the dinoflagellate *H. triquetra* dominated at most of the stations in the northern Gulf (10–53% of total wet weight

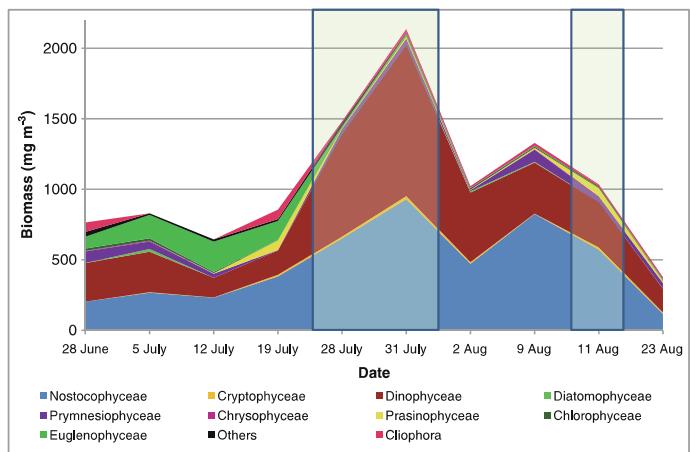
biomass). According to the research vessel data (used to fill in the gap in the Ferrybox data) collected from the upper layer (1–5 m) in the vicinity of the buoy profiler on 28 and 31 July, the community was clearly dominated by cyanobacteria and dinoflagellates (Fig. 5) in late July. Dominant species on both days were *Aphanizomenon* sp. (37% and 29%, respectively) and *H. triquetra* (32% and 27%). The biomass increase on 31 July was mainly due to the appearance of *Nodularia spumigena* Mertens and higher biomass of *D. acuminata* in the whole community.

On 2 August, *Aphanizomenon* sp. and *H. triquetra* were dominant in the southern Gulf (21–32% and 27–57% of total wet weight, respectively; Ferrybox data). The more saline water mass just northward from the buoy station (see Fig. 4b) was characterized by a lower *Aphanizomenon* sp. contribution (below 10%) and high dominance of *H. triquetra* (58–72%). One week later, on 9 August, *Aphanizomenon* sp. and *H. triquetra* were more or less evenly distributed across the Gulf (11–44% and 10–32%, respectively). The cyanobacterium *N. spumigena* had a significant share in the total biomass in the whole sampling area (6–46%). On 11 August, the samples collected aboard the research vessel showed an overall decrease in phytoplankton biomass and the dominance of filamentous cyanobacteria in the community. On 23 August, *Aphanizomenon* sp. continued to dominate in the southern part of the Gulf (40–50%); however, the total phytoplankton biomass was clearly lower than that of previous sampling days (Fig. 5).

3.4 Vertical migration of phytoplankton

To verify whether the observed short-term variations in Chl *a* distribution (Fig. 2) were consistent with a diurnal vertical migration pattern of phytoplankton, the average daily courses of Chl *a* were constructed for the entire deployment

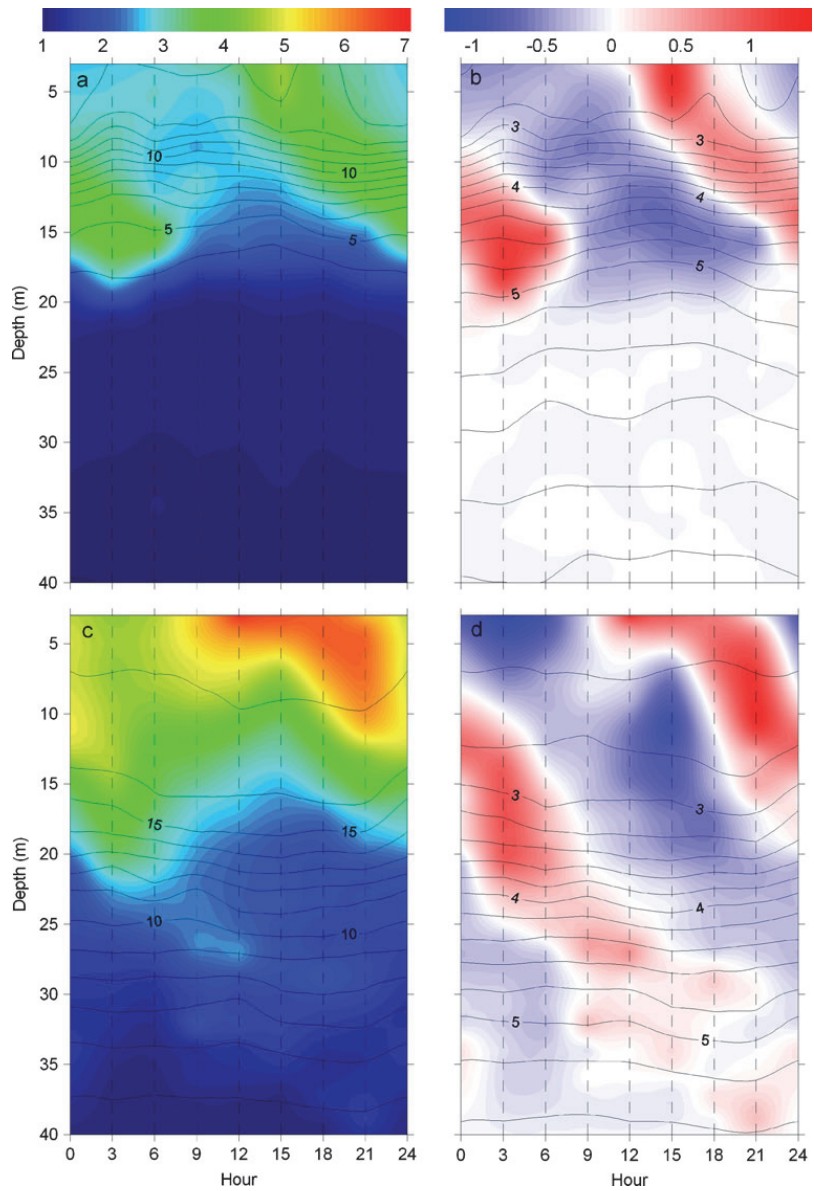
Fig. 5 Temporal dynamics of phytoplankton in the Gulf of Finland in summer 2009 in the vicinity of the buoy profiler. Ferrybox data collected from the depth of 4 m in the evening are complemented by research vessel data (marked as shaded areas) collected from the surface layer 1–5 m during daytime



period and for several distinct periods of atmospheric–oceanographic forcing and species composition. Due to the high variability at other time scales, the amplitude of the diurnal cycle, revealed using the data from the entire deployment period, was low in comparison to the overall variability (calculated as the standard deviation of Chl *a* at a fixed depth). Clear diurnal patterns in the Chl *a* dynamics were detected in the period of dominance of euglenophytes (*Eutreptiella* spp.)

at the beginning of July and in the period of dominance of the dinoflagellate *H. triquetra* in late July–early August (Fig. 6). In the former period, the Chl *a* values were relatively low (mainly $<5 \text{ mg m}^{-3}$), the maximum at the surface (3 m) was observed at 3 p.m. and the maximum at 15–17 m depth at 3 a.m. The changes in the Chl *a* distribution were restricted to the upper 20 m layer where the water temperature and density anomaly were $>4^\circ\text{C}$ and $<5 \text{ kg m}^{-3}$, respectively. We

Fig. 6 The daily average variations of Chl *a* and deviations from the mean Chl *a* at each depth in the layer 3–40 m from 5 July to 9 July (a and b, respectively) and from 25 July to 2 August (c, d). Both Chl *a* scales are in milligram per cubic metre. Average temperature (degree Celsius; a, c) and density anomaly (kilogram per cubic metre; b, d) distributions are shown by solid lines



interpret the observed Chl *a* dynamics as diurnal vertical migration of phytoplankton with a clear downward migration at night. Two features of the Chl *a* dynamics in the time–depth plot (Fig. 6a, b) are consistent with the upward migration of phytoplankton—the upward directed branches of slightly higher values with the starting points at 3 a.m., 8–10 m and at 6 a.m., 15 m (Fig. 6a, b). However, we note that the related temporal changes were statistically not significant due to the high day-to-day variability and too short period with this migration pattern observed at the buoy profiler.

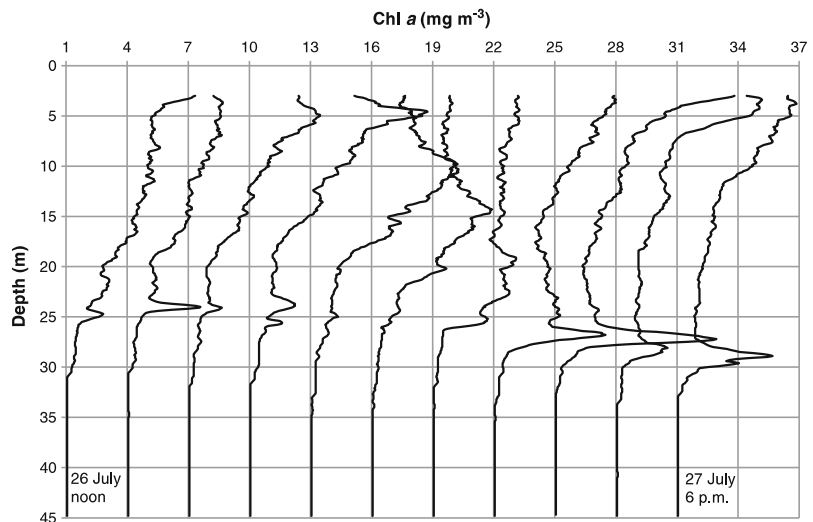
In late July–early August, the maximum Chl *a* concentrations at the surface were observed between noon and 6 p.m. and the minimum at 3 a.m. (Fig. 6c, d). Clear diurnal cycles, but with the daily maximum and minimum at the different times of day, occurred also in the sub-surface layer, while below the depth of the strongest density gradient (on average at 21–23 m), a possible cyclical migration pattern was masked by occasionally observed patches of high Chl *a*. It has to be noted that the daily maximum and minimum Chl *a* values were significantly different only in the upper 12-m layer. Due to a relatively strong vertical gradient of average Chl *a* in the upper 20 m layer (Fig. 6c), the diurnal cycle can be better examined with a graph of Chl *a* deviations (calculated against the daily averages at each depth) in a time–depth plot (Fig. 6d). The maximum Chl *a* values at 6–12 m were observed at 9 p.m. and the minimum at 3 p.m., while the maximum and minimum at 14–20 m were observed at 3 a.m. and 6–9 p.m., respectively. On the basis of the described Chl *a* dynamics, we suggest that, on average, after accumulation at the very surface at 3 p.m. the phytoplankton experienced downward migration reaching 20 m at 3 a.m., whereas

sinking was faster in the almost mixed upper layer (see vertical density distribution in Fig. 6d). After 3 a.m., some part of the community continued downward migration and penetrated into the water layer below the strongest density gradient while some part returned, reaching the surface at noon. Although we do not have clear evidence that phytoplankton appearing below the thermocline returned, it can be assumed that part of the deep population could join the maximum at about 20 m depth at 3 a.m. the next day and thus could have a bi-diurnal migration pattern.

To illustrate the described diurnal (and possible bi-diurnal) migration pattern, a series of consecutive vertical profiles of Chl *a* collected from noon on 26 July to 6 p.m. on 27 July is presented (Fig. 7). According to this example, at 9 p.m., the maximum in the vertical profile of Chl *a* was measured at 4.6 m. During the night, the Chl *a* maximum was deeper and was at 10.4 m at midnight and 14.3 m at 3 a.m. Three hours later, Chl *a* was distributed almost evenly in the whole water layer from 3 to 25 m with local maxima at 5.5 and 19.2 m. Within the next 6 h, two clear maxima developed—one near the surface (at 3 m) and the other at 27 m. At the same time, Chl *a* concentration decreased in the water layer between 13 and 23 m. The strongest density gradient during the described period was at 21–23 m. The presented evolution of Chl *a* distribution showed that the Chl *a* maximum moves downward during the night with an approximate speed of 1.6 m h^{-1} . The splitting of the community into two at 9 a.m. could indicate that part of the community returns to the sea surface and the other part continues downward migration until getting below the thermocline.

On 11–12 August, vertical sampling was performed in the vicinity of the buoy profiler aboard the research vessel

Fig. 7 Changes in the vertical distribution of Chl *a* at the buoy station from noon on 26 July until 9 p.m. on 27 July 2009. Values on the x-axis are correct for the first profile. Each subsequent profile is shifted to the right by 3 mg m^{-3} in relation to the preceding one



SALME—from 5 p.m. until 9 a.m. with a time resolution of 2–3 h. No Chl *a* fluorescence maxima were found below the seasonal thermocline and no temporal changes of profiles, which could be related to the vertical migration of phytoplankton, were observed. The contribution of cyanobacteria and dinoflagellates to the phytoplankton total wet weight biomass at 2 m was 53–87% and 6–27%, respectively, while *H. triquetra* biomass was low—it formed only 2–13% of phytoplankton biomass. However, the temporal changes in the vertical distribution of *H. triquetra* were in accordance with a diurnal migration pattern—the biomass maximum was at a depth of 2 m in the evening, at 10–15 m at midnight and at 3 a.m. and in the upper 5 m layer by 6 a.m. It has to be noted that although fluorescence profiles did not show maxima in the thermocline, we observed relatively high biomass of heterotrophic dinoflagellates at 20 m depth in all samples. The phytoplankton biomass was between 600 and 1,400 mg m⁻³ and the heterotrophic dinoflagellates formed 84–99% of the total wet weight.

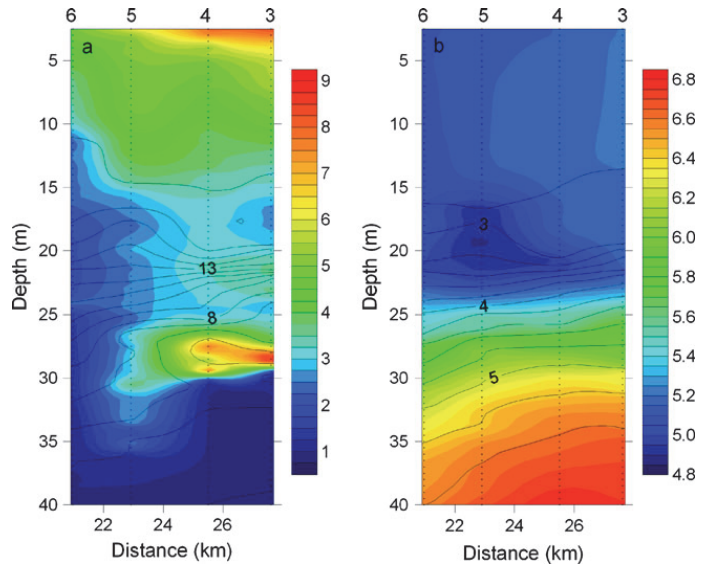
3.5 Sub-surface patches of high phytoplankton biomass

On 28 July, when the maximum Chl *a* concentration was recorded by the autonomous profiler in the sub-surface layer (at 32 m at 9 a.m.), a north–south-oriented transect of four stations close to the mooring was sampled twice—2–3.5 h later and 5.5–7 h later. Extremely layered vertical distributions of temperature, salinity and Chl *a* with

substantial horizontal gradients of all parameters in the thermocline were recorded (Fig. 8). Isopycnals below the thermocline (below the depth of the strongest density gradient) had a shallower position in the northern part of the section and a cold intrusion extended from the north towards the buoy profiler. There was a less saline layer (well visible at station 5) in the upper part of the thermocline beneath the more saline surface layer (Fig. 8b). A relatively intense sub-surface Chl *a* maximum layer, which was thinner and more intense in the northern part and thicker (consisting of a few sub-layers) near the buoy profiler (station 5), was detected. At the two northernmost stations, the maximum Chl *a* concentration and thickness of the layer (determined as described by Lips et al. (2010)) were 9.9 mg m⁻³ and 3.9 m and 9.2 mg m⁻³ and 5.0 m, respectively. The sub-surface Chl *a* maximum layer coincided with the cold intrusion. The vertical distribution of nutrients revealed that nitrates–nitrites were depleted (concentration <0.1 μM) and only low concentrations of phosphates were measured (0.15 μM) in the water column above the Chl *a* maximum layer while relatively high concentrations were measured in it (0.5 μM of NO₃⁻+NO₂⁻ and 0.54 μM of PO₄³⁻).

Phytoplankton had the highest total biomass (2,300 mg m⁻³) in the surface layer at the northernmost station (station 3), where at a depth of 2 m, 75% of the biomass was dinoflagellates (69% of total wet weight was formed by *H. triquetra*) and 20% cyanobacteria. At 28 m depth, in the Chl *a* maximum layer, a phytoplankton biomass of 1,700 mg m⁻³

Fig. 8 Vertical sections of Chl *a* and temperature (a; colour scale, milligram per cubic metre and solid lines, degree Celsius, respectively), and salinity and density anomaly (b; colour scale, without units and solid lines, kilogram per cubic metre, respectively) along a north–south transect in the vicinity of the buoy profiler (station 5 was located close to the buoy) sampled on 28 July. Distance in kilometres corresponding to the distance in Fig. 4 is shown on the x-axis and station numbers are indicated above the plots



was measured. About 90% of biomass in this layer was formed by dinoflagellates—half of it by *H. triquetra* and the other half by larger heterotrophic species. By microscopic examination, it could be seen that heterotrophic species were feeding on *H. triquetra*. At the next station (located 2.2 km southward), the total biomass at 28 m depth was slightly lower (1,200 mg m⁻³), but it was mostly (96%) formed by dinoflagellates with a clear dominance of *H. triquetra* (90%). Near the buoy profiler (station 5), the biomass maximum was thicker and the biomass values at the sampling depths of 25–31 m were lower (340–600 mg m⁻³). *H. triquetra* formed 50–83% of total wet weight biomass. At the same time in the surface layer, the biomass (1,600 mg m⁻³) was dominated by cyanobacteria (51%) while the contribution of dinoflagellates to the total wet weight biomass was 43% (*H. triquetra* formed 29% and *D. acuminata* 10%).

Similar to that described above, a layered structure of vertical temperature, salinity and Chl *a* distribution was observed during the second sampling on 28 July. A very intense sub-surface phytoplankton biomass maximum was detected at 33 m (at station 9, which was close to station 4 in Fig. 8). The maximum Chl *a* concentration and thickness of the layer detected at the measured vertical Chl *a* profile were 26.6 mg m⁻³ and 1.3 m, respectively. This Chl *a* maximum layer coincided with a warm intrusion, which occurred below the cold intrusion where the Chl *a* maximum at stations 3 and 4 was detected 4 h earlier (Fig. 8). Phytoplankton counting gave a very high abundance and biomass of *H. triquetra* in the water sample collected from the maximum layer at station 9—2,523,000 cells l⁻¹ and 3,390 mg m⁻³ (forming 95% of the total phytoplankton biomass). The Chl *a* fluorescence value measured when the water bottle was closed corresponded to a Chl *a* value of 42.8 mg m⁻³.

On 31 July, the transect consisting of four stations was sampled again. In the surface layer, dinoflagellates and cyanobacteria formed an equal share (close to 50%) of the total phytoplankton biomass at all stations. Only moderate sub-surface maxima were observed with a *H. triquetra* biomass of up to 300 mg m⁻³. In most samples from 25 to 32 m, the heterotrophic dinoflagellates were dominant in the phytoplankton community with biomasses of between 500 and 600 mg m⁻³.

4 Discussion

High-resolution vertical profiling has revealed remarkable variations of the vertical distribution of temperature, salinity and Chl *a* in the Gulf of Finland in July–August 2009. Vertical dynamics of phytoplankton was described to a large extent using Chl *a* fluorescence data. It is well known that the fluorescence quenching effect can influence

the results at high daytime irradiances (Sackmann et al. 2008), even up to 30%. During our study, the daily maximum Chl *a* values near the sea surface were recorded at daytime and the minimum values at night (Fig. 6). Thus, if the quenching effect could influence the fluorescence data, the amplitude of diurnal variation at the sea surface could be underestimated, rather than overestimated. In addition, the Secchi depth measured aboard the research vessel on 28 July, 31 July and 11–12 August did not exceed 4 m. Consequently, the euphotic depth in the study area was about 12.8 m (or less) in late July–early August 2009. It allows us to assume that the quenching effect could not affect the Chl *a* fluorescence measurements in the sub-surface layer where, on average, the Chl *a* maximum was observed at 3 a.m. and the minimum at 3 p.m.

We explain the observed changes in vertical dynamics of phytoplankton by prevailing meteorological and oceanographic forcing and related shifts between dominant species/taxonomic groups of phytoplankton. The most prominent variations in the vertical Chl *a* distribution were observed in late July–early August when the phytoplankton community was dominated by *H. triquetra*. While at our measurement site this period was relatively short, *H. triquetra* was the dominant species in the community in the northern Gulf by early July and in the central Gulf by mid-July. Thus, similar migration patterns of phytoplankton as observed in the southern Gulf in late July–early August and formation of sub-surface layers of high phytoplankton biomass could have occurred in those areas for a longer period. This suggestion has to be taken into account when extrapolating our observational results over the larger area in the Gulf of Finland, e.g. when estimating the role of sub-surface biomass maxima in summer phytoplankton assemblages. One question to be answered is why the dominance of *H. triquetra* in the phytoplankton community at our measurement site was restricted only to late July and first days of August. Vertical migration of phytoplankton was evident also in the first half of July when euglenophytes (*Eutreptiella* spp.) dominated the phytoplankton community in the UML. Although we did not collect samples for phytoplankton counting from the sub-surface layer to confirm that *Eutreptiella* spp. were dominating there as well, the revealed diurnal migration pattern is in accordance with earlier findings on migration behaviour of these species. Figueroa et al. (1998) have shown that *Eutreptiella* sp. aggregated at the surface in maximum numbers at noon and migrated through the pycnocline (at depth of 6 m) at night. The winds favourable for the development of upwelling events near the southern coast of the Gulf of Finland prevailed, and the seasonal thermocline had a quite shallow position in early July. Most probably, the latter and related shallow position of nutriclines (e.g. Laanemets et al. 2004) created favourable conditions also for smaller sized species,

which should have lower swimming speeds than bigger sized species (e.g. Smayda 2010), to undertake nutrient-gathering migrations to nutrient-rich layers.

In the beginning of August, a secondary thermocline developed close to the sea surface and the UML temperature increased to 19.2°C. It resulted in the dominance of cyanobacteria and appearance of *N. spumigena* in the community. This observational result confirms that the vertical stratification in the surface layer is favourable for cyanobacteria, especially for *N. spumigena* (e.g. Kanoshina et al. 2003). Thus, the nitrogen uptake strategy of dinoflagellates by vertical migration through the secondary and seasonal thermoclines seems to be less competitive than the nitrogen fixation by cyanobacteria in warm stratified surface waters. Deepening of the UML, observed after 16 August at the buoy station due to the development of downwelling near the southern coast, did not result in *H. triquetra* dominance and related migration pattern. Most probably, in this case, the nutrient-rich waters were pushed too deep, to depths >35–40 m. A reason for the observed overall decline in phytoplankton biomass in the second half of August (Fig. 5) could be the deep UML as well; the UML depth was about two times deeper than the estimated euphotic depth.

Many dinoflagellates are known to be capable of vertical migration, and the measured maximum swimming speeds of different phytoplankton species range from 139 to 1,667 $\mu\text{m s}^{-1}$ (Smayda 2010). Swimming enables nutrient-deficient cells to migrate to the deeper layers where they dark-assimilate NO_3^- for photosynthetic incorporation upon swimming back up into the euphotic zone (Fauchot et al. 2005). The ability of *H. triquetra* to uptake nitrate in the dark was shown by Paasche et al. (1984). The maximum swimming speed of *H. triquetra*, as measured by laboratory experiments, is as high as 467 $\mu\text{m s}^{-1}$ (average 370 $\mu\text{m s}^{-1}$; Jeong et al. 2002). We presented in situ evidence that the summer phytoplankton dominated by the dinoflagellate *H. triquetra* in the stratified Gulf of Finland experiences vertical migration, and the speed of downward migration could be as high as 1.6 mh^{-1} (equal to 444 $\mu\text{m s}^{-1}$). During mesocosm experiments conducted by Olli and Seppälä (2001), clear diurnal vertical migration of *H. triquetra* was detected in the 11-m water column in 24 h. We observed a similar diurnal migration pattern by direct measurements on 11–12 August in a situation when *H. triquetra* had low biomass in the community dominated by cyanobacteria, and the vertical migration range of cells was only 15 m.

During the period of dominance of *H. triquetra* in late July–early August, the detectable amounts of nutrients were measured below the strongest density gradient at depths >25 m. The estimated mean spherical diameter of *H. triquetra* in the sub-surface biomass maxima layers was

21.5 μm . As motility progressively increases with cell size up to a threshold of 35 μm (Kamykowski et al. 1992), the depths of 28–34 m, where phytoplankton biomass maxima were observed, are in principle reachable by diurnal migratory behaviour. However, the observed swimming speed of 1.6 mh^{-1} is not enough for cells to sink to a depth >25 m, uptake nitrogen, and swim back to the surface in 24 h. Furthermore, we have measured many profiles with two vertically separated maxima of Chl *a* during daytime. Therefore, we suggest that the migration cycle for those cells of *H. triquetra* which reach the high nutrient resources below the thermocline could be longer, e.g. bi-diurnal. Ralston et al. (2007) have shown in their modelling exercise that asynchronous vertical migrations in cases when the migration cycle cannot be completed in 24 h could result in a bimodal vertical distribution of phytoplankton cells. As suggested by Townsend et al. (2005), the cells that swim downward would most likely stop upon encountering the nitracline, and likewise, those swimming upwards would concentrate near the surface. Our results indicate that the downward migration is clearly synchronous while the upward migration could be asynchronous and depend on the time period needed to reach the nutrient-rich layer and uptake enough nitrogen.

Dortch and Maske (1982) have proposed that only part of the population migrates to the full depth necessary to reach the nitracline in response to the depletion of internal stores of nitrogen. We also showed the splitting of the community into two. One half stayed in the upper mixed layer and was moving to the surface by noon, while the other half continued downward migration (Fig. 7). The downward migrating phytoplankton cells did not stop at the depths with the strongest density gradient and formed patches of high biomass just a few metres below h_{maxN} . The presence of phytoplankton maxima below h_{maxN} has been shown in the Adriatic Sea (Revelante and Gilmartin 1995), indicating that the formation of these maxima are not connected to the accumulation of organisms at a marked density gradient as it has been reported in many other studies (e.g. Velo-Suarez et al. 2010). The latter and the fact that in these layers high enough nutrient concentrations were measured support the suggestion that the downward migration was caused by physiological needs of phytoplankton. The split of one species community during migration and the formation of a double peak in vertical profiles was demonstrated by Olli and Seppälä (2001) in their mesocosm experiment and found by Holligan et al. (1984) in field measurements. The downward movement of dinoflagellates has been suggested to be triggered by inorganic nutrient depletion in the surface layers. However, laboratory experiments (Olli and Seppälä 2001; Jephson and Carlsson 2009) have shown downward migrations to be present also in nutrient-sufficient conditions.

In many studies, it has been argued that physical processes are able to shape the vertical distribution of phytoplankton into thin layers of high biomass (e.g. Veloso-Suarez et al. 2010). Sullivan et al. (2010) have concluded that even though physical forcing affects the spatial-temporal dynamics of thin phytoplankton layers, biological processes and behaviour can be equally, if not more important. Ross and Sharples (2007) showed that motility could give an advantage to the phytoplankton in competing for the nutrients in the thermocline. Our results indicate that the sub-surface maxima of *H. triquetra* are fuelled by synchronous downward migration of cells at night. Since the physical processes in the tideless Gulf of Finland do not reveal a diurnal cycle, we suggest that this migration pattern occurs as an adaptation of phytoplankton to migrate to the deeper nutrient resources at low irradiances (when photosynthesis rate is low) in response to the inorganic nutrient depletion at the surface. On the other hand, we suggest that the success of this strategy depends on hydrophysical background, mostly at a mesoscale, e.g. the appearance of a more saline water mass, which could be interpreted as an anticyclonic eddy, at the study site coincided with the clear vertical migration of phytoplankton and formation of biomass maxima in the sub-surface layer. Similar suggestions on the importance of mesoscale processes were made in the earlier studies by Kononen et al. (2003) and Lips et al. (2010).

The most intense sub-surface maxima observed in our study area were associated with the intrusions (with both, warm and cold ones) indicating that physical processes at a sub-mesoscale are also important. However, since on some occasions the biomass is much higher in the sub-surface maxima than that in the surface layer, it is not possible to explain the phenomenon by physical processes alone. The question in this context is why the downward migration of cells stops at a very restricted depth range? Thus, we still do not know the exact mechanisms of formation of these very thin layers with a very high biomass. We have not discussed the possible influence of grazing, although direct evidence of feeding of large heterotrophic dinoflagellates on *H. triquetra* was found. A topic which has to be studied in more detail in the future is related to the heterotrophic communities in the sub-surface layers in general. Local biomass maxima of heterotrophic phytoplankton at most sampling stations were detected in the thermocline, but the observed biomasses were not as high as for *H. triquetra*. Equipment suitable to locate similar layers of very high biomass of heterotrophic phytoplankton has to be used in these studies.

5 Conclusions

We have observed pronounced oceanographic processes and related changes in the horizontal and vertical distribu-

tions of temperature; salinity; and Chl *a* in the Gulf of Finland in July and August 2009. Based on our observations, we suggest that the conditions caused by the prevailing atmospheric and oceanographic forcing (wind, dynamics of vertical stratification, basin-wide, mesoscale and sub-mesoscale processes) are preferred by certain species/taxonomic groups (small flagellates, dinoflagellate *H. triquetra* or cyanobacteria) and explain the migration patterns of phytoplankton. Downward migration of *H. triquetra* with a speed up to 1.6 mh^{-1} and splitting of the community into two, resulting in a bimodal vertical distribution of organisms were documented. The areas and periods where and when this migration pattern and the sub-surface biomass maxima occur are suggested to be defined by mesoscale processes and vertical stratification of the water column. To understand the role of the sub-surface phytoplankton biomass maxima in the total primary production and internal nutrient cycling in stratified estuaries, further studies are needed.

Acknowledgements This work was financially supported by the Estonian Science Foundation (grant no. 6955). We thank the Finnish Meteorological Institute for providing wind data at Kalbådagrund station, AS Tallink Group for cooperation on Ferrybox measurements and our colleagues and crew members for participation in the field measurements.

References

- Alenius P, Myrberg K, Nekrasov A (1998) The physical oceanography of the Gulf of Finland: a review. *Boreal Environ Res* 3:97–125
- APHA (1992) APHA, AWWA, and WPCF standard methods for the examination of water and wastewater, 18th edn. American Public Health Association, Washington
- Dortch Q, Maske H (1982) Dark uptake of nitrate and nitrate reductase activity of a red-tide population off Peru. *Mar Ecol Prog Ser* 9:299–303
- Elken J, Raudsepp U, Lips U (2003) On the estuarine transport reversal in deep layers of the Gulf of Finland. *J Sea Res* 49:267–274
- Fauchot J, Levasseur M, Roy S (2005) Daytime and nighttime vertical migrations of *Alexandrium tamarens* in the St. Lawrence estuary (Canada). *Mar Ecol Prog Ser* 296:241–250
- Figuerola FL, Niell FX, Figueiras FG, Villarino ML (1998) Diel migration of phytoplankton and spectral light field in the Ría de Vigo NW Spain. *Mar Biol* 130:491–499
- HELCOM (1988) Guidelines for the Baltic monitoring programme for the third stage. Part D. Biological determinants. *Baltic Sea Environ Proc* 27D:1–161
- HELCOM (2002) Environment of the Baltic Sea area 1994–1998; background document. *Baltic Sea Environ Proc* 82B:1–215
- Holligan PM, Balch WM, Yentsch CM (1984) The significance of subsurface chlorophyll, nitrate and ammonium maxima in relation to nitrogen for phytoplankton growth in stratified waters of the Gulf of Maine. *J Mar Res* 42:1051–1073
- Jeong HJ, Yoon JY, Kim JS, Yoo YO, Seong KA (2002) Growth and grazing rates of the prostomidian ciliate *Tiarina fusus* on red tide and toxic algae. *Aquat Microb Ecol* 28:289–297

- Jephson T, Carlsson P (2009) Species- and stratification-dependent diel vertical migration behaviour of three dinoflagellate species in a laboratory study. *J Plankton Res* 31:1353–1362
- Kamykowski D, Reed RE, Kirkpatrick GJ (1992) Comparison of sinking velocity, swimming velocity, rotation and path characteristics among six marine dinoflagellate species. *Mar Biol* 113:319–328
- Kanoshina I, Lips U, Leppänen JM (2003) The influence of weather conditions (temperature and wind) on cyanobacterial bloom development in the Gulf of Finland (Baltic Sea). *Harmful Algae* 2:29–41
- Kononen K, Kuparinen J, Mäkelä K, Laanemets J, Pavelson J, Nömmann S (1996) Initiation of cyanobacterial blooms in a frontal region at the entrance of the Gulf of Finland, Baltic Sea. *Limnol Oceanogr* 41:98–112
- Kononen K, Huttunen M, Hällfors S, Gentien P, Lunven M, Huttala T, Laanemets J, Lilover M, Pavelson J, Stips A (2003) Development of a deep chlorophyll maximum of *Heterocapsa triquetra* Ehrenb. at the entrance to the Gulf of Finland. *Limnol Oceanogr* 48:594–607
- Laanemets J, Kononen K, Pavelson J, Poutanen EL (2004) Vertical location of seasonal nutriclines in the western Gulf of Finland. *J Mar Syst* 52:1–13
- Lips I, Lips U (2008) Abiotic factors influencing cyanobacterial bloom development in the Gulf of Finland (Baltic Sea). *Hydrobiologia* 614:133–140
- Lips I, Lips U (2010) Phytoplankton dynamics affected by the coastal upwelling events in the Gulf of Finland in July–August 2006. *J Plankton Res* 32:1269–1282
- Lips I, Lips U, Liblik T (2009) Consequences of coastal upwelling events on physical and chemical patterns in the central Gulf of Finland (Baltic Sea). *Cont Shelf Res* 29:1836–1847
- Lips U, Lips I, Liblik T, Kuvaldina N (2010) Processes responsible for the formation and maintenance of sub-surface chlorophyll maxima in the Gulf of Finland. *Estuar Coast Shelf Sci* 88:339–349
- Olli K, Seppälä J (2001) Vertical niche separation of phytoplankton: large-scale mesocosm experiments. *Mar Ecol Prog Ser* 217: 219–233
- Paasche E, Bryceson I, Tangen K (1984) Interspecific variation in dark nitrogen uptake by dinoflagellates. *J Phycol* 20:394–401
- Pavelson J, Kononen K, Laanemets J (1999) Chlorophyll distribution patchiness caused by hydrodynamical processes: a case study in the Baltic Sea. *ICES J Mar Sci* 56S:87–99
- Ralston DK, McGillicuddy DJ, Townsend DW (2007) Asynchronous vertical migration and bimodal distribution of motile phytoplankton. *J Plankton Res* 29:803–821
- Revelante N, Gilmartin M (1995) The relative increase of larger phytoplankton in a subsurface chlorophyll maximum in Northern Adriatic Sea. *J Plankton Res* 17:1535–1562
- Ross ON, Sharples J (2007) Phytoplankton motility and the competition for nutrients in the thermocline. *Mar Ecol Prog Ser* 347:21–38
- Sackmann BC, Perry MJ, Eriksen CC (2008) Seaglider observations of variability in daytime fluorescence quenching of chlorophyll-*a* in Northeastern Pacific coastal waters. *Biogeosciences Discuss* 5:2839–2865
- Shlitzer R (2010) Ocean data view, <http://odv.awi.de>. Accessed 15 Jul 2010
- Smayda TJ (2010) Adaptation and selection of harmful and other dinoflagellate species in upwelling system. Motility and migratory behaviour. *Prog Oceanogr* 85:71–91
- Sullivan JM, Donaghay PL, Rines JEB (2010) Coastal thin layer dynamics: consequences to biology and optics. *Cont Shelf Res* 30:50–65
- Townsend DW, Bennett SL, Thomas MA (2005) Diel vertical distributions of the red tide dinoflagellate *Alexandrium fundyense* in the Gulf of Maine. *Deep Sea Res Pt II* 52:2593–2602
- Utermöhl H (1958) Zur Vervollkommnung der quantitativen Phytoplanktonmethodik. *Mittelungen des Internationale Vereinigung für Theoretische und Angewandte Limnologie* 9:1–38
- Vahtera E, Laanemets J, Pavelson J, Huttunen M, Kononen K (2005) Effect of upwelling on the pelagic environment and bloom-forming cyanobacteria in the western Gulf of Finland, Baltic Sea. *J Mar Syst* 58:67–82
- Velo-Suarez L, Fernand M, Gentien P, Reguera B (2010) Hydrodynamic conditions associated with the formation, maintenance and dissipation of a phytoplankton thin layer in a coastal upwelling system. *Cont Shelf Res* 30:193–202
- Zhurbas V, Laanemets J, Vahtera E (2008) Modeling of the mesoscale structure of coupled upwelling/downwelling events and related input of nutrients to the upper mixed layer in the Gulf of Finland, Baltic Sea. *J Geophys Res* 113:C05004

Paper IV

Uiboupin, R., Laanemets, J., Sipelgas, L., Raag, L., Lips, I., Buhhalko, N. 2012. Monitoring the effect of upwelling on the chlorophyll *a* distribution in the Gulf of Finland (Baltic Sea) using remote sensing and in situ data. *Oceanologia*, 54(3), 395-419.

**Monitoring the effect
of upwelling on the
chlorophyll *a* distribution
in the Gulf of Finland
(Baltic Sea) using remote
sensing and in situ data***

doi:10.5697/oc.54-3.395
OCEANOLOGIA, 54 (3), 2012.
pp. 395–419.

© Copyright by
Polish Academy of Sciences,
Institute of Oceanology,
2012.

KEYWORDS
MERIS
MODIS
Upwelling
Chlorophyll *a*
SST
Baltic Sea
Gulf of Finland

RIVO UIBOUPIN*
JAAN LAANEMETS
LIIS SIPELGAS
LAURA RAAG
INGA LIPS
NATALIA BUHHALKO

Marine Systems Institute,
Tallinn University of Technology,
Akadeemia 15a, Tallinn 12618, Estonia;

e-mail: rivo.uiboupin@msi.ttu.ee

*corresponding author

Received 12 March 2012, revised 17 April 2012, accepted 8 May 2012.

Abstract

The spatio-temporal variability of chlorophyll *a* (Chl *a*) caused by a sequence of upwelling events in the Gulf of Finland in July–August 2006 was studied using remote sensing data and field measurements. Spatial distributions of sea surface temperature (SST) and Chl *a* concentration were examined using MODIS and MERIS data respectively. The MERIS data were processed with an algorithm

* The study was supported by the Estonian Science Foundation (grants No. 7467, No. 6752, No. 7633, No. 7581 & No. 8968). The remote sensing data were provided by ESA via Cat-1 project No. 6855.

The complete text of the paper is available at <http://www.iopan.gda.pl/oceanologia/>

developed by the Free University of Berlin (FUB) for case 2 waters. Evaluation of MERIS Chl *a* versus in situ Chl *a* showed good correlation ($r^2 = 0.67$), but the concentration was underestimated. The linear regression for a 2 h window was applied to calibrate MERIS Chl *a*. The spatio-temporal variability exhibited the clear influence of upwelling events and related filaments on Chl *a* distribution in the western and central Gulf. The lowest Chl *a* concentrations were recorded in the upwelled water, especially at the upwelling centres, and the highest concentrations (13 mg m^{-3}) were observed about two weeks after the upwelling peak along the northern coast. The areas along the northern coast of upwelled water (4879 km^2) on the SST map, and increased Chl *a* (5526 km^2) two weeks later, were roughly coincident. The effect of upwelling events was weak in the eastern part of the Gulf, where Chl *a* concentration was relatively consistent throughout this period.

1. Introduction

Remote sensing data have been widely used for monitoring the ecological and physical state of the Baltic Sea. Satellite imagery has been used for detecting interannual, seasonal and mesoscale variability of the sea surface temperature (SST) (Horstmann 1983, Gidhagen et al. 1987, Siegel et al. 1994, Krężel et al. 2005a, Siegel et al. 2006, Bradtke et al. 2010). Previous studies have demonstrated that remote sensing imagery can be used for the systematic monitoring of the chlorophyll *a* (Chl *a*) distribution and variability (Krężel et al. 2005b, Koponen et al. 2007, Kratzer et al. 2008). Coastal upwelling is an important process that brings cold, nutrient-rich deep water to the surface layer, and can be monitored using different remote sensing data (Krężel et al. 2005a, Lass et al. 2010). The combined use of SST and Chl *a* imagery, complemented by in situ measurements and wind information, provides a basis for describing and analysing the spatial variability of phytoplankton blooms promoted by upwelling.

The Gulf of Finland is an area of the Baltic Sea well known for frequent upwelling events (Kahru et al. 1995, Myrberg & Andrejev 2003, Lehmann & Myrberg 2008, Myrberg et al. 2008). Satellite SST data have shown that during the strongest upwelling events along the northern and southern coasts of the Gulf of Finland, the upwelled water can cover remarkably large areas, corresponding to about 40% and 20%, respectively, of the total surface area of the Gulf (which is about $29\,500 \text{ km}^2$) (Uiboupin & Laanemets 2009). During upwelling events the surface phytoplankton community is transported offshore and replaced by species normally resident in the upper part of the thermocline (Kanoshina et al. 2003, Vahtera et al. 2005, Lips & Lips 2010). Numerical simulations by Zhurbas et al. (2008) and field measurements by Lips et al. (2009) have shown that in the narrow, elongated Gulf of Finland, upwelling along one coast is accompanied by downwelling along the opposite coast, i.e. two longshore baroclinic jets and

their related thermohaline fronts develop simultaneously. The instability of a longshore baroclinic jet leads to the increasing development of filaments and eddies, and thus coastal offshore mixing, resulting in a substantial horizontal variability of the surface layer temperature, upwelled nutrients and phytoplankton/chlorophyll.

The spatio-temporal variability of hydrographic and biological-chemical parameters can be regularly monitored from autonomous ship-of-opportunity measurements that collect temperature, salinity and chlorophyll *a* fluorescence data, as well as water samples for nutrient and phytoplankton analysis, along fixed transects in the Baltic Sea (Rantajärvi et al. 1998, Lips & Lips 2008, Petersen et al. 2008). However, for obtaining information about the phytoplankton abundance/biomass, and surface distribution over large sea areas, remote sensing imagery is invaluable. The Baltic Sea (including the Gulf of Finland) comprises optically complex case 2 waters that are dominated by coloured dissolved organic matter, and it is therefore a considerable challenge to produce accurate estimates of water quality parameters from remote sensing imagery (Schroeder et al. 2007a, Sorensen et al. 2007, Kratzer et al. 2008). This optical complexity affects satellite Chl *a* retrievals, so it is important to validate the algorithm using in situ measurements. Satellite imagery with sufficient temporal resolution is regularly available from MERIS (Medium Resolution Imaging Spectrometer) and MODIS (Moderate Resolution Imaging Spectroradiometer) for the Baltic Sea region. MERIS was designed to monitor coastal waters (Doerffer et al. 1999), and it therefore has sufficient spectral resolution in the visible range to monitor turbid waters like the Baltic Sea. In principle, MERIS operates in a range enabling the detection of pigments like phycocyanin (cyanobacteria), which have specific absorption minima near wavelength 630 nm and local maxima at wavelength 650 nm (Kutser et al. 2006).

A series of upwelling events along the northern and southern coasts of the Gulf of Finland occurred in July–August 2006. Westerly winds were dominant in July, generating moderate upwelling along the northern coast of the Gulf. Easterly winds then prevailed during the whole of August, and as a result, very intense upwelling was observed along the southern coast. The upwelling events were well documented by several studies based on in situ measurements of physical, biological and chemical parameters (Suursaar & Aps 2007, Lips et al. 2009, Lips & Lips 2010). In addition, remote sensing data (MERIS and MODIS) are available from that period to monitor the variability of SST and phytoplankton chlorophyll *a* fields.

The objectives of this study were: (1) to validate the MERIS chlorophyll product retrieved with the Free University of Berlin (FUB) case 2 waters processor using in situ measurements of Chl *a*, and (2) to assess the spatial

and temporal variability of the Chl *a* field caused by consecutive upwelling events using MERIS data.

This paper is structured as follows: section 2 describes the in situ, remote sensing and wind data, as well as the methodology; in section 3, the comparability of in situ and satellite chlorophyll *a* data is evaluated, the sequence of upwelling events is described on the basis of MODIS SST, MERIS chlorophyll is compared with in situ chlorophyll *a*, and the upwelling-related variability of the chlorophyll *a* field from MERIS data is described; section 4 discusses the results of the SST and chlorophyll *a* surface distributions; the final conclusions are drawn in section 5.

2. Data and methodology

2.1. In situ data

The in situ data were obtained during five surveys (Table 1) conducted along the same transect between Tallinn and Helsinki (Kuvaldina et al. 2010). Water samples for phytoplankton and Chl *a* analysis were collected from 14 stations, each about 5.2 km apart (Figure 1). Three (but two in the case of the shallow upper mixed layer) water samples were taken from the upper mixed layer (UML, from a depth of 1 m down to the seasonal thermocline) to form a pooled sample for each station. The depth of the UML was determined from the CTD profile, which preceded water sampling. Chl *a* content was measured spectrophotometrically (Thermo Helios γ ; photometric accuracy: ± 0.005 A at 1 A) from the pooled samples in the laboratory (HELCOM 1988). On 19–20 July, two (TH19, TH21) out of five pooled samples were cloud-free on the satellite imagery. Because of inclement weather conditions, only surface samples ($n = 8$) were collected at stations TH1–TH15.

Phytoplankton species composition and biomass were analysed for each survey from pooled samples (Lips & Lips 2010).

Table 1. In situ sampling and MERIS acquisition dates, times (UTC) and number of samples used (N) in July–August 2006. The figures in brackets indicate the number of samples collected within the 2 h interval from the satellite overpass. On 19–20 July, 2 pooled samples and 8 surface samples were collected

Sampling date	N	MERIS date	MERIS time
11 Jul.	14 (3)	11 Jul.	9.35
19–20 Jul.	10	18 Jul.	9.15
25 Jul.	14 (4)	25 Jul.	8.55
8 Aug.	12	7 Aug.	8.46
15–16 Aug.	9	16 Aug.	9.03

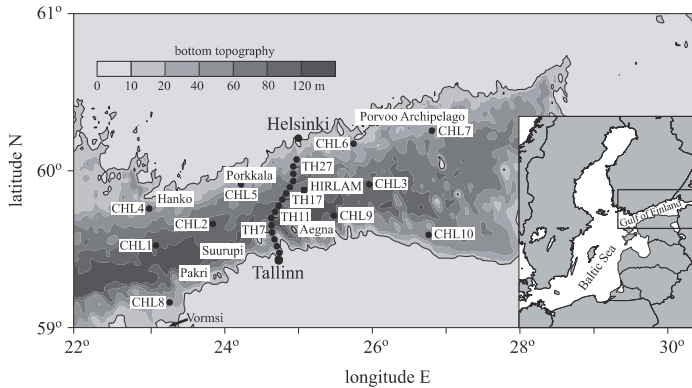


Figure 1. Map of the study area in the Gulf of Finland. The solid circles (●) represent the locations of the in situ sampling stations (TH1–TH27) and the locations of the MERIS chlorophyll time series (CHL1–CHL10, TH7 and TH27). The solid square (■) represents the location of the HIRLAM grid point where wind data were extracted. The bottom topography is drawn from the gridded topography in metres (Seifert et al. 2001)

2.2. MERIS data

MERIS reduced-resolution (about 1×1 km) images from 10 July to 18 August 2006 (altogether 31 sufficiently cloud free images) were used to analyse the spatio-temporal variability of the Chl *a* field. The MERIS images were processed using an algorithm developed by FUB for case 2 waters (Schroeder et al. 2007a, b) to apply an atmospheric correction and to obtain the reflectance values used to calculate the Chl *a* concentration. For the purposes of comparison, we also calculated Chl *a* and reflectance values using the case 2 regional water (C2RW) processor (Doerffer & Schiller 2007).

To compare the MERIS and in situ Chl *a* data, two time frames were selected at 24 h and 2 h intervals (before, or after) from the satellite overpass (Table 1). According to Kratzer et al. (2008) a 2 h window is sufficient for validating satellite Chl *a* measurements with in situ data. The MERIS image pixel covering the location of the sampling station within the given time window was extracted.

To evaluate the suitability of MERIS data for the detection of moderate concentrations of cyanobacteria, the normalized reflectance spectra were calculated according to Wu (2004).

For the detection of surface phytoplankton accumulations a Maximum Chlorophyll Index (MCI) was calculated for each MERIS image using the algorithm provided in Gower et al. (2008).

2.3. MODIS data

To determine the extent of the upwelling zone and to describe the temporal course of SST at selected locations, MODIS data (standard level 2 MODIS SST products) from 10 July to 18 August 2006 were used (<http://oceancolor.gsfc.nasa.gov>). Altogether 200 MODIS/Terra and MODIS/Aqua images (1×1 km pixel spacing) were examined in order to extract the SST data from 60 images that were sufficiently cloud-free.

2.4. Wind data

Wind-induced mixing largely determines the distribution of phytoplankton in the upper layer. To evaluate the comparability of satellite and in situ Chl *a* measurements, wind data from the version of HIRLAM (High Resolution Limited Area Model) of the Estonian Meteorological and Hydrological Institute (Männik & Merilain 2007) were interpolated to the location ($25^{\circ}7.5'E$, $59^{\circ}51.9'N$) close to the measurement transect in July–August 2006 (Figure 1). The spatial resolution of HIRLAM is 11 km, and the forecast interval of 1 h ahead of 54 h is recalculated after every 6 h. To characterize wind-induced mixing we used the depth of the turbulent Ekman boundary layer estimated by the formula $h = 0.1u_* / f$ (Csanady 1982), where $u_* = (\tau / \rho_w)^{1/2}$ is the friction velocity, $\tau = \rho_a C_a u^2$ is the wind stress, $\rho_a = 1.3 \text{ kg m}^{-3}$ is the air density, $C_a = 1.2 \times 10^{-3}$ is the dimensionless wind drag coefficient, u is the wind speed, $\rho_w = 1005 \text{ kg m}^{-3}$ is the water density, and $f = 1.25 \times 10^{-4} \text{ s}^{-1}$ is the Coriolis parameter.

3. Results

3.1. Comparability of in situ and satellite Chl *a*

Generally speaking, remote sensing imagery represents the situation at the sea surface. Variable wind conditions prevailed during July and August, whilst wind speeds were mainly moderate but with some gusts over 10 m s^{-1} (Figure 2b). In this study, the pooled sample represents the UML, and therefore we suggest that these two datasets are comparable if the depth of the turbulent Ekman boundary layer largely persists during the time interval between the acquisition of the MERIS image and the collection of the water samples. The average UML depths estimated from the CTD profiles within

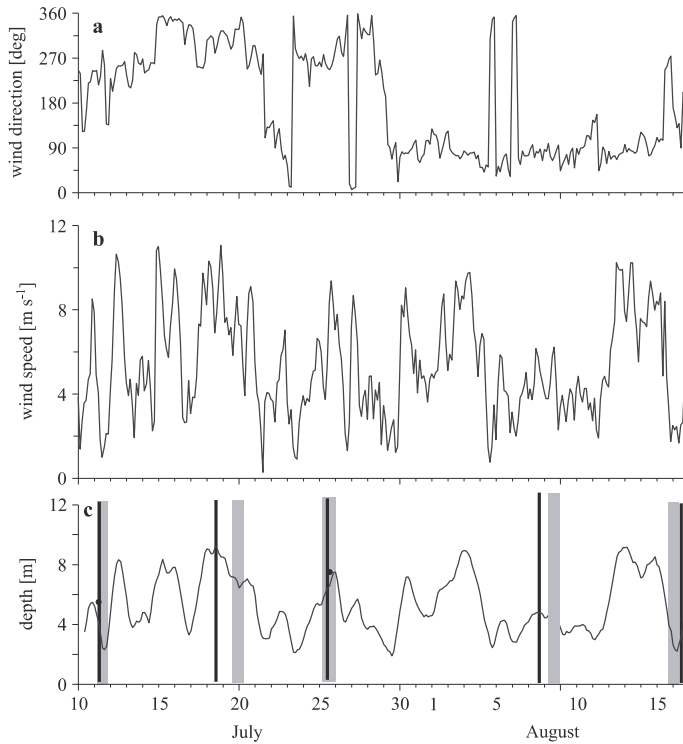


Figure 2. Wind direction (a), wind speed derived from HIRLAM data in July–August 2006 (b), depth of turbulent Ekman boundary layer (c). The grey rectangles mark the time of in situ measurements and the bold lines mark the times of MERIS image acquisition. The black dots represent the UML depths estimated from CTD measurements during the 2 h window on 11 and 25 July

the 2 h windows on 11 July (5.5 m) and 25 July (7.5 m) coincided well with the UML depths estimated from HIRLAM wind data (Figure 2c).

Comparability of in situ and MERIS Chl *a* data is also supported by the MCI calculated from all the MERIS data used. The MCI showed that no surface algal accumulations were observed during the study period. The highest MCI values were observed on 6 August 2006, when a maximum MCI value of $0.9 \text{ mW}/(\text{m}^2 \text{ sr nm})$ was recorded at the location of a filament at the entrance to the Gulf of Finland. The MCI index was close to zero most of the time.

3.2. Upwelling events in July–August

Westerly winds dominated in the Gulf area from 10 to 29 July (Figure 2a). The development of upwelling along the northern coast of the Gulf was observed from 10 July (Figures 3 and 5a), and the temperature difference between the upwelling and the surrounding water was around 5°C for most of the time, according to the MODIS SST data. However, the temperature difference was larger for the upwelling centres because of the

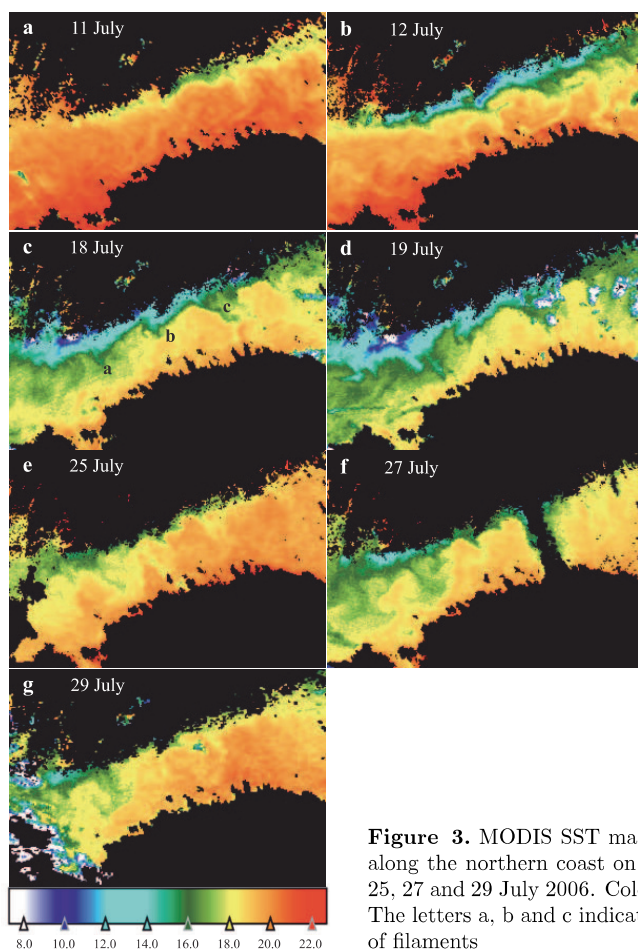


Figure 3. MODIS SST maps of upwelling along the northern coast on 11, 12, 18, 19, 25, 27 and 29 July 2006. Colour scale in °C. The letters a, b and c indicate the locations of filaments

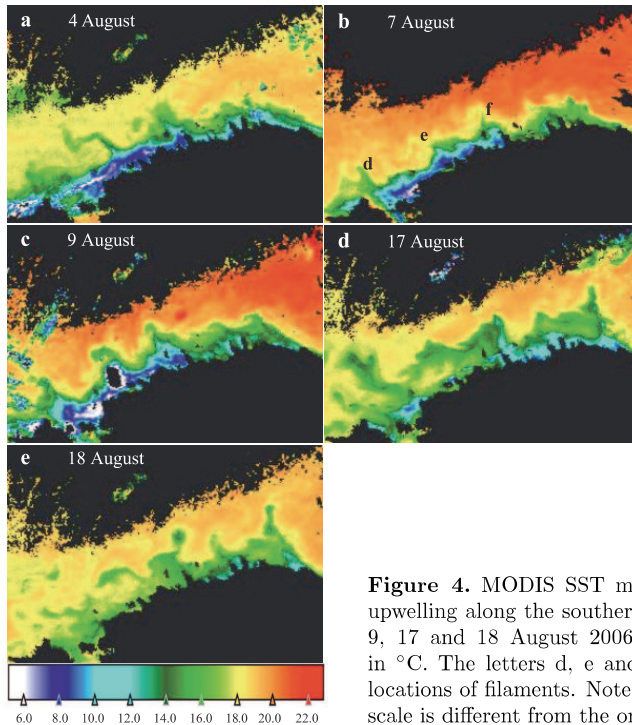


Figure 4. MODIS SST maps of stronger upwelling along the southern coast on 4, 7, 9, 17 and 18 August 2006. Colour scale in °C. The letters d, e and f indicate the locations of filaments. Note that the colour scale is different from the one in Figure 3

significantly lower temperature in the upwelled water. On 12 July the water temperature in the upwelling centre near the Porkkala Peninsula dropped to 8°C (Figure 3b). At the peak of upwelling on 19 July, the upwelling centre was near the Hanko Peninsula (due to the NW wind), and the temperature dropped to 6°C (Figures 3d and 5a), whilst in the middle of the Gulf the temperature was around 16°C, and near the southern coast it was over 18°C (Figure 3d). In the Porkkala region, where the upwelling centre was located on 12 July, the temperature rose to 13°C by 19 July. Relaxation of upwelling along the northern coast started after 20 August as a result of a change in wind forcing (Figure 2). The temperature in the upwelling zone on 25 and 27 July was then in the 14–16°C range, and the surrounding area had temperatures of around 19°C (Figures 3e and f). Because of the start of the upwelling relaxation after 20 July, cold filaments developed off the Hanko and Porkkala Peninsulas, and off the Porvoo Archipelago during the upwelling along the northern coast (Figure 3c).

After 29 July, easterly winds were dominant in the Gulf of Finland area until 16 August (Figure 2a), and as a result, a zone of upwelling formed along the southern coast (Figure 4). The strongest such zone developed along the NW coast of Estonia, from Vormsi Island to Aegna Island, with several upwelling centres near the Pakri Islands, Vormsi Island and off the coast of the Suurupi Peninsula, where the minimum temperature of the upwelled water was about 2°C (Figure 4 and 5b). The temperature difference between the upwelled and the surrounding water was as much as 18°C (Figures 4 and 5b), and the upwelled water covered 31% of the western Gulf area

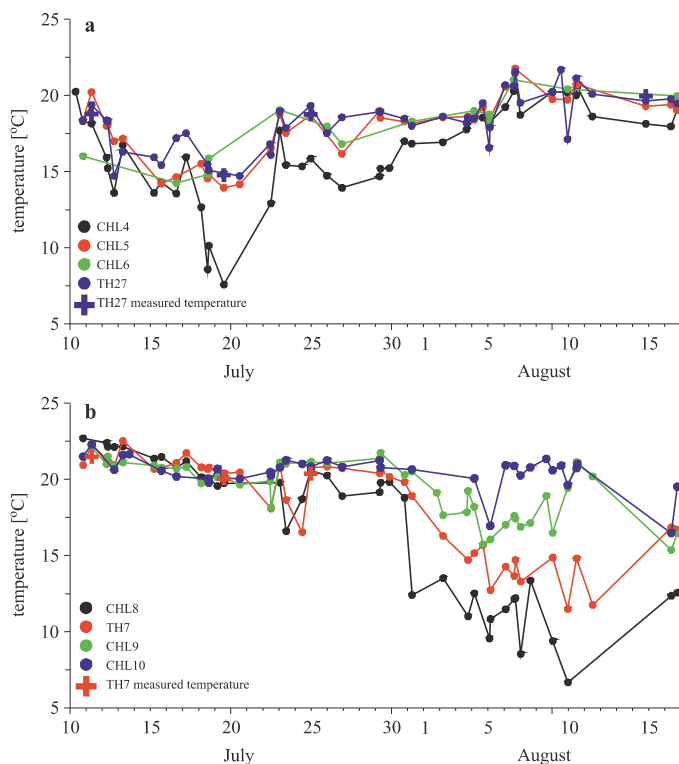


Figure 5. Temporal courses of surface layer temperature (MODIS SST) from 10 July to 16 August 2006 at stations CHL4, CHL5, CHL6 and TH27 (northern part of the Gulf) (a) and at stations CHL8, CHL9, CHL10 and TH7 (southern part of the Gulf) (b). The in situ surface temperature (bold cross) is given for stations TH7 and TH27

(22–26°E) on 9 August. After 16 August, the wind turned to the S and SW (data not shown), thus causing the upwelling to relax. Several cold upwelling filaments developed along the southern coast between longitudes 23 and 27°E, and a few of them transformed into eddies (Figure 4). The filaments were persistent at three locations: north of Hiiumaa, and off Pakri and Tallinn (Figure 4b).

3.3. Evaluation of the FUB Chl *a* processor using in situ Chl *a*

In situ Chl *a* concentrations along the transect varied in a wide range from 1.57 to 15.54 mg m⁻³ during the period of field measurements (Figure 6). Low Chl *a* values were observed during the first half of July in the upwelling region along the northern coast. From 25 July, when upwelling along the northern coast was in the relaxation phase, the Chl *a* concentrations increased off the northern coast, and decreased off the southern coast. The highest (15.5 mg m⁻³) and lowest (1.6 mg m⁻³) Chl *a* concentrations were observed on 8 August off the northern and southern coasts respectively.

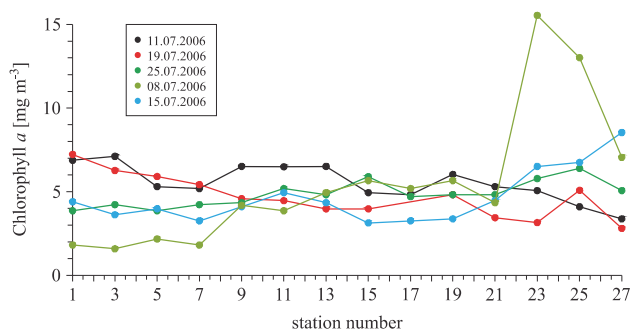


Figure 6. In situ Chl *a* distribution along the sampling transect on 11, 19 and 25 July, and 8 and 15 August 2006

The Chl *a* concentrations calculated with the FUB processor from the MERIS data was correlated with in situ Chl *a* for two time windows: 24 h and 2 h intervals (before or after) from the satellite overpass. A scatterplot of selected data pairs is shown in Figure 7. A total of 7 data pairs fulfilled the 2 h criterion: 3 samples (TH9, TH11 and TH13) from 11 July and 4 samples (TH11, TH13, TH15 and TH17) from 25 July (Table 1). For the 2 h window the FUB processor underestimated Chl *a* compared with in situ Chl *a* (Figure 7); the average underestimation was 25% (1.3 mg m⁻³),

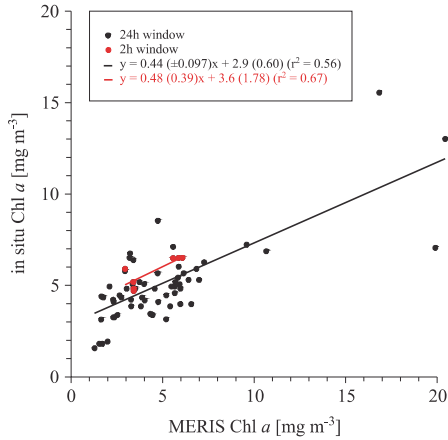


Figure 7. Scatterplot of in situ Chl *a* and MERIS Chl *a* derived by the FUB processor. Black dots represent all data pairs from 11, 18 and 25 July, and 7 and 16 August 2006 (24 h window), and red dots represent data pairs from 11 and 25 July 2006 (2 h window). The data corresponding to the 2 h window were used to estimate bias and to calibrate the FUB Chl *a* processor. The correlation (r^2) for 24 h window data points was 0.56 and for the 2 h window it was 0.67

which is of the same magnitude as in previous studies in the Baltic Sea (Kratzer et al. 2008). The correlation (r^2) for data points within the 2 h window was 0.67 and for the 24 h window was also relatively high at 0.56. The linear regression for the 2 h window with 95% confidence limits was $\text{Chl } a = 0.48(\pm 0.39) \times X + 3.6(\pm 1.8)$, where X is the FUB processor output. The standard deviation of the residuals (i.e. standard error of the estimation – SEE) was 0.51. For the 24 h window the slope and y-intercept of the linear regression were 0.44 (± 0.097) and 2.9 (± 0.60) respectively. The standard deviation of the residuals for the 24 h window was 1.43.

In addition to the FUB processor we also evaluated the case 2 regional water processor (C2RW) for Chl *a* (data not shown). The correlation for the FUB processor (0.67) was much higher compared to the C2RW processor (0.17). Also, the Chl *a* overestimation of C2RW by 52% is poorer compared to the underestimation (25%) by the FUB processor.

On the basis of the above analysis, the FUB algorithm was used to calculate Chl *a* from MERIS data in the Gulf of Finland. The equation obtained with linear regression for the 2 h window was applied to calibrate MERIS Chl *a* data.

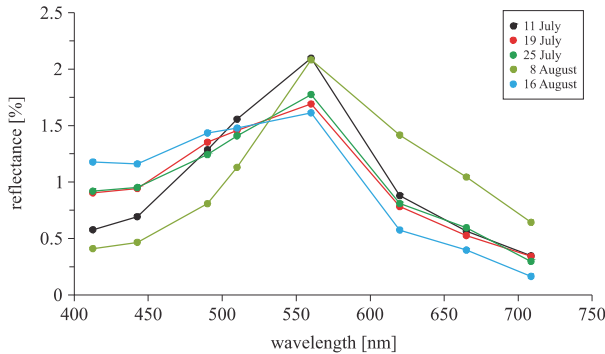


Figure 8. Normalized reflectance spectra calculated according to Wu (2004) on 11, 19 and 26 July; 8 and 16 August 2006 at location TH25

In order to assess the suitability of MERIS data (processed with the FUB algorithm) for detecting cyanobacteria, we analysed the temporal changes of reflectance spectra at the location of the largest increase in Chl *a* off the northern coast (Figure 6). We used MERIS images with the smallest time displacement from the time of the in situ measurements (Table 1). The distinct peak around wavelengths 620–650 nm, which is related to phycocyanin, was not detected on any of the normalized spectra (Figure 8).

3.4. Upwelling-related Chl *a* variability from MERIS imagery

To describe the spatio-temporal variability of the Chl *a* field, we used maps (Figures 9 and 10) and time series (Figure 11) at selected locations (Figure 1) formed from calibrated MERIS Chl *a* data. Different locations were selected to describe the temporal variability of Chl *a* along the northern and southern coasts, and along the axis of the Gulf (open sea area).

In July–August the Chl *a* concentrations were generally higher along the northern coast compared with those in the open sea area, and along the southern coast (Figure 11). In July the Chl *a* concentrations along the northern coast varied in the range of 4–9 mg m⁻³ (Figure 11a). After the relaxation of upwelling along the northern coast, Chl *a* concentrations reached high values of up to 13–14 mg m⁻³ at locations CHL5 and TH27 on 7 August. The increase in Chl *a* was also observed at other locations along the northern coast, reaching values of up to 8.5 mg m⁻³. Elevated Chl *a* along the northern coast and in the filaments was observed starting from 23 July and peaked on 6–7 August (Figures 9e, 10b and c). By 6 August, 26% of the area between longitudes 23–27°E was covered by Chl *a*

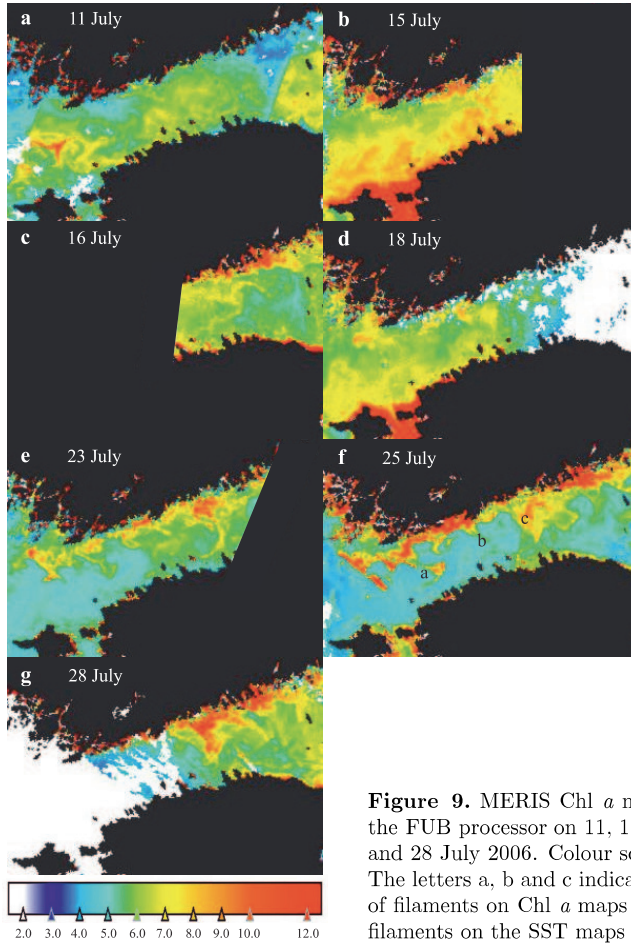


Figure 9. MERIS Chl *a* maps derived by the FUB processor on 11, 15, 16, 18, 23, 25 and 28 July 2006. Colour scale in mg m^{-3} . The letters a, b and c indicate the locations of filaments on Chl *a* maps coincident with filaments on the SST maps (see Figure 3c)

concentrations above 7 mg m^{-3} (Figure 10b and c). The development of the Chl *a* field was characterized by high spatial and temporal variability; standard deviations were 2.1 and 2.4 mg m^{-3} at locations CHL5 and TH27 respectively. Chlorophyll-rich filaments were observed off the Hanko and Porkkala Peninsulas and the Porvoo Archipelago after 23 July, when upwelling along the northern coast was in the relaxation phase. Relatively high and persistent Chl *a* concentrations were observed in the easternmost

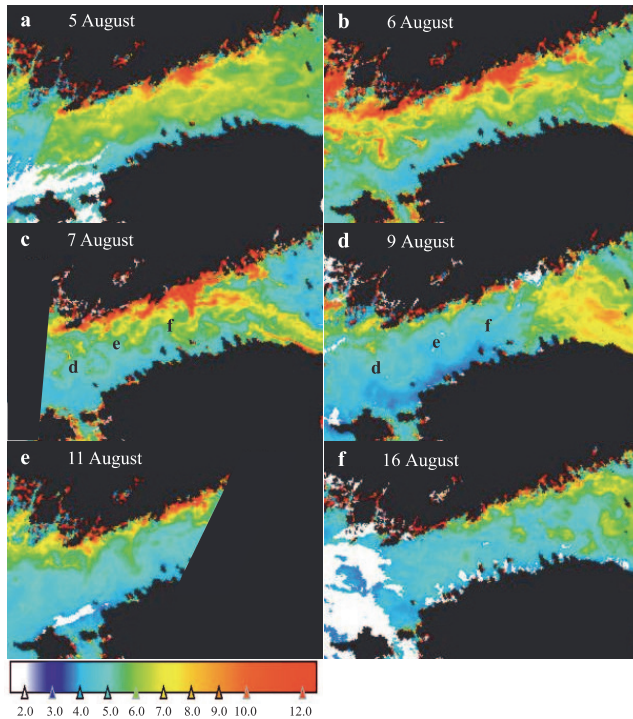


Figure 10. MERIS Chl *a* maps derived by the FUB processor on 5, 6, 7, 9, 11 and 16 August 2006. Colour scale in mg m^{-3} . The letters d, e and f indicate the locations of filaments on Chl *a* maps coincident with filaments on SST maps (see Figures 4b and 4c)

part of the study area (CHL7, mean = 5.9 mg m^{-3} , SD = 1.1 mg m^{-3}) throughout the period.

Along the southern coast, Chl *a* concentrations varied between 4 and 8.5 mg m^{-3} in July–August (Figure 11c). Higher Chl *a* concentrations (up to 8.5 mg m^{-3}) were observed in the western part of the Gulf (CHL8 and TH7) during the upwelling along the northern coast between 11 to 18 July. In early August, when upwelling developed along the southern coast, the temperature dropped below 12°C (Figure 4b), and measured Chl *a* concentrations were below 5 mg m^{-3} (Figure 10c) in a narrow area along the southern coast. The temporal course of Chl *a* along the southern coast was less variable compared with the northern coast during the whole study

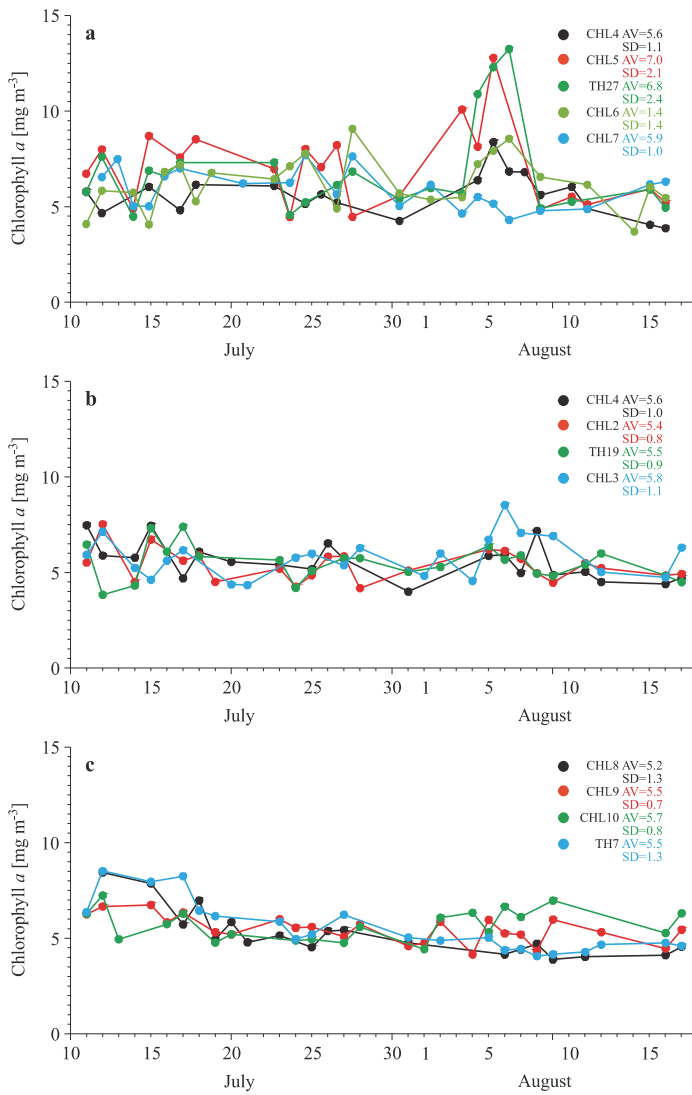


Figure 11. Distribution of MERIS Chl *a* at selected locations (see Figure 1) along the northern coast (a), along the Gulf axis (b), and along the southern coast (c) in July–August 2006

period (Figure 11c). By 16 (and 18) August, when upwelling started to relax (Figure 4e), the Chl *a* concentrations increased slightly in the upwelling region (Figure 9c, CHL8 and TH7). Again, relatively high and persistent Chl *a* concentrations were found in the easternmost part of the study area (CHL10, mean = 5.7 mg m⁻³, SD = 0.8 mg m⁻³).

During the whole study period the temporal course of Chl *a* along the Gulf axis (Figure 11b) displayed less variability, mainly between 4 and 8 mg m⁻³, compared with the northern coast. Chl *a* variations were larger between 11 and 18 July (Figures 9 and 11b), when the upwelling front and related filaments with low chlorophyll contents (Figures 3a–d) reached the open part of the Gulf. The high variability of Chl *a* at locations along the Gulf axis observed in August (Figure 11b, CHL1, CHL2 and TH19) was a result of chlorophyll-rich filaments from the northern, and chlorophyll-poor filaments from the southern, coastal sea areas (Figure 10).

4. Discussion

July–August 2006 was characterized by quite a rare wind regime in the Gulf of Finland: westerly winds prevailed until 29 July, whereas after 30 July easterly winds remained dominant for quite a long time. In the long, narrow Gulf of Finland, westerly winds cause upwelling along the northern coast, and downwelling along the southern coast, and vice versa when winds are blowing from the east. A high-resolution numerical study showed that the instability of the longshore baroclinic jet and related thermohaline fronts, caused by coupled upwelling and downwelling events, leads to the development of cold and warm mesoscale filaments and eddies contributing to coastal offshore exchange (Zhurbas et al. 2008). The maps of mean mesoscale (eddy) kinetic energy in the surface layer (simulation for July–August 2006), showed that the coastal offshore exchange caused by filaments and eddies is larger in the narrow western and the central parts of the Gulf (Laanemets et al. 2011).

Spatio-temporal variability of the Chl *a* field observed from MERIS imagery in July–August 2006 clearly reflected the influence of mesoscale physical processes, coupled upwelling/downwelling events and related filaments. Wind mixing may also decrease the surface Chl *a* concentration by mixing phytoplankton deeper into the water column. Chl *a* concentrations varied in a wide range, from 4 to 14 mg m⁻³, which is also expressed in the variations of mean concentrations (5.2–7.0 mg m⁻³) and standard deviations (SD = 1.4–2.4 mg m⁻³) (Figures 9, 10 and 11). Chl *a* concentrations were the lowest in the upwelling zones along both coasts. The highest mean Chl *a* and standard deviation were recorded along the northern coast: up to 7.0 and 2.4 mg m⁻³ respectively. In this region the upwelling and possible

upwelling-related nutrient input to the surface layer occurred earlier, during the first half of July, and therefore most likely promoted phytoplankton growth after the relaxation of the upwelling and the warming of the surface layer.

At locations along the Gulf axis in the western and central Gulf of Finland, the variability of the surface Chl *a* field (Figure 11b) was related to mesoscale activity. In July, when upwelling was taking place along the northern coast, filaments carried cold water with low chlorophyll concentrations offshore. In August, filaments carried chlorophyll-poor water from the southern upwelling zone and chlorophyll-rich water from the northern downwelling zone, into the central part of the Gulf.

In the shallower eastern part of the Gulf, the mesoscale activity estimated from SST imagery (Kahru et al. 1995, Uiboupin & Laanemets 2009) and numerical simulations (Laanemets et al. 2011) was lower. This was also reflected by the MERIS Chl *a* data, as concentrations were relatively persistent (mean 5.7–5.9 mg m⁻³) with small standard deviations (0.8–1.1 mg m⁻³).

The largest increase in Chl *a* was observed from 4 to 8 August along the northern coast (Figures 11a and 12) after the decrease of the surface Chl *a* concentration from 31 July to 4 August (Figures 11a and b), which was most likely caused by a strong wind event increasing the UML depth (Figures 2b and c) and mixing the phytoplankton deeper. There are probably two reasons for the increase of Chl *a* concentration in the narrow northern coastal zone and the cold filaments (Figure 9e) starting after the peak of upwelling

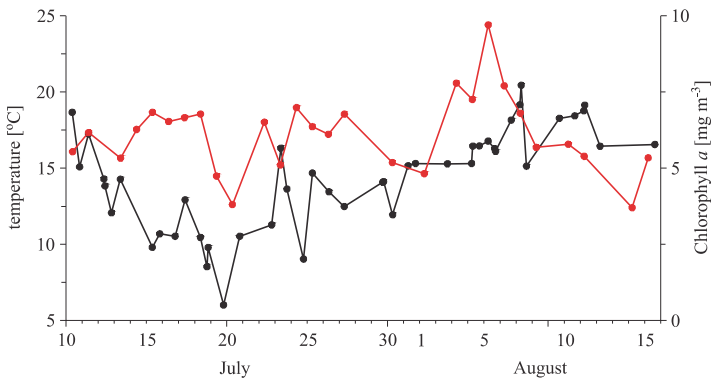


Figure 12. Temporal course of average (CHL4, CHL5 and CHL6) Chl *a* concentration (red line), and SST (black line) on the northern coast in July–August 2006

on 20 July (Figure 12). One reason could be the phytoplankton growth promoted by nutrient input during the upwelling in July along the northern coast. The numerical simulation of nutrient transport during upwelling events in summer 2006 showed that the main area along the northern coast of the Gulf, where nutrients (nitrogen and phosphorus) were brought to the surface layer, was from the Hanko Peninsula to the Porvoo Archipelago region (Laanemets et al. 2011). By 20 July most of the nitrogen and phosphorus (about 325 and 400 tonnes respectively) had been brought into the upper layer (Laanemets et al. 2009). This area coincided with the area of intensive upwelling along the northern coast depicted on the SST maps (Figures 3b and c). After the upwelling began to relax, the temperature in the northern coastal zone rose to above 15°C by 23 July (Figures 5a and 12). Previous studies have shown that phytoplankton growth is promoted in an area covered by upwelled nutrient-rich water (Vahtera et al. 2005). To confirm this assumption, we also compared the upwelled water area and the extended Chl *a* area along the northern coast. The area where the temperature was < 14°C, i.e. the narrow area along the northern coast where nutrients were probably brought to the surface layer, was 1317 km² (about 7% of the study area) on 18 July. Moreover, the area along the coast of water with a temperature < 17°C due to offshore transport and also covering the filaments was 4879 km² (about 25%). The upwelling-induced area with a slightly increased Chl *a* (concentrations over 7 mg m⁻³) on 25 July was 5507 km². This area remained approximately the same until 6 August (the bloom peak) – 5526 km². This suggests that the observed phytoplankton increase occurred mainly in the region of possible nutrient input by upwelling with a two week lag. Of course, some differences in the spatial distribution were due to the development of upwelling along the southern coast (Figures 4a and b).

The second possible reason responsible for the higher Chl *a* concentrations and variability along the northern coast could be the Ekman transport of phytoplankton biomass in the surface layer from the open sea area towards the northern coast during the upwelling event along the southern coast and the simultaneous downwelling along the northern coast in early August. Surface transport and a higher Chl *a* concentration in the downwelling zone were also observed in previous studies (Pavelson et al. 1999, Kanoshina et al. 2003, Lips & Lips 2010). In addition, Lips & Lips (2010) found a relationship between high phytoplankton biomass and a mesoscale anticyclonic feature in the northern part of the study area on 8 August. This corresponds to Zhurbas et al. (2006), who showed that instability of the longshore baroclinic jet, associated with downwelling, results in the formation of an anticyclonic eddy. The highest biomass values in the same area coincided

with this mesoscale feature, where domed isopycnals caused shallowing of the UML to only 5 m, against the background of a relatively deep UML in the remainder of the downwelling area on the transect. The northward surface transport of cold upwelled water and the spreading of filaments with low chlorophyll content are clearly visible on the SST and Chl *a* maps (Figures 4a, b, c and 10a, b, c, d).

The distinct feature (the peak around 630 nm) in the red part of the reflectance spectrum can be used to detect phycocyanin (cyanobacteria) (Dekker 1993, Dekker & Peters 1993, Reinart & Kutser 2006, Kutser et al. 2006). Bio-optical modelling results by Metsamaa et al. (2006) showed that MERIS bands 6 and 7 can be used to separate cyanobacteria and green algae if the concentration of Chl *a* in the cyanobacteria is 8–10 mg m⁻³. The calculated reflectance spectra showed that despite the dominance of phycocyanin-containing cyanobacteria (Chl *a* about 9 mg m⁻³) off the northern coast on 8 August (Lips & Lips 2010), the peak around 630 nm was not detected (Figure 8). Thus, our estimates based on in situ data confirmed the bio-optical modelling result. Previous field measurements have shown that Chl *a* in cyanobacteria during blooms were usually 10 mg m⁻³ in the Gulf of Finland area (Kononen et al. 1996, Vahtera et al. 2005, Suikkanen et al. 2007), i.e. cyanobacteria blooms are not detectable on MERIS imagery before the appearance of surface accumulations.

5. Conclusions

Upwelling events along the northern (southern) coast of the Gulf of Finland led to a minimum temperature of around 6°C (2°C) with a temperature difference between the upwelled and surrounding water of up to 12°C (18°C).

The Chl *a* concentration obtained from MERIS data using the FUB processor was well correlated with in situ measurements ($r^2 = 0.67$), but was underestimated on average by 25%. The Chl *a* concentration in cyanobacteria was not high enough to detect the characteristic feature of phycocyanin around wavelengths 620–650 nm in the reflectance spectra.

The spatio-temporal variability of Chl *a* estimated from MERIS data showed the evident influence of upwelling events and related filaments. The variability of Chl *a* was largest in the western and central parts of the Gulf, where mesoscale activity was the highest.

The highest Chl *a* concentrations (up to 14 mg m³) along the northern coast were observed about two weeks after the upwelling peak. The high Chl *a* was induced by (1) growth of phytoplankton promoted by nutrient input, and (2) the northward Ekman transport of surface waters caused by easterly wind forcing at the beginning of August.

Comparison of the upwelling areas on the SST images and high Chl *a* areas on MERIS images showed structural similarities. The upwelling area along the northern coast (4879 km²) and the high Chl *a* area (5526 km²) about two weeks later were roughly coincident. Also, the filaments with high Chl *a* coincided with the locations of cold filaments extending from the upwelling front along the northern coast. In the case of intensive upwelling along the southern coast, the low Chl *a* regions coincided with the cold filaments.

Upwelling events had only a minor influence in the eastern part of the study area, where Chl *a* concentrations were relatively high and persistent throughout the study period.

Acknowledgements

Our thanks go to the staff of the Marine Systems Institute who conducted the measurement campaigns.

References

- Bradtke K., Herman A., Urbański J. A., 2010, *Spatial and interannual variations of seasonal sea surface temperature patterns in the Baltic Sea*, *Oceanologia*, 52 (3), 345–362, <http://dx.doi.org/10.5697/oc.52-3.345>.
- Csanady G. T., 1982, *Circulation in the coastal ocean*, D. Reidel Publ. Co., Dordrecht, 279 pp.
- Dekker A. G., 1993, *Detection of optical water quality parameters for eutrophic waters by high resolution remote sensing*, Ph.D. thesis, Free University, Amsterdam.
- Dekker A. G., Peters S. W. M., 1993, *The use of the thematic mapper for the analysis of eutrophic lakes – a case-study in the Netherlands*, *Int. J. Remote Sens.*, 14 (5), 799–821, <http://dx.doi.org/10.1080/01431169308904379>.
- Doerffer R., Sorensen K., Aiken J., 1999, *MERIS potential for coastal zone applications*, *Int. J. Remote Sens.*, 20 (9), 1809–1818, <http://dx.doi.org/10.1080/014311699212498>.
- Doerffer R., Schiller H., 2007, *The MERIS case 2 water algorithm*, *Int. J. Remote Sens.*, 28 (3–4), 517–535, <http://dx.doi.org/10.1080/01431160600821127>.
- Gidhagen L., 1987, *Coastal upwelling in the Baltic – satellite and in situ measurements of sea surface temperatures indicating coastal upwelling*, *Estuar. Coast. Shelf Sci.*, 24 (4), 449–462, [http://dx.doi.org/10.1016/0272-7714\(87\)90127-2](http://dx.doi.org/10.1016/0272-7714(87)90127-2).
- Gower J., King S., Borstad G., Brown L., 2008, *The importance of a band at 709 nm for interpreting water-leaving spectral radiance*, *Can. J. Remote Sens.*, 34 (3), 287–295.

- HELCOM, 1988, *Guidelines for the Baltic Monitoring Programme for the third stage*, Baltic Sea Environ. Proc., 27D.
- Horstmann U., 1983, *Distribution patterns of temperature and water colour in the Baltic Sea as recorded in satellite images: Indicators for phytoplankton growth*, Ber. Inst. Meeresk., Kiel, 106, 147 pp.
- Kahru M.H., Håkansson B., Rud O., 1995, *Distributions of the sea-surface temperature fronts in the Baltic Sea as derived from satellite imagery*, Cont. Shelf Res., 15 (6), 663–679, [http://dx.doi.org/10.1016/0278-4343\(94\)E0030-P](http://dx.doi.org/10.1016/0278-4343(94)E0030-P).
- Kanoshina I., Lips U., Leppänen J.-M., 2003, *The influence of weather conditions (temperature and wind) on cyanobacterial bloom development in the Gulf of Finland (Baltic Sea)*, Harmful Algae, 2 (1), 29–41, [http://dx.doi.org/10.1016/S1568-9883\(02\)00085-9](http://dx.doi.org/10.1016/S1568-9883(02)00085-9).
- Kononen K., Kuparinen J., Mäkelä K., Laanemets J., Pavelson J., Nömmann S., 1996, *Initiation of cyanobacterial blooms in a frontal region at the entrance to the Gulf of Finland, Baltic Sea*, Limnol. Oceanogr., 41 (1), 98–112.
- Koponen S., Attila J., Pulliainen J., Kallio K., Pyhälähti T., Lindfors A., Rasmus K., Hallikainen M., 2007, *A case study of airborne and satellite remote sensing of a spring bloom event in the Gulf of Finland*, Cont. Shelf Res., 27 (2), 228–244, <http://dx.doi.org/10.1016/j.csr.2006.10.006>.
- Kratzer S., Brockmann C., Moore G., 2008, *Using MERIS full resolution data to monitor coastal waters – A case study from Himmerfjärden, a fjord-like bay in the northwestern Baltic Sea*, Remote Sens. Environ., 112 (5), 2284–2300, <http://dx.doi.org/10.1016/j.rse.2007.10.006>.
- Krzęzał A., Ostrowski M., Szymelfenig M., 2005a, *Sea surface temperature distribution during upwelling along the Polish Baltic coast*, Oceanologia, 47 (4), 415–432.
- Krzęzał A., Szymanek L., Kozłowski L., Szymelfenig M., 2005b, *Influence of coastal upwelling on chlorophyll a concentration in the surface water along the Polish coast of the Baltic Sea*, Oceanologia, 47 (4), 433–452.
- Kutser T., Metsamaa L., Strömbeck N., Vahtmäe E., 2006, *Monitoring cyanobacterial blooms by satellite remote sensing*, Estuar. Coast. Shelf Sci., 67 (1–2), 303–312, <http://dx.doi.org/10.1016/j.ecss.2005.11.024>.
- Kuvaldina N., Lips I., Lips U., Liblik T., 2010, *The influence of a coastal upwelling event on chlorophyll a and nutrient dynamics in the surface layer of the Gulf of Finland, Baltic Sea*, Hydrobiologia, 639 (1), 221–230, <http://dx.doi.org/10.1007/s10750-009-0022-4>.
- Laanemets J., Väli G., Zhurbas V., Elken J., Lips I., Lips U., 2011, *Simulation of mesoscale structures and nutrient transport during summer upwelling events in the Gulf of Finland in 2006*, Boreal Environ. Res., 16 (suppl. A), 15–26.
- Laanemets J., Zhurbas V., Elken J., Vahtera E., 2009, *Dependence of upwelling-mediated nutrient transport on wind forcing, bottom topography and stratification in the Gulf of Finland: model experiments*, Boreal Environ. Res., 14 (1), 213–225.

- Lass H. U., Mohrholz V., Nausch G., Siegel H., 2010, *On phosphate pumping into the surface layer of the eastern Gotland Basin by upwelling*, J. Marine Syst., 80 (1–2), 71–89, <http://dx.doi.org/10.1016/j.jmarsys.2009.10.002>.
- Lehmann A., Myrberg K., 2008, *Upwelling in the Baltic Sea – A review*, J. Marine Syst., 74 (Suppl.), S3–S12, <http://dx.doi.org/10.1016/j.jmarsys.2008.02.010>.
- Lips I., Lips U., 2008, *Abiotic factors influencing cyanobacterial bloom development in the Gulf of Finland (Baltic Sea)*, Hydrobiologia, 614 (1), 133–140, <http://dx.doi.org/10.1007/s10750-008-9449-2>.
- Lips I., Lips U., 2010, *Phytoplankton dynamics affected by the coastal upwelling events in the Gulf of Finland in July–August 2006*, J. Plankton Res., 32 (9), 1269–1282, <http://dx.doi.org/10.1093/plankt/fbq049>.
- Lips I., Lips U., Liblik T., 2009, *Consequences of coastal upwelling events on physical and chemical patterns in the central Gulf of Finland (Baltic Sea)*, Cont. Shelf Res., 29 (15), 1836–1847, <http://dx.doi.org/10.1016/j.csr.2009.06.010>.
- Männik A., Merilain M., 2007, *Verification of different precipitation forecasts during extended winter-season in Estonia*, HIRLAM Newsletter, 52, 65–70.
- Metsamaa L., Kutser T., Strombeck N., 2006, *Recognising cyanobacterial blooms based on their optical signature: a modelling study*, Boreal Environ. Res., 11 (6), 493–506.
- Myrberg K., Andrejev O., 2003, *Main upwelling regions in the Baltic Sea – a statistical analysis based on three-dimensional modelling*, Boreal Environ. Res., 8 (2), 97–112.
- Myrberg K., Lehmann A., Raudsepp U., Szymelfenig M., Lips I., Lips U., Matciak M., Kowalewski M., Krężel A., Burska D., Szymanek L., Ameryk A., Bielecka L., Bradtke K., Gałkowska A., Gromisz S., Jędrasik J., Kaluźny M., Kozłowski L., Krajewska-Sołtys A., Oldakowski B., Ostrowski M., Zalewski M., Andrejev O., Suomi I., Zhurbas V., Kauppinen O.-K., Soosaar E., Laanemets J., Uiboupin R., Talpsepp L., Golenko M., Golenko N., Vahtera E., 2008, *Upwelling events, coastal offshore exchange, links to biogeochemical processes – Highlights from the Baltic Sea Science Congress at Rostock University, Germany, 19–22 March 2007*, Oceanologia, 50 (1), 95–113.
- Pavelson J., Kononen K., Laanemets J., 1999, *Chlorophyll distribution patchiness caused by hydrodynamical processes: a case study in the Baltic Sea*, ICES J. Mar. Sci., 56 (Suppl.), 87–99, <http://dx.doi.org/10.1006/jmsc.1999.0610>.
- Petersen W., Wehde H., Krasernann H., Colijn F., Schroeder F., 2008, *FerryBox and MERIS – Assessment of coastal and shelf sea ecosystems by combining in situ and remotely sensed data*, Estuar. Coast. Shelf Sci., 77 (2), 296–307, <http://dx.doi.org/10.1016/j.ecss.2007.09.023>.
- Rantajärvi E., Olsonen R., Hallfors S., Leppanen J. M., Raateoja M., 1998, *Effect of sampling frequency on detection of natural variability in phytoplankton: unattended high-frequency measurements on board ferries in the Baltic Sea*, ICES J. Mar. Sci., 55 (4), 697–704, <http://dx.doi.org/10.1006/jmsc.1998.0384>.

- Reinart A., Kutser T., 2006, *Comparison of different satellite sensors in detecting cyanobacterial bloom events in the Baltic Sea*, Remote Sens. Environ., 102 (1–2), 74–85.
- Schroeder T., Behnert I., Schaale M., Fischer J., Doerffer R., 2007a, *Atmospheric correction algorithm for MERIS above Case-2 waters*, Int. J. Remote Sens., 28 (7), 1469–1486, <http://dx.doi.org/10.1080/01431160600962574>.
- Schroeder T., Schaale M., Fischer J., 2007b, *Retrieval of atmospheric and oceanic properties from MERIS measurements: A new Case-2 water processor for BEAM*, Int. J. Remote Sens., 28 (24), 5627–5632, <http://dx.doi.org/10.1080/01431160701601774>.
- Seifert T., Tauber F., Kayser B., 2001, *A high resolution spherical grid topography of the Baltic Sea – 2nd edition*, Baltic Sea Science Congress, Stockholm 25–29 November 2001, Poster No. 147, [<http://www.io-warnemuende.de/iowtopo>].
- Siegel H., Gerth M., Rudloff R., Tschersich G., 1994, *Dynamic features in the western Baltic Sea investigated using NOAA-AVHRR data*, Dt. Hydrogr. Zet., 46, 191–209, <http://dx.doi.org/10.1007/BF02226949>.
- Siegel H., Gerth M., Tschersich G., 2006, *Sea surface temperature development of the Baltic Sea in the period 1990–2004*, Oceanologia, 48 (S), 119–131.
- Sorensen K., Aas E., Hokedal J., 2007, *Validation of MERIS water products and bio-optical relationships in the Skagerrak*, Int. J. Remote Sens., 28 (3–4), 555–568, <http://dx.doi.org/10.1080/01431160600815566>.
- Suikkanen S., Laamanen M., Huttunen M., 2007, *Long-term changes in summer phytoplankton communities of the open northern Baltic Sea*, Estuar. Coast. Shelf Sci., 71 (3–4), 580–592, <http://dx.doi.org/10.1016/j.ecss.2006.09.\break004>.
- Suursaar Ü., Aps R., 2007, *Spatio-temporal variations in hydrophysical and chemical parameters during a major upwelling event off the southern coast of the Gulf of Finland in summer 2006*, Oceanologia, 49 (2), 209–229.
- Uiboupin R., Laanemets J., 2009, *Upwelling characteristics derived from satellite sea surface temperature data in the Gulf of Finland, Baltic Sea*, Boreal Environ. Res., 14 (2), 297–304.
- Vahtera E., Laanemets J., Pavelson J., Huttunen M., Kononen K., 2005, *Effect of upwelling on the pelagic environment and bloom-forming cyanobacteria in the western Gulf of Finland, Baltic Sea*, J. Marine Syst., 58 (1–2), 67–82, <http://dx.doi.org/10.1016/j.jmarsys.2005.07.001>.
- Wu C., 2004, *Normalized spectral mixture analysis for monitoring urban composition using ETM plus imagery*, Remote Sens. Environ., 93 (4), 480–492, <http://dx.doi.org/10.1016/j.rse.2004.08.003>.
- Zhurbas V. M., Laanemets J., Vahtera E., 2008, *Modeling of the mesoscale structure of coupled upwelling/downwelling events and the related input of nutrients to the upper mixed layer in the Gulf of Finland, Baltic Sea*, J. Geophys. Res., 113 (C5), C05004, <http://dx.doi.org/10.1029/2007JC004280>.

Zhurbas V., Oh I.S., Park T., 2006, *Formation and decay of a longshore baroclinic jet associated with transient coastal upwelling and downwelling: A numerical study with applications to the Baltic Sea*, J. Geophys. Res., 111 (C4), C04014, <http://dx.doi.org/10.1029/2005JC003079>.

ACKNOWLEDGEMENTS

I would like to thank my supervisor Inga Lips for her help, support, inspiration and opportunities in the marine science. I am thankful to colleagues in Marine Systems Institute and co-authors of papers: Kristi Altoja, Villu Kikas, Jaan Laanemets, Taavi Liblik, Urmas Lips, Laura Raag, Nelli Rünk, Liis Sipelgas and Rivo Uiboupin. I am grateful to Kai Künis-Beres for reviewing the thesis and her helpful comments.

In addition, I thank AS Tallink Group for cooperation on Ferrybox measurements and our colleagues and crew members for participation in the field measurements.

This work was financially supported by the Estonian Science Foundation (grants no. 6752, 6955) and Foundation Innove (grant no. 1.0101-0279), ESF Programm DoRa, student scholarship from the Bat Sheva de Rothschild Fund. Writing of the thesis was supported by institutional research funding IUT (19-6) of the Estonian Ministry of Education.

I would like to thank my family and especially my husband Kirill for supporting me.

ABSTRACT

The aim of this thesis was to verify influence, and importance of varying meso-scale hydrophysical processes on the dynamics of nutrients and phytoplankton chlorophyll *a* in summer in stratified Gulf of Finland, Baltic Sea. The study was based on combination of different approaches, including traditional measurements aboard research vessel coupled with latest technological capabilities using autonomous horizontal and vertical high-resolution measuring devices. In summer, when the water column in the Gulf of Finland is thermally stratified and euphotic layer is exhausted of inorganic nutrients necessary for phytoplankton growth, the spatial distribution of phytoplankton is highly influenced by prevailing hydrophysical features caused by variable wind impulses. Wind induced processes, like upwelling/downwelling, eddies, coastal currents and jets, in the background of estuarine circulation cause movements of water-masses (and substances in it) both horizontally and vertically.

Major upwelling and coupled downwelling created drastic simultaneous changes in the horizontal and vertical distribution of inorganic nutrient field and phytoplankton communities along the entire cross-section in the central part of Gulf of Finland in 2006. During the observed upwelling event the horizontal Ekman transport was the major process shaping the distribution of phytoplankton biomass in size-fraction $>20\ \mu\text{m}$. The warmer surface layer was transported towards the opposite coast off from the upwelling region, concentrating pre upwelling phytoplankton communities in the downwelling area, whereas, the upwelled waters had low Chl *a* concentration. At the stabilization and relaxation of upwelling nanoflagellates responded faster to the upwelled nutrients compared with phytoplankton in size-fraction $>20\ \mu\text{m}$.

Phytoplankton sub-surface or deep maxima are common features in summer in thermally stratified Gulf of Finland. The formation of sub-surface phytoplankton layers in the Gulf of Finland is the combination of physical, chemical and biological processes. These maxima usually locate at the base of thermocline and coincide well with the depth of nutriclines. Clear diurnal and bi-diurnal vertical patterns of chlorophyll *a* were observed when dinoflagellate *Heterocapsa triquetra* was dominating in the community. The descend speed of this species, estimated on the basis of vertical dynamics of chlorophyll *a*, was $1.6\ \text{m h}^{-1}$. This is the first documented migration speed record for this species in the field. The asynchronous upward migration pattern often created bimodal distribution of chlorophyll *a* in the stratified water column.

Chl *a* concentrations can be used with high confidence to assess the effects of measures taken to reduce eutrophication and improve the ecological status of the water body. However, due to variations in freshwater run-off, light climate, and internal cycling processes, trends in Chl *a* concentrations as such cannot be directly related to measures, but must be evaluated in a broader context.

RESÜMEE

Käesoleva doktoritöö raames uuriti erinevate mesomastaapsete hüdrofüüsikaliste protsesside mõju anorgaaniliste toitainete ja fütoplanktoni ajalis-ruumilisele jaotusele vertikaalselt kihistunud Soome lahes. Ökosüsteemile avalduva antropogeense mõju hindamisel ja eutrofeerumise vähendamiseks kohaldatavate meetmete rakendamisel on oluline mõista looduslikku varieeruvust ja kliimaatiliste tegurite mõju hinnatavatele parameetritele.

Doktoritöö käigus kasutati andmete kogumiseks erinevaid tehnilisi lähenemisi, sh mõõtmised ja proovikogumised uurimislaeva pardalt ning horisontaalsete ja vertikaalsete jaotuste kaardistamised kasutades autonoomseid platvorme (ferrybox ja profileeriv poijaam). Töös on käsitletud andmeid, mis koguti 2006. ja 2009. aasta suvel Soome lahe keskosas erineva ruumilise lahutuse ja ajalise sammuga. Vertikaalsed jaotused registreeriti diskreetsusega 10 cm kuni 10 m ja ajalise sammuga 3 h kuni 2 nädalat. Horisontaalsete jaotuste kaardistamisel oli ruumiline lahutus 150 m kuni 5 km ja ajaline samm 1 päev kuni 1 nädal.

Veesamba tugev termiline kihistus suveperioodil loob fütoplanktoni kasvuks vajalike ressursside vertikaalse eraldatuse – ülemine valgusküllane kiht on toitainetevaene, alumises toitainerikas kihis aga pole piisavalt valgust fotosünteesimiseks. Taolise ressursside jaotuse puhul muutuvad ülioluliseks hüdrofüüsikalised protsessid, mis toovad toitaineid alumistest kihtidest üles ja loovad seeläbi fütoplanktoni kasvuks soodsad tingimused. Ida-lääne sihis väljavenitatud Soome lahes on lisaks estuaarsele veeliikumisele olulised vee ja selles olevate ainete transporti ja segunemist soodustavad mesomastaapsed protsessid: tuule tekitatud rannikumere apvelling/daunvelling, pöörised, rannikumere jugahoovused. Lisaks on peale füüsikaliste protsesside ning nendega seotud toitainete voogude olulised ka suvise fütoplanktoni koosluse liigispetsiifilised kohastumused nagu võime omastada molekulaarset lämmastikku, migreeruda vertikaalselt kihistunud veesambas, talletada toitaineid nende ainete poolt limiteeritud tingimustes kasutamiseks, omastada toitaineid pimedas.

Käesoleva doktoritöö peamised tulemused võib kokku võtta järgnevalt:

- Soome lahes esinevad rannikumere apvellingud toovad kaasa laiaulatuslikke muutusi temperatuuri, soolsuse ja klorofüll *a* sisalduse horisontaalses ja vertikaalses jaotuses ning on väga olulised protsessid toitainete transpordil alumistest kihtidest ülemisse toitainetevaesesse eufootsesse kihti.
- Intensiivse rannikumere apvellingu ajal on suuremõõtmelise (> 20 µm) fütoplanktoni jaotus pinnakihi määratud peamiselt horisontaalse Ekmani transpordiga ja vähem vertikaalse toitainete vooga. Soe pindmine veekiht koos pinnakihi fütoplanktoni kooslustega transporditakse apvellingu piirkonnast vastas ranniku suunas ning altpoolt üles liikuvad veemassid on vähese klorofüll sisaldusega.
- Erinevalt Maailmamere püsivate apvellingu alade fütoplanktoni kooslustest, kus domineerivad suuremõõtmelised ränivetikad, saavad Läänemeres

apvellingu stabiliseerumise järgselt esmalt eelise nanoflagellaadid, kes reageerivad kiiremini ülemisse kihti transporditud toitainetele.

- Tugev termaalne kihistumine suvel takistab ülemise toitainetevaese pinnakihi ja termokliini all asuva toitainerikka kihi segunemist. Töös on näidatud, et suvises toitainete poolt limiteeritud pinnakihis saavad fütoplanktoni koosluses konkurentsieelise liigid, mis on võimelised vertikaalselt migreeruma ja assimileerima pimedas toitaineid.
- Fütoplanktoni pinnaaluste ja sügavate maksimumide esinemine on suvel tavapärane nähtus tugevalt kihistunud Soome lahes. Pinnaaluste klorofüllid maksimumide teke ja jaotus on tihedalt seotud vertikaalse stratifikatsiooniga – maksimumid paiknevad termokliini alaosas ja ühtivad nitrakliiniga.
- Juulis Soome lahes esinevates pinnaalustes ja sügavates fütoplanktoni maksimumides domineerib dinoflagellaat *Heterocapsa triquetra*. Esmakordselt hinnati looduses, antud liigi poolt domineeritud koosluse klorofüllid sisalduse ööpäevaseid dünaamikaid kaardistades, *H. triquetra* laskumiskiirus. *H. triquetra* migreerub sügavamatesse kihtidesse hinnanguliselt 1.6 m h^{-1} , mis on märkimisväärne arvestades antud liigi suurust (20-25 μm).
- Fütoplanktoni vertikaalses migratsioonis domineerib teatud hüdrofüüsikaliste tingimuste puhul ööpäevane tsükkel. Samas võib sageli täheldada sünkroonset allapoole migreerumist ja asünkroonset pinnakihti migreerumist, mille tagajärjel tekib veesambas fütoplanktoni bimodaalne jaotus.
- Fütoplanktoni liikide võime migreeruda sügavamatesse kihtidesse, omastada pimedas vajalikke toitaineid ja kasutada neid peale ülemisse kihti tagasi jõudmist fotosünteesis on oluline ka sellepöolest, et nii püsib ülemine segunenud veekiht produktiivsena ka toitainete ammendumisel eufootses kihist.
- Suure ajalis-ruumilise lahutusega teostatud proovikogumised ja mõõtmised võimaldasid usaldusväärsemalt hinnata hüdrofüüsikaliste protsesside mõju fütoplanktoni ja selle kasvuks vajalike toitainete vertikaalsele ja horisontaalsele jaotusele.

ELULOOKIRJELDUS

1. Isikuandmed

Ees- ja perekonnanimi Natalja Buhhalko (neiupõlvenimi Kuvaldina)
Sünniaeg ja -koht 04. aprill 1983, Venemaa
Kodakondsus Eesti
E-posti aadress natalja.buhhalko@msi.ttu.ee

2. Hariduskäik

Õppeasutus (nimetus lõpetamise ajal)	Lõpetamise aeg	Haridus (eriala/kraad)
Narva Humanitaargümnaasium	2001	Keskharidus
Tallinna Ülikool	2008	Merebioloogia/M.Sc.

3. Keelteoskus (alg-, kesk- või kõrgtase)

Keel	Tase
Eesti keel	Kõrgtase
Inglise keel	Keskstase
Vene keel	Emakeel

4. Teenistuskäik

Töötamise aeg	Töötaja nimetus	Ametikoht
2006-2010	TTÜ Meresüsteemide Instituut	Tehnik
2010-tänapäevani	TTÜ Meresüsteemide Instituut	Insener

5. Teadustegevus

- Uiboupin, R., Laanemets, J., Sipelgas, L., Raag, L., Lips, I., Buhhalko, N. (2012). Monitoring the effect of upwelling on the chlorophyll *a* distribution in the Gulf of Finland (Baltic Sea) using remote sensing and in situ data. *Oceanologia*, 54(3), 395-419.
- Lips, U., Lips, I., Liblik, T., Kikas, V., Altoja, K., Buhhalko, N., Rünk, N. (2011). Vertical dynamics of summer phytoplankton in a stratified estuary (Gulf of Finland, Baltic Sea). *Ocean Dynamics*, 61, 903-915.
- Buschmann, F., Erm, A., Konts, M.-L., Buhhalko, N. (2011). Optical Monitoring of NW Estonian coastal waters in 2008 - 2010. In: *Book of Abstract: 8th Baltic Sea Science Congress [BSSC]: 22-26, August 2011, St.Petersburg, Russia*. RSHU, 275.

- Rünk, N., Meerits, A., Buhhalko, N., Lips, I., Kikas, V., Liblik, T., Lips, U. (2011). Dynamics of nutrients and phytoplankton Chl a influenced by meso-scale and sub-meso-scale physical processes in the Gulf of Finland (Baltic Sea). *In: Geophysical Research Abstracts: European Geosciences Union General Assembly 2011, Vienna, Austria, May 3 – 8.*
- Lips, U., Lips, I., Liblik, T., Kuvaldina, N. (2010). Processes responsible for the formation and maintenance of sub-surface chlorophyll maxima in the Gulf of Finland. *Estuarine, coastal and shelf science*, 88, 339 - 349.
- Kuvaldina, N., Lips, I., Lips, U., Liblik, T. (2010). The influence of a coastal upwelling event on chlorophyll *a* and nutrient dynamics in the surface layer of the Gulf of Finland, Baltic Sea. *Hydrobiologia*, 639(1), 221 - 230.
- Lips, U., Lips, I., Kikas, V., Kuvaldina, N. (2008). Ferrybox measurements: a tool to study meso-scale processes in the Gulf of Finland (Baltic Sea). US/EU-Baltic Symposium "Ocean Observations, Ecosystem-Based Management & Forecasting", Tallinn, 27-29 May, 2008. IEEE, (IEEE Conference Proceedings), 1 - 6.
- Lips, I., Lips, U., Liblik, T., Kuvaldina, N. (2008). An upwelling event in the Gulf of Finland (Baltic Sea) in August 2006: Observational results. *In: Meeting Abstracts: 2008 Ocean Sciences Meeting, Orlando, March 2-7, 2008.* , 268.

6. Kaitstud lõputööd

Magistritöö, 2008. Toitainete ja klorofüllü ajalis-ruumiline muutlikkus Soome lahes lõikel Tallinn-Helsinki 2006. a. suvel. Tallinna Ülikool.

7. Kursused

14.11-26.11.2010 – Läänemere fütoplanktoni kursus, (Tvärminne, Soome)

16.08-19.12.2009 – Vahetusüliõpilane in Oregon Health and Science University, Portland, USA.

- 07-19.06.2009 – Rahvusvaheline kursus doktorantidele „Flow Cytometry“ (Kalmar, Rootsi)
- 11-16.05.2009 – Suvekool Physical Oceanography of the Baltic Sea, (Tvärminne, Soome)
- 16-26.03.2009 – Rahvusvaheline kursus Phosphorus cycling in the aquatic environment, (Umeå, Rootsi)
- 23-30.11.2008 – The Bat Sheva De Rothschild seminar fütoplanktonist füüsikalises keskkonnas: The 15th workshop of the international association of phytoplankton taxonomy and ecology (IAP), (Ramot, Iisrael)
- 20.06.2008 – Valgusmikroskoobi tehnikad, (Tallinn, Eesti)
- 19.06.2008 – Valgusmikroskoobikasutaja baaskoolitus, (Tallinn, Eesti)
- 18.06.2008 – Epi-fluorestsents seminar, (Tallinn, Eesti)
- 09-16.03.2007 – kursus Methods in Algae Research, (Turku, Soome)
- 01.09.2006 – 07.01.2007 – kursus Microbial Ecology, (Umeå, Rootsi)
- 07.06-11.08.2006 – kursus The Brackish Water Ecology, (Umeå, Rootsi)
- 14-18.04.2004 – kursus Building the Baltic Sea Region, (Borki, Poland)

CURRICULUM VITAE

1. Personal data

Name Natalja Buhhalko (maiden name Kuvaldina)
Date and place of birth 04 Aprill 1983, Russia
E-mail address natalja.buhhalko@msi.ttu.ee

2. Education

Educational institution	Graduation year	Education (field of study/degree)
NHG	2001	Secondary
Tallinn University	2008	Marine biology/ M.Sc

3. Language competence/skills (fluent, average, basic skills)

Language	Level
Estonian	Fluent
English	Average
Russian	Native language

4. Professional employment

Period	Organisation	Position
2006-2010	Marine Systems Institute	Technician
2010-present	Marine Systems Institute	Engineer

5. Scientific work

- Uiboupin, R., Laanemets, J., Sipelgas, L., Raag, L., Lips, I., Buhhalko, N. (2012). Monitoring the effect of upwelling on the chlorophyll *a* distribution in the Gulf of Finland (Baltic Sea) using remote sensing and in situ data. *Oceanologia*, 54(3), 395-419.
- Lips, U., Lips, I., Liblik, T., Kikas, V., Altoja, K., Buhhalko, N., Rünk, N. (2011). Vertical dynamics of summer phytoplankton in a stratified estuary (Gulf of Finland, Baltic Sea). *Ocean Dynamics*, 61, 903-915.
- Buschmann, F., Erm, A., Konts, M.-L., Buhhalko, N. (2011). Optical Monitoring of NW Estonian coastal waters in 2008 - 2010. *In: Book of Abstract: 8th Baltic Sea Science Congress [BSSC]: 22-26, August 2011, St.Petersburg, Russia.* RSHU, 275.
- Rünk, N., Meerits, A., Buhhalko, N., Lips, I., Kikas, V., Liblik, T., Lips, U. (2011). Dynamics of nutrients and phytoplankton Chl *a* influenced by meso-scale and sub-meso-scale physical processes in the Gulf of Finland (Baltic Sea). *In:*

Geophysical Research Abstracts: European Geosciences Union General Assembly 2011, Vienna, Austria, May 3 – 8.

- Lips, U., Lips, I., Liblik, T., Kuvaldina, N. (2010). Processes responsible for the formation and maintenance of sub-surface chlorophyll maxima in the Gulf of Finland. *Estuarine, coastal and shelf science*, 88, 339 - 349.
- Kuvaldina, N., Lips, I., Lips, U., Liblik, T. (2010). The influence of a coastal upwelling event on chlorophyll *a* and nutrient dynamics in the surface layer of the Gulf of Finland, Baltic Sea. *Hydrobiologia*, 639(1), 221 - 230.
- Lips, U., Lips, I., Kikas, V., Kuvaldina, N. (2008). Ferrybox measurements: a tool to study meso-scale processes in the Gulf of Finland (Baltic Sea). *US/EU-Baltic Symposium "Ocean Observations, Ecosystem-Based Management & Forecasting"*, Tallinn, 27-29 May, 2008. IEEE, (IEEE Conference Proceedings), 1 - 6.
- Lips, I., Lips, U., Liblik, T., Kuvaldina, N. (2008). An upwelling event in the Gulf of Finland (Baltic Sea) in August 2006: Observational results. *In: Meeting Abstracts: 2008 Ocean Sciences Meeting, Orlando, March 2-7, 2008.* , 268.

6. Defended theses

Spatio-temporal variability of nutrients and chlorophyll in the Gulf of Finland on section Tallinn-Helsinki in summer 2006. Tallinn University.

7. Special courses

14.11-26.11.2010 – Baltic Sea Phytoplankton course, (Tvärminne, Soome)

16.08-19.12.2009 – Exchange student at Oregon Health and Science University, Portland, USA

07-19.06.2009 – „Flow Cytometry“ (Kalmar, Rootsi)

11-16.05.2009 – Summerschool Physical Oceanography of the Baltic Sea, (Tvärminne, Soome)

16-26.03.2009 – Phosphorus cycling in the aquatic environment, (Umeå, Rootsi)

23-30.11.2008 – The Bat Sheva De Rothschild seminar on phytoplankton in the physical environment: The 15th workshop of the international association of phytoplankton taxonomy and ecology (IAP), (Ramot, Iisrael)

20.06.2008 – Lightmicroscopy techniques, (Tallinn, Eesti)

19.06.2008 – Basic course of lightmicroscopy, (Tallinn, Eesti)

18.06.2008 – Epi-fluorescency seminar, (Tallinn, Eesti)

09-16.03.2007 – Methods in Algae Research, (Turku, Soome)

01.09.2006 – 07.01.2007 – Microbial Ecology, (Umeå, Rootsi)

07.06-11.08.2006 – The Brackish Water Ecology, (Umeå, Roots)

14-18.04.2004 – Building the Baltic Sea Region, (Borki, Poland)

**DISSERTATIONS DEFENDED AT
TALLINN UNIVERSITY OF TECHNOLOGY ON
NATURAL AND EXACT SCIENCES**

1. **Olav Kongas**. Nonlinear Dynamics in Modeling Cardiac Arrhythmias. 1998.
2. **Kalju Vanatalu**. Optimization of Processes of Microbial Biosynthesis of Isotopically Labeled Biomolecules and Their Complexes. 1999.
3. **Ahto Buldas**. An Algebraic Approach to the Structure of Graphs. 1999.
4. **Monika Drews**. A Metabolic Study of Insect Cells in Batch and Continuous Culture: Application of Chemostat and Turbidostat to the Production of Recombinant Proteins. 1999.
5. **Eola Valdre**. Endothelial-Specific Regulation of Vessel Formation: Role of Receptor Tyrosine Kinases. 2000.
6. **Kalju Lott**. Doping and Defect Thermodynamic Equilibrium in ZnS. 2000.
7. **Reet Koljak**. Novel Fatty Acid Dioxygenases from the Corals *Plexaura homomalla* and *Gersemia fruticosa*. 2001.
8. **Anne Paju**. Asymmetric oxidation of Prochiral and Racemic Ketones by Using Sharpless Catalyst. 2001.
9. **Marko Vendelin**. Cardiac Mechanoenergetics *in silico*. 2001.
10. **Pearu Peterson**. Multi-Soliton Interactions and the Inverse Problem of Wave Crest. 2001.
11. **Anne Menert**. Microcalorimetry of Anaerobic Digestion. 2001.
12. **Toomas Tiivel**. The Role of the Mitochondrial Outer Membrane in *in vivo* Regulation of Respiration in Normal Heart and Skeletal Muscle Cell. 2002.
13. **Olle Hints**. Ordovician Scolecodonts of Estonia and Neighbouring Areas: Taxonomy, Distribution, Palaeoecology, and Application. 2002.
14. **Jaak Nõlvak**. Chitinozoan Biostratigraphy in the Ordovician of Baltoscandia. 2002.
15. **Liivi Kluge**. On Algebraic Structure of Pre-Operad. 2002.
16. **Jaanus Lass**. Biosignal Interpretation: Study of Cardiac Arrhythmias and Electromagnetic Field Effects on Human Nervous System. 2002.
17. **Janek Peterson**. Synthesis, Structural Characterization and Modification of PAMAM Dendrimers. 2002.
18. **Merike Vaher**. Room Temperature Ionic Liquids as Background Electrolyte Additives in Capillary Electrophoresis. 2002.
19. **Valdek Mikli**. Electron Microscopy and Image Analysis Study of Powdered Hardmetal Materials and Optoelectronic Thin Films. 2003.
20. **Mart Viljus**. The Microstructure and Properties of Fine-Grained Cermets. 2003.
21. **Signe Kask**. Identification and Characterization of Dairy-Related *Lactobacillus*. 2003.
22. **Tiiu-Mai Laht**. Influence of Microstructure of the Curd on Enzymatic and Microbiological Processes in Swiss-Type Cheese. 2003.
23. **Anne Kuusksalu**. 2–5A Synthetase in the Marine Sponge *Geodia cydonium*. 2003.
24. **Sergei Bereznev**. Solar Cells Based on Polycrystalline Copper-Indium Chalcogenides and Conductive Polymers. 2003.

25. **Kadri Kriis.** Asymmetric Synthesis of C₂-Symmetric Bimorpholines and Their Application as Chiral Ligands in the Transfer Hydrogenation of Aromatic Ketones. 2004.
26. **Jekaterina Reut.** Polypyrrole Coatings on Conducting and Insulating Substrates. 2004.
27. **Sven Nõmm.** Realization and Identification of Discrete-Time Nonlinear Systems. 2004.
28. **Olga Kijatkina.** Deposition of Copper Indium Disulphide Films by Chemical Spray Pyrolysis. 2004.
29. **Gert Tamberg.** On Sampling Operators Defined by Rogosinski, Hann and Blackman Windows. 2004.
30. **Monika Übner.** Interaction of Humic Substances with Metal Cations. 2004.
31. **Kaarel Adamberg.** Growth Characteristics of Non-Starter Lactic Acid Bacteria from Cheese. 2004.
32. **Imre Vallikivi.** Lipase-Catalysed Reactions of Prostaglandins. 2004.
33. **Merike Peld.** Substituted Apatites as Sorbents for Heavy Metals. 2005.
34. **Vitali Syritski.** Study of Synthesis and Redox Switching of Polypyrrole and Poly(3,4-ethylenedioxythiophene) by Using *in-situ* Techniques. 2004.
35. **Lee Põllumaa.** Evaluation of Ecotoxicological Effects Related to Oil Shale Industry. 2004.
36. **Riina Aav.** Synthesis of 9,11-Secosterols Intermediates. 2005.
37. **Andres Braunbrück.** Wave Interaction in Weakly Inhomogeneous Materials. 2005.
38. **Robert Kitt.** Generalised Scale-Invariance in Financial Time Series. 2005.
39. **Juss Pavelson.** Mesoscale Physical Processes and the Related Impact on the Summer Nutrient Fields and Phytoplankton Blooms in the Western Gulf of Finland. 2005.
40. **Olari Ilison.** Solitons and Solitary Waves in Media with Higher Order Dispersive and Nonlinear Effects. 2005.
41. **Maksim Säkki.** Intermittency and Long-Range Structurization of Heart Rate. 2005.
42. **Enli Kiipli.** Modelling Seawater Chemistry of the East Baltic Basin in the Late Ordovician–Early Silurian. 2005.
43. **Igor Golovtsov.** Modification of Conductive Properties and Processability of Polyparaphenylene, Polypyrrole and polyaniline. 2005.
44. **Katrin Laos.** Interaction Between Furcellaran and the Globular Proteins (Bovine Serum Albumin β -Lactoglobulin). 2005.
45. **Arvo Mere.** Structural and Electrical Properties of Spray Deposited Copper Indium Disulphide Films for Solar Cells. 2006.
46. **Sille Ehala.** Development and Application of Various On- and Off-Line Analytical Methods for the Analysis of Bioactive Compounds. 2006.
47. **Maria Kulp.** Capillary Electrophoretic Monitoring of Biochemical Reaction Kinetics. 2006.
48. **Anu Aaspõllu.** Proteinases from *Vipera lebetina* Snake Venom Affecting Hemostasis. 2006.
49. **Lyudmila Chekulayeva.** Photosensitized Inactivation of Tumor Cells by Porphyrins and Chlorins. 2006.
50. **Merle Uudsemaa.** Quantum-Chemical Modeling of Solvated First Row Transition Metal Ions. 2006.

51. **Tagli Pitsi**. Nutrition Situation of Pre-School Children in Estonia from 1995 to 2004. 2006.
52. **Angela Ivask**. Luminescent Recombinant Sensor Bacteria for the Analysis of Bioavailable Heavy Metals. 2006.
53. **Tiina Lõugas**. Study on Physico-Chemical Properties and Some Bioactive Compounds of Sea Buckthorn (*Hippophae rhamnoides* L.). 2006.
54. **Kaja Kasemets**. Effect of Changing Environmental Conditions on the Fermentative Growth of *Saccharomyces cerevisiae* S288C: Auxo-accelerostat Study. 2006.
55. **Ildar Nisamedtinov**. Application of ¹³C and Fluorescence Labeling in Metabolic Studies of *Saccharomyces* spp. 2006.
56. **Alar Leibak**. On Additive Generalisation of Voronoï's Theory of Perfect Forms over Algebraic Number Fields. 2006.
57. **Andri Jagomägi**. Photoluminescence of Chalcopyrite Tellurides. 2006.
58. **Tõnu Martma**. Application of Carbon Isotopes to the Study of the Ordovician and Silurian of the Baltic. 2006.
59. **Marit Kauk**. Chemical Composition of CuInSe₂ Monograin Powders for Solar Cell Application. 2006.
60. **Julia Kois**. Electrochemical Deposition of CuInSe₂ Thin Films for Photovoltaic Applications. 2006.
61. **Iiona Oja Ačik**. Sol-Gel Deposition of Titanium Dioxide Films. 2007.
62. **Tiia Anmann**. Integrated and Organized Cellular Bioenergetic Systems in Heart and Brain. 2007.
63. **Katrin Trummal**. Purification, Characterization and Specificity Studies of Metalloproteinases from *Vipera lebetina* Snake Venom. 2007.
64. **Gennadi Lessin**. Biochemical Definition of Coastal Zone Using Numerical Modeling and Measurement Data. 2007.
65. **Enno Pais**. Inverse problems to determine non-homogeneous degenerate memory kernels in heat flow. 2007.
66. **Maria Borissova**. Capillary Electrophoresis on Alkylimidazolium Salts. 2007.
67. **Karin Valmsen**. Prostaglandin Synthesis in the Coral *Plexaura homomalla*: Control of Prostaglandin Stereochemistry at Carbon 15 by Cyclooxygenases. 2007.
68. **Kristjan Piirimäe**. Long-Term Changes of Nutrient Fluxes in the Drainage Basin of the Gulf of Finland – Application of the PolFlow Model. 2007.
69. **Tatjana Dedova**. Chemical Spray Pyrolysis Deposition of Zinc Sulfide Thin Films and Zinc Oxide Nanostructured Layers. 2007.
70. **Katrin Tomson**. Production of Labelled Recombinant Proteins in Fed-Batch Systems in *Escherichia coli*. 2007.
71. **Cecilia Sarmiento**. Suppressors of RNA Silencing in Plants. 2008.
72. **Vilja Mardla**. Inhibition of Platelet Aggregation with Combination of Antiplatelet Agents. 2008.
73. **Maie Bachmann**. Effect of Modulated Microwave Radiation on Human Resting Electroencephalographic Signal. 2008.
74. **Dan Hüvonen**. Terahertz Spectroscopy of Low-Dimensional Spin Systems. 2008.
75. **Ly Villo**. Stereoselective Chemoenzymatic Synthesis of Deoxy Sugar Esters Involving *Candida antarctica* Lipase B. 2008.

76. **Johan Anton.** Technology of Integrated Photoelasticity for Residual Stress Measurement in Glass Articles of Axisymmetric Shape. 2008.
77. **Olga Volobujeva.** SEM Study of Selenization of Different Thin Metallic Films. 2008.
78. **Artur Jõgi.** Synthesis of 4'-Substituted 2,3'-dideoxynucleoside Analogues. 2008.
79. **Mario Kadastik.** Doubly Charged Higgs Boson Decays and Implications on Neutrino Physics. 2008.
80. **Fernando Pérez-Caballero.** Carbon Aerogels from 5-Methylresorcinol-Formaldehyde Gels. 2008.
81. **Sirje Vaask.** The Comparability, Reproducibility and Validity of Estonian Food Consumption Surveys. 2008.
82. **Anna Menaker.** Electrosynthesized Conducting Polymers, Polypyrrole and Poly(3,4-ethylenedioxythiophene), for Molecular Imprinting. 2009.
83. **Lauri Ilson.** Solitons and Solitary Waves in Hierarchical Korteweg-de Vries Type Systems. 2009.
84. **Kaia Ernits.** Study of In₂S₃ and ZnS Thin Films Deposited by Ultrasonic Spray Pyrolysis and Chemical Deposition. 2009.
85. **Veljo Sinivee.** Portable Spectrometer for Ionizing Radiation "Gammamapper". 2009.
86. **Jüri Virkepu.** On Lagrange Formalism for Lie Theory and Operadic Harmonic Oscillator in Low Dimensions. 2009.
87. **Marko Piirsoo.** Deciphering Molecular Basis of Schwann Cell Development. 2009.
88. **Kati Helmja.** Determination of Phenolic Compounds and Their Antioxidative Capability in Plant Extracts. 2010.
89. **Merike Sõmera.** Sobemoviruses: Genomic Organization, Potential for Recombination and Necessity of P1 in Systemic Infection. 2010.
90. **Kristjan Laes.** Preparation and Impedance Spectroscopy of Hybrid Structures Based on CuIn₃Se₅ Photoabsorber. 2010.
91. **Kristin Lippur.** Asymmetric Synthesis of 2,2'-Bimorpholine and its 5,5'-Substituted Derivatives. 2010.
92. **Merike Luman.** Dialysis Dose and Nutrition Assessment by an Optical Method. 2010.
93. **Mihhail Berezovski.** Numerical Simulation of Wave Propagation in Heterogeneous and Microstructured Materials. 2010.
94. **Tamara Aid-Pavlidis.** Structure and Regulation of BDNF Gene. 2010.
95. **Olga Bragina.** The Role of Sonic Hedgehog Pathway in Neuro- and Tumorigenesis. 2010.
96. **Merle Randrüüt.** Wave Propagation in Microstructured Solids: Solitary and Periodic Waves. 2010.
97. **Marju Laars.** Asymmetric Organocatalytic Michael and Aldol Reactions Mediated by Cyclic Amines. 2010.
98. **Maarja Grossberg.** Optical Properties of Multinary Semiconductor Compounds for Photovoltaic Applications. 2010.
99. **Alla Maloverjan.** Vertebrate Homologues of Drosophila Fused Kinase and Their Role in Sonic Hedgehog Signalling Pathway. 2010.
100. **Priit Pruunsild.** Neuronal Activity-Dependent Transcription Factors and Regulation of Human *BDNF* Gene. 2010.

101. **Tatjana Knjazeva.** New Approaches in Capillary Electrophoresis for Separation and Study of Proteins. 2011.
102. **Atanas Katerski.** Chemical Composition of Sprayed Copper Indium Disulfide Films for Nanostructured Solar Cells. 2011.
103. **Kristi Timmo.** Formation of Properties of CuInSe_2 and $\text{Cu}_2\text{ZnSn}(\text{S,Se})_4$ Monograin Powders Synthesized in Molten KI. 2011.
104. **Kert Tamm.** Wave Propagation and Interaction in Mindlin-Type Microstructured Solids: Numerical Simulation. 2011.
105. **Adrian Popp.** Ordovician Proetid Trilobites in Baltoscandia and Germany. 2011.
106. **Ove Pärn.** Sea Ice Deformation Events in the Gulf of Finland and This Impact on Shipping. 2011.
107. **Germo Väli.** Numerical Experiments on Matter Transport in the Baltic Sea. 2011.
108. **Andrus Seiman.** Point-of-Care Analyser Based on Capillary Electrophoresis. 2011.
109. **Olga Katargina.** Tick-Borne Pathogens Circulating in Estonia (Tick-Borne Encephalitis Virus, *Anaplasma phagocytophilum*, *Babesia* Species): Their Prevalence and Genetic Characterization. 2011.
110. **Ingrid Sumeri.** The Study of Probiotic Bacteria in Human Gastrointestinal Tract Simulator. 2011.
111. **Kairit Zovo.** Functional Characterization of Cellular Copper Proteome. 2011.
112. **Natalja Makarytsheva.** Analysis of Organic Species in Sediments and Soil by High Performance Separation Methods. 2011.
113. **Monika Mortimer.** Evaluation of the Biological Effects of Engineered Nanoparticles on Unicellular Pro- and Eukaryotic Organisms. 2011.
114. **Kersti Tepp.** Molecular System Bioenergetics of Cardiac Cells: Quantitative Analysis of Structure-Function Relationship. 2011.
115. **Anna-Liisa Peikolainen.** Organic Aerogels Based on 5-Methylresorcinol. 2011.
116. **Leeli Amon.** Palaeoecological Reconstruction of Late-Glacial Vegetation Dynamics in Eastern Baltic Area: A View Based on Plant Macrofossil Analysis. 2011.
117. **Tanel Peets.** Dispersion Analysis of Wave Motion in Microstructured Solids. 2011.
118. **Liina Kaupmees.** Selenization of Molybdenum as Contact Material in Solar Cells. 2011.
119. **Allan Olsper.** Properties of VPg and Coat Protein of Sobemoviruses. 2011.
120. **Kadri Koppel.** Food Category Appraisal Using Sensory Methods. 2011.
121. **Jelena Gorbatšova.** Development of Methods for CE Analysis of Plant Phenolics and Vitamins. 2011.
122. **Karin Viipsi.** Impact of EDTA and Humic Substances on the Removal of Cd and Zn from Aqueous Solutions by Apatite. 2012.
123. **David Schryer.** Metabolic Flux Analysis of Compartmentalized Systems Using Dynamic Isotopologue Modeling. 2012.
124. **Ardo Illaste.** Analysis of Molecular Movements in Cardiac Myocytes. 2012.
125. **Indrek Reile.** 3-Alkylcyclopentane-1,2-Diones in Asymmetric Oxidation and Alkylation Reactions. 2012.
126. **Tatjana Tamberg.** Some Classes of Finite 2-Groups and Their Endomorphism Semigroups. 2012.
127. **Taavi Liblik.** Variability of Thermohaline Structure in the Gulf of Finland in Summer. 2012.

128. **Priidik Lagemaa**. Operational Forecasting in Estonian Marine Waters. 2012.
129. **Andrei Errapart**. Photoelastic Tomography in Linear and Non-linear Approximation. 2012.
130. **Külliki Krabbi**. Biochemical Diagnosis of Classical Galactosemia and Mucopolysaccharidoses in Estonia. 2012.
131. **Kristel Kaseleht**. Identification of Aroma Compounds in Food using SPME-GC/MS and GC-Olfactometry. 2012.
132. **Kristel Kodar**. Immunoglobulin G Glycosylation Profiling in Patients with Gastric Cancer. 2012.
133. **Kai Rosin**. Solar Radiation and Wind as Agents of the Formation of the Radiation Regime in Water Bodies. 2012.
134. **Ann Tiiman**. Interactions of Alzheimer's Amyloid-Beta Peptides with Zn(II) and Cu(II) Ions. 2012.
135. **Olga Gavrilo**va. Application and Elaboration of Accounting Approaches for Sustainable Development. 2012.
136. **Olesja Bondarenko**. Development of Bacterial Biosensors and Human Stem Cell-Based *In Vitro* Assays for the Toxicological Profiling of Synthetic Nanoparticles. 2012.
137. **Katri Muska**. Study of Composition and Thermal Treatments of Quaternary Compounds for Monograin Layer Solar Cells. 2012.
138. **Ranno Nahku**. Validation of Critical Factors for the Quantitative Characterization of Bacterial Physiology in Accelerostat Cultures. 2012.
139. **Petri-Jaan Lahtvee**. Quantitative Omics-level Analysis of Growth Rate Dependent Energy Metabolism in *Lactococcus lactis*. 2012.
140. **Kerti Orumets**. Molecular Mechanisms Controlling Intracellular Glutathione Levels in Baker's Yeast *Saccharomyces cerevisiae* and its Random Mutagenized Glutathione Over-Accumulating Isolate. 2012.
141. **Loreida Timberg**. Spice-Cured Sprats Ripening, Sensory Parameters Development, and Quality Indicators. 2012.
142. **Anna Mihhalevski**. Rye Sourdough Fermentation and Bread Stability. 2012.
143. **Liisa Arike**. Quantitative Proteomics of *Escherichia coli*: From Relative to Absolute Scale. 2012.
144. **Kairi Otto**. Deposition of In₂S₃ Thin Films by Chemical Spray Pyrolysis. 2012.
145. **Mari Sepp**. Functions of the Basic Helix-Loop-Helix Transcription Factor TCF4 in Health and Disease. 2012.
146. **Anna Suhhova**. Detection of the Effect of Weak Stressors on Human Resting Electroencephalographic Signal. 2012.
147. **Aram Kazarjan**. Development and Production of Extruded Food and Feed Products Containing Probiotic Microorganisms. 2012.
148. **Rivo Uiboupin**. Application of Remote Sensing Methods for the Investigation of Spatio-Temporal Variability of Sea Surface Temperature and Chlorophyll Fields in the Gulf of Finland. 2013.
149. **Tiina Kriščiunaite**. A Study of Milk Coagulability. 2013.
150. **Tuuli Levandi**. Comparative Study of Cereal Varieties by Analytical Separation Methods and Chemometrics. 2013.
151. **Natalja Kabanova**. Development of a Microcalorimetric Method for the Study of Fermentation Processes. 2013.

152. **Himani Khanduri**. Magnetic Properties of Functional Oxides. 2013.
153. **Julia Smirnova**. Investigation of Properties and Reaction Mechanisms of Redox-Active Proteins by ESI MS. 2013.
154. **Mervi Sepp**. Estimation of Diffusion Restrictions in Cardiomyocytes Using Kinetic Measurements. 2013.
155. **Kersti Jääger**. Differentiation and Heterogeneity of Mesenchymal Stem Cells. 2013.
156. **Victor Alari**. Multi-Scale Wind Wave Modeling in the Baltic Sea. 2013.
157. **Taavi Päll**. Studies of CD44 Hyaluronan Binding Domain as Novel Angiogenesis Inhibitor. 2013.
158. **Allan Niidu**. Synthesis of Cyclopentane and Tetrahydrofuran Derivatives. 2013.
159. **Julia Geller**. Detection and Genetic Characterization of *Borrelia* Species Circulating in Tick Population in Estonia. 2013.
160. **Irina Stulova**. The Effects of Milk Composition and Treatment on the Growth of Lactic Acid Bacteria. 2013.
161. **Jana Holmar**. Optical Method for Uric Acid Removal Assessment During Dialysis. 2013.
162. **Kerti Ausmees**. Synthesis of Heterobicyclo[3.2.0]heptane Derivatives *via* Multicomponent Cascade Reaction. 2013.
163. **Minna Varikmaa**. Structural and Functional Studies of Mitochondrial Respiration Regulation in Muscle Cells. 2013.
164. **Indrek Koppel**. Transcriptional Mechanisms of BDNF Gene Regulation. 2014.
165. **Kristjan Pilt**. Optical Pulse Wave Signal Analysis for Determination of Early Arterial Ageing in Diabetic Patients. 2014.
166. **Andres Anier**. Estimation of the Complexity of the Electroencephalogram for Brain Monitoring in Intensive Care. 2014.
167. **Toivo Kallaste**. Pyroclastic Sanidine in the Lower Palaeozoic Bentonites – A Tool for Regional Geological Correlations. 2014.
168. **Erki Kärber**. Properties of ZnO-nanorod/In₂S₃/CuInS₂ Solar Cell and the Constituent Layers Deposited by Chemical Spray Method. 2014.
169. **Julia Lehner**. Formation of Cu₂ZnSnS₄ and Cu₂ZnSnSe₄ by Chalcogenisation of Electrochemically Deposited Precursor Layers. 2014.
170. **Peep Pitk**. Protein- and Lipid-rich Solid Slaughterhouse Waste Anaerobic Co-digestion: Resource Analysis and Process Optimization. 2014.
171. **Kaspar Valgepea**. Absolute Quantitative Multi-omics Characterization of Specific Growth Rate-dependent Metabolism of *Escherichia coli*. 2014.
172. **Artur Noole**. Asymmetric Organocatalytic Synthesis of 3,3'-Disubstituted Oxindoles. 2014.
173. **Robert Tsanev**. Identification and Structure-Functional Characterisation of the Gene Transcriptional Repressor Domain of Human Gli Proteins. 2014.
174. **Dmitri Kartofelev**. Nonlinear Sound Generation Mechanisms in Musical Acoustic. 2014.
175. **Sigrid Hade**. GIS Applications in the Studies of the Palaeozoic Graptolite Argillite and Landscape Change. 2014.
176. **Agne Velthut-Meikas**. Ovarian Follicle as the Environment of Oocyte Maturation: The Role of Granulosa Cells and Follicular Fluid at Pre-Ovulatory Development. 2014.

177. **Kristel Hälvin**. Determination of B-group Vitamins in Food Using an LC-MS Stable Isotope Dilution Assay. 2014.
178. **Mailis Päre**. Characterization of the Oligoadenylate Synthetase Subgroup from Phylum Porifera. 2014.
179. **Jekaterina Kazantseva**. Alternative Splicing of *TAF4*: A Dynamic Switch between Distinct Cell Functions. 2014.
180. **Jaanus Suurväli**. Regulator of G Protein Signalling 16 (RGS16): Functions in Immunity and Genomic Location in an Ancient MHC-Related Evolutionarily Conserved Synteny Group. 2014.
181. **Ene Viiard**. Diversity and Stability of Lactic Acid Bacteria During Rye Sourdough Propagation. 2014.
182. **Kristella Hansen**. Prostaglandin Synthesis in Marine Arthropods and Red Algae. 2014.
183. **Helike Lõhelaid**. Allene Oxide Synthase-lipoxygenase Pathway in Coral Stress Response. 2015.
184. **Normunds Stivrīnš**. Postglacial Environmental Conditions, Vegetation Succession and Human Impact in Latvia. 2015.
185. **Mary-Liis Kütt**. Identification and Characterization of Bioactive Peptides with Antimicrobial and Immunoregulating Properties Derived from Bovine Colostrum and Milk. 2015.
186. **Kazbulat Šogenov**. Petrophysical Models of the CO₂ Plume at Prospective Storage Sites in the Baltic Basin. 2015.
187. **Taavi Raadik**. Application of Modulation Spectroscopy Methods in Photovoltaic Materials Research. 2015.
188. **Reio Pöder**. Study of Oxygen Vacancy Dynamics in Sc-doped Ceria with NMR Techniques. 2015.
189. **Sven Siir**. Internal Geochemical Stratification of Bentonites (Altered Volcanic Ash Beds) and its Interpretation. 2015.
190. **Kaur Jaanson**. Novel Transgenic Models Based on Bacterial Artificial Chromosomes for Studying BDNF Gene Regulation. 2015.
191. **Niina Karro**. Analysis of ADP Compartmentation in Cardiomyocytes and Its Role in Protection Against Mitochondrial Permeability Transition Pore Opening. 2015.
192. **Piret Laht**. B-plexins Regulate the Maturation of Neurons Through Microtubule Dynamics. 2015.
193. **Sergei Žari**. Organocatalytic Asymmetric Addition to Unsaturated 1,4-Dicarbonyl Compounds. 2015.